CAPITAL UNIVERSITY OF SCIENCE AND
TECHNOLOGY, ISLAMABAD

Investigation of Darcy-Forchheimer Model with Two-Level Galerkin Finite Element Method

by

Muhammad Nadeem

A thesis submitted in partial fulfillment for the
degree of Master of Philosophy

in the

Faculty of Computing
Department of Mathematics

2025

I dedicate my thesis to

my beloved family, friends specially

***My Mother(Haneefa Zaheer)**,*

A determined and aristocratic embodiment who educate me to belief in ALLAH,

believe in hard work and that so much could be done with little,

My Father(Muhammad Zaheer)

I quote the remarkable words of Hadith,

"A father gives his child nothing better than good education."

CERTIFICATE OF APPROVAL

Investigation of Darcy-Forchheimer Model with Two-Level Galerkin Finite Element Method

by

Muhammad Nadeem

(MMT231011)

THESIS EXAMINING COMMITTEE

S. No.	Examiner	Name	Organization
(a)	External Examiner	Dr. Qazi Mehmood ul Hassan	UOW, Wah
(b)	Internal Examiner	Dr. Abid Kamran	CUST, Islambad
(c)	Supervisor	Dr. Muhammad Sabeel Khan	CUST, Islamabad

Dr. Muhammad Sabeel Khan
Thesis Supervisor
August, 2025

Dr. Muhammad Sagheer
Head
Dept. of Mathematics
August, 2025

Dr. M. Abdul Qadir
Dean
Faculty of Computing
August, 2025

Author's Declaration

I, **Muhammad Nadeem** hereby state that my MPhil thesis titled "**Investigation of Darcy-Forchheimer Model with Two-Level Galerkin Finite Element Method**" is my own work and has not been submitted previously by me for taking any degree from Capital University of Science and Technology, Islamabad or anywhere else in the country/abroad.

At any time if my statement is found to be incorrect even after my graduation, the University has the right to withdraw my MPhil Degree.

(Muhammad Nadeem)

Registration No: MMT231011

Plagiarism Undertaking

I solemnly declare that research work presented in this thesis titled "**Investigation of Darcy-Forchheimer Model with Two-Level Galerkin Finite Element Method**" is solely my research work with no significant contribution from any other person. Small contribution/help wherever taken has been duly acknowledged and that complete thesis has been written by me.

I understand the zero tolerance policy of the HEC and Capital University of Science and Technology towards plagiarism. Therefore, I as an author of the above titled thesis declare that no portion of my thesis has been plagiarized and any material used as reference is properly referred/cited.

I undertake that if I am found guilty of any formal plagiarism in the above titled thesis even after award of MPhil Degree, the University reserves the right to withdraw/revoke my MPhil degree and that HEC and the University have the right to publish my name on the HEC/University website on which names of students are placed who submitted plagiarized work.

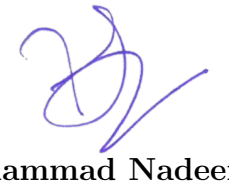

(Muhammad Nadeem)
Registration No: MMT231011

Acknowledgement

In the name of **ALLAH**, the Most Merciful and Beneficent, who created the universe and bestowed upon humankind the wisdom and intellect to uncover its mysteries.

I express my deepest gratitude and sincere respect to my supervisor, **Dr. Muhammad Sabeel Khan**, for his unwavering support, expert guidance and genuine encouragement throughout this research journey. His insightful feedback, patience, and constant motivation have been instrumental in shaping the direction and quality of this thesis.

I am deeply grateful to all my teachers for their motivation and emphasis on striving for excellence in the pursuit of knowledge. I extend my sincere gratitude to the **Capital University of Science and Technology (CUST)** for providing a supportive environment that greatly facilitated this research. I would like to express my heartfelt appreciation to my wife, **Maria Arshad Janjua**, whose unwavering love and support have been my guiding light. Her constant encouragement and prayers have been my greatest strength throughout this journey. Her belief in me has always inspired me to persevere and achieve my goals.

Finally, I would like to express my sincere thanks to my friends and fellow researchers at **CUST** for their valuable discussions and support throughout this research. Their camaraderie and insightful contributions have greatly enriched my experience and I am truly grateful to have shared this journey with them.

(Muhammad Nadeem)
Registration No: MMT231011

Abstract

This research focuses on the application and enhancement of the Darcy-Forchheimer model for fluid flow in porous media, considering higher-grade modifications to account for complex behaviors like non-linearity and heat transfer enhancement. The study employs the two-level algorithm with coarse and finer mesh strategies to improve the accuracy and computational efficiency of simulations. The numerical experiments are conducted using the open-source **FreeFEM++** platform, which facilitates the modeling and solution of coupled flow and heat transfer problems. The results highlight the significant role of the Forchheimer number in non-linear flow regimes and demonstrate how mesh refinement enhances the precision of the computed velocity and temperature distributions. By integrating the two-level algorithm, the research ensures a balance between computational cost and solution accuracy, especially for problems involving intricate geometries and boundary conditions. Additionally, the study investigates the impact of various parameters, including Reynolds, Prandtl, Forchheimer, Hartmann, Grashof, and Porosity numbers, on the system's performance. This work provides valuable insights for future studies on fluid dynamics in porous media and contributes to the development of more efficient simulation techniques for complex engineering applications.

Contents

List of Figures

List of Tables

Abbreviations

CFD	Computational Fluid Dynamics
FEM	Finite Element Method
FDM	Finite Difference Method
FVM	Finite Volume Method
GFEM	Galerkin Finite Element Method
IVP	Initial Value Problem
MHD	Magnetohydrodynamics
MMR	Micromagnetorotation
MFEM	Mixed Finite Element Method
ODEs	Ordinary Differential Equations
PDEs	Partial Differential Equations
RBF	Radial Basis Function
WRM	Weighted Residue Method

Symbols

B_0	Constant magnetic field
B_θ	Variable magnetic field
σ	Electrical conductivity
g	Gravitational acceleration
C_f	Skin-friction coefficient
C_p	Specific heat
$\mathbf{u}$	Velocity vector
E	Electric field
K	Permeability parameter
M $\times H$	Micromagnetorotation term
P_r	Prandtl number
Q	Dimensionless heat source
R_e	Reynolds number
ψ	Stream function
μ_θ	Reference dynamic viscosity
p	Pressure
γ	Viscous elasticity
μ_o	Dynamic viscosity
ρ	Fluid density
ϕ	Porosity
θ	Dimensionless temperature
$\mathbf{g}$	Gravity vector
H_a	Hartmann number
F_r	Forchheimer number

G_r	Grashof number
κ	Thermal conductivity
α	Thermal diffusivity

Chapter 1

Introduction and Literature Survey

The study of heat equations dates back to the pioneering work of Joseph Fourier in the 19th century. Fourier in his monograph "The Analytical Theory of Heat" (1822) introduced the first mathematical formulation of heat conduction, establishing the foundation for modern thermal analysis [1]. The classical heat equation is a parabolic partial differential equation (PDE) that describes the distribution of temperature over time in a given domain. Over the years, researchers extended Fourier's work to cover complex scenarios such as transient heat conduction, phase-change materials, and anisotropic heat diffusion [2] and [3]. The role of heat equations in various scientific and industrial applications has expanded significantly, driving researchers to develop improved numerical methods for solving complex heat transfer problems with high accuracy and computational efficiency [4].

Heat transfer problems arise in various engineering and scientific applications, including energy systems, aerospace engineering, biomedical engineering, and electronics cooling. The three primary modes of heat transfer—conduction, convection, and radiation—play crucial roles in these applications. Conduction, governed by Fourier's law, describes heat flow through solid materials [5]. Convection involves heat transfer in fluids due to bulk motion, characterized by the Navier-Stokes and energy equations [6]. Radiation, modeled using the Stefan-Boltzmann

law, accounts for thermal energy exchange without direct contact between surfaces [7]. Over time, advancements in computational tools and numerical methods have enabled more detailed and accurate simulations of heat transfer mechanisms across various disciplines [8]. Recent developments in fluid and heat transport through porous media have highlighted the limitations of classical Darcy's law, especially under moderate-to-high velocity conditions. To overcome this, the Darcy–Forchheimer model has been extensively adopted, incorporating non-linear inertial effects to more accurately describe flow behavior in porous structures [9]. Several investigations [10] have examined how parameters such as permeability and the Forchheimer coefficient influence thermal and momentum transport in porous media. Numerical investigations based on detailed simulations [11] have provided insights into heat transfer patterns in Forchheimer-type porous media, contributing to improved understanding of energy-efficient thermal system design. However, despite these advancements, many existing models still assume idealized boundary conditions or overlook the impact of coupled heat and momentum interactions under varying porosity, which this study aims to address. Several numerical methods have been employed to solve the heat equation, including the Finite Difference Method (FDM), Finite Volume Method (FVM), Finite Element Method (FEM), and meshless techniques. Each method has its advantages and limitations. This Finite difference method discretizes the spatial and temporal derivatives using difference equations. It is simple and efficient for structured grids but struggles with complex geometries[3]. The accuracy of FDM is highly dependent on the grid resolution, and high-order schemes are often required for improved precision [12]. Finite Volume Method Commonly used in computational fluid dynamics, FVM ensures local conservation of mass, momentum, and energy, making it suitable for heat transfer in fluid flow problems [13]. The flexibility of FVM allows it to handle complex boundary conditions and transient simulations efficiently [14] and [15]. Finite Element method (FEM) is highly versatile and allows for flexible meshing, making it well-suited for solving heat conduction problems in complex geometries [16]. Unlike FDM and FVM, FEM can easily incorporate anisotropic and heterogeneous materials [17]. The adaptability of FEM makes it an essential tool in modern engineering applications, including thermal stress analysis and multiphysics problems [18].Meshless methods like the Radial

Basis Function (RBF) approach have been explored for heat transfer simulations without the need for mesh generation [19]. These methods are gaining attention for problems involving free-surface flows, deformable media, and phase-change materials, as they eliminate the challenges associated with mesh distortion and refinement[20, 21].

The heat transfer of porous media has broad applications in environmental engineering, petroleum extraction, and bioengineering. In such systems, the presence of pores significantly alters the flow behavior and heat conduction mechanisms. The governing equations for heat transfer in porous media often incorporate both Darcy's law and the energy equation, modified to include effective thermal conductivity [22]. Porous structures play a crucial role in enhancing heat dissipation in heat exchangers, insulation materials, and catalytic reactors. Recent research has also explored the impact of fluid flow in porous domains, leading to improved heat transfer efficiency in industrial processes [23, 24]. Several studies have focused on numerically simulating magnetically induced flow within rectangular channels, using higher-order continuum mechanics and tools like FreeFem++. These models, often based on the micropolar continuum theory, describe the coupled dynamics of velocity, induction, and microrotation fields under laminar, incompressible flow, with an applied external magnetic field and corresponding boundary conditions [25].

The objective of the present study is to analyze the velocity and temperature profiles of a steady, incompressible, two-dimensional fluid flow and heat transfer in a rectangular cavity with embedded semi-circular heaters and a lid-driven top boundary, using the Mixed Finite Element Method (MFEM). The investigation incorporates the heat equation to examine thermal behavior, considering the influence of parameters such as the Darcy-Forchheimer number, Reynolds number, and Hartmann number. By employing the two-level Galerkin finite element method, the characteristic behavior of the model is effectively captured, providing insights into fluid dynamics and heat transfer characteristics. Graphical representations of the dimensionless temperature and velocity fields are provided to illustrate key findings and physical interpretations.

1.1 Thesis Contribution

In this thesis, we present a higher-grade Darcy-Forchheimer porous flow model in a rectangular cavity with three cylindrical heaters positioned at the bottom wall. The governing dynamics of the flow and heat transfer are formulated using PDEs and solved by Two-Level FEM. The model is non-dimensionalized through appropriate transformations, incorporating key dimensionless parameters such as the Reynolds number, Prandtl number, Forchheimer number, and Hartmann number.

A weak formulation of the problem is derived and numerically implemented in FreeFEM++. The computational framework employs two-level methods to enhance solution accuracy and efficiency. The study further explores the influence of different inflow boundary conditions, particularly parabolic inflow, on the velocity and pressure distribution. The effects of external heat sources and varying heater temperatures on convective heat transfer are also examined.

Mesh independence of the solutions is carried out, and results are presented in tabular and graphical forms. The findings are analyzed for different physical parameters of interest, providing insights into optimizing heat transfer performance in porous media applications

1.2 Thesis Layout

This thesis is further composed of the following chapters:

- **Chapter 2**, introduces the fundamental principles of fluid flow and heat transfer in porous media. It defines key concepts, outlines the governing equations of fluid motion, and explores the Darcy-Forchheimer model for non-linear flow through porous structures. The discussion covers the conservation laws of mass, momentum, and energy, emphasizing their formulation in the presence of external heat sources.

- **Chapter 3**, explains the finite element method by considering an example of a second-order non-homogeneous differential equation. The example is

used to illustrate the numerical procedure involved in solving such equations and obtaining reliable computational results.

- **Chapter 4**, focuses on the numerical investigation of heat transfer and fluid flow in a porous medium within a two-dimensional rectangular enclosure, incorporating three semicircular heat sources along the lower boundary and accounting for the effects of external heating The Darcy-Forchheimer model is employed to account for non-linear flow characteristics, and the Two-Level FEM is utilized for the numerical solution. The governing equations (mass, momentum, and energy conservation) are converted to dimensionless form to study the problem's scaled behavior. Carefully selected boundary conditions ensure physical accuracy in simulating fluid flow and heat transfer dynamics.

  For numerical solution, the dimensional equations are first transformed into dimensionless weak formulations. These are integrated across the computational domain and converted from strong to weak form using compatible test functions. The study employs an innovative two-level mesh algorithm that strategically combines coarse and fine grids . Localized trial functions generate domain-specific approximations, enabling an optimized Two-Level FEM approach for the Darcy-Forchheimer model.

  The chapter presents comprehensive graphical results demonstrating how key parameters influence thermal-fluid behavior. These visualizations validate the effectiveness of the two-level FEM framework in solving complex porous media problems.

- **Chapter 5** Contains the conclusion, summarizing the key findings of this work and outline potential avenues for further investigation.

Chapter 2

Basic Terminologies

This chapter provides a comprehensive discussion on the fundamental principles, key terminologies, and governing equations of fluid dynamics. Additionally, it introduces dimensionless parameters that play a crucial role in the mathematical formulation and analysis presented in subsequent chapters.

2.1 Fundamental definitions

2.1.1 Fluid

"A fluid will continuously deform when subjected to shear (tangential) stress, regardless of how small the stress may be." [26]

2.1.2 Fluid Mechanics

'Fluid mechanics is the branch of science that studies the behavior of fluids (liquids or gases) both at rest and in motion." [27]

2.1.3 Fluid Dynamics

"When pressure forces are also considered in the study of fluids in motion, the branch of science is known as fluid dynamics." [27]

2.1.4 Fluid Statics

"Fluid statics is the study of fluids at rest." [27]

2.1.5 Viscosity

"*Viscosity* refers to the property of a fluid that resists the movement of one layer of fluid over another adjacent layer. Mathematically,

$$\mu = \frac{\tau}{\frac{\partial u}{\partial y}}, \tag{2.1}$$

where μ is the viscosity coefficient, τ is the shear stress, and $\frac{\partial u}{\partial y}$ represents the velocity gradient." [27]

2.1.6 Kinematic Viscosity

"*Kinematic viscosity* is the ratio of the dynamic viscosity to the density of a fluid. It is denoted by the symbol ν, called *nu*. Mathematically,

$$\nu = \frac{\mu}{\rho}, \tag{2.2}$$

where ν is the kinematic viscosity, μ is the dynamic viscosity, and ρ is the density of the fluid." [27]

2.1.7 Thermal Conductivity

"The Fourier heat conduction law states that heat flow is proportional to the temperature gradient. The proportionality constant is known as the *thermal conductivity*, which may depend on various variables." [28]

2.1.8 Thermal Diffusivity

"The rate at which heat diffuses by conduction through a material depends on the *thermal diffusivity* and can be defined as,

$$\alpha = \frac{k}{\rho C_p}, \tag{2.3}$$

where α is the thermal diffusivity, k is the thermal conductivity, ρ is the density, and C_p is the specific heat at constant pressure." [29]

2.1.9 Mass Density or Density

Mass density, denoted by ρ, is a fundamental property of a substance that represents its mass per unit volume. It quantifies how much mass is contained within a given volume and is mathematically expressed as:

$$\rho = \frac{m}{V}, \tag{2.4}$$

where:

- ρ = Density ($\mathrm{kg/m^3}$)
- m = Mass of the substance (kg)
- V = Volume of the substance ($\mathrm{m^3}$)

The **SI unit** of density is **kilogram per cubic meter ($\mathbf{kg/m^3}$)**. Density plays a crucial role in fluid dynamics, determining buoyancy, pressure distribution, and flow characteristics. Incompressible fluids maintain a constant density, whereas compressible fluids exhibit density variations under changing pressure and temperature conditions.

2.1.10 Pressure

Pressure, denoted by P, is defined as the force exerted per unit area on a surface. It describes the intensity of a force acting normally to a given area and is mathematically expressed as:

$$P = \frac{F}{A}, \tag{2.5}$$

where:

P	Pressure (Pa or $\mathrm{N/m^2}$)
F	Force applied (N)
A	Area over which the force is distributed ($\mathrm{m^2}$)

The **SI unit** of pressure is **Pascal ($\mathbf{Pa = N/m^2}$)**. Pressure plays a fundamental role in fluid mechanics, influencing fluid motion, buoyancy, and the behavior of gases and liquids under different conditions. In a static fluid, pressure increases with depth due to the weight of the overlying fluid column, following the hydrostatic pressure equation.

2.2 Types of Fluid

2.2.1 Ideal Fluid

"A fluid that is incompressible and has no viscosity is called an *ideal fluid*. An ideal fluid is a theoretical concept, as all real fluids have some viscosity." [27]

2.2.2 Real Fluid

"A *real fluid* is a fluid that has viscosity. In practice, all fluids are real fluids." [27]

2.2.3 Newtonian Fluid

"A *Newtonian fluid* is a real fluid in which the shear stress is directly proportional to the rate of shear strain (or velocity gradient)." [27]

2.2.4 Non-Newtonian Fluid

"A real fluid in which the shear stress is not directly proportional to the rate of shear strain (or velocity gradient) is called a *non-Newtonian fluid*. The relationship between shear stress and velocity gradient for such fluids can be expressed as,

$$\tau_{xy} \propto \left(\frac{du}{dy}\right)^m, \quad m \neq 1, \tag{2.6}$$

or equivalently,

$$\tau_{xy} = \mu \left(\frac{du}{dy}\right)^m, \tag{2.7}$$

where τ_{xy} is the shear stress, $\dfrac{du}{dy}$ is the rate of shear strain, μ is the viscosity, and m is a constant that is not equal to 1." [27]

2.3 Types of flow

2.3.1 Rotational Flow

"*Rotational flow* refers to a type of fluid flow in which fluid particles, while moving along streamlines, also rotate about their own axis." [27]

2.3.2 Irrotational Flow

"*Irrotational flow* refers to a type of fluid flow in which fluid particles, while moving along streamlines, do not rotate about their own axis." [27]

2.3.3 Compressible Flow

"*Compressible flow* is characterized by changes in fluid density at different points. In other words, the density (ρ) of the fluid is not constant. Mathematically,

$$\rho \neq c, \tag{2.8}$$

where c is a constant." [27]

2.3.4 Incompressible Flow

"*Incompressible flow* refers to a type of flow where the fluid's density remains constant. Liquids are typically incompressible, whereas gases are generally compressible. Mathematically,

$$\rho = c, \tag{2.9}$$

where c is a constant." [27]

2.3.5 Steady Flow

"*Steady flow* occurs when the flow characteristics, such as velocity, depth, or rate of flow, remain constant over time at any given point in an open channel. Mathematically,

$$\frac{\partial Q}{\partial t} = 0, \tag{2.10}$$

where Q represents any fluid property." [27]

2.3.6 Unsteady Flow

"*Unsteady flow* refers to a flow condition where the velocity, depth, or rate of flow varies with time at any given point in an open channel. Mathematically,

$$\frac{\partial Q}{\partial t} \neq 0, \tag{2.11}$$

where Q represents any fluid property." [27]

2.3.7 Internal Flow

"*Internal flow* describes fluid flow that is entirely confined within solid boundaries, such as in pipes or ducts." [26]

2.3.8 External Flow

"*External flow* occurs when a fluid flows around a body that is immersed in an unbounded fluid domain, such as the flow over an aircraft wing or a cylinder." [26]

2.4 Modes of Heat Transfer

2.4.1 Heat Transfer

"*Heat transfer* is a phenomenon focused on the movement of thermal energy from one location to another within a medium or between different media due to a temperature difference." [28]

2.4.2 Conduction

"*Conduction* refers to the transfer of heat within a material through the process of diffusion." [28]

2.4.3 Convection

"*Convection* is the transfer of heat that occurs through energy transport facilitated by fluid motion. Heat transfer between two different media via convection follows Newton's law of cooling." [28]

2.4.4 Advection

"*Advection* is the transport of heat or matter that occurs purely due to the bulk motion of a fluid, without involving molecular conduction. It represents the physical movement of a quantity with the flowing medium." [28]

2.4.5 Thermal Radiation

"*Thermal radiation* is radiant energy, in the form of electromagnetic waves, emitted by a medium solely as a result of its temperature." [28]

2.4.6 Magnetohydrodynamics (MHD)

Magnetohydrodynamics (MHD) refers to the study of the dynamics of electrically conducting fluids, such as liquid metals, plasmas, saltwater, or electrolytes, under the influence of electromagnetic fields. It combines the principles of fluid mechanics and electromagnetism to describe the behavior of such flows. In MHD, the interaction between the magnetic field and the moving fluid generates Lorentz forces, which can significantly alter the flow characteristics.

The governing equations for MHD flow are obtained by coupling the Navier–Stokes equations with Maxwell's equations. For incompressible, Newtonian, and electrically conducting fluids, the MHD equations are typically written as, Momentum Equation:

$$\rho\left(\frac{\partial \mathbf{u}}{\partial t} + (\mathbf{u}\cdot\nabla)\mathbf{u}\right) = -\nabla p + \mu\nabla^2\mathbf{u} + \mathbf{J}\times\mathbf{B}, \tag{2.12}$$

where:

ρ is the fluid density,

$\mathbf{u}$ is the velocity vector,

p is the pressure,

μ is the dynamic viscosity,

$\mathbf{J}$ is the current density,

$\mathbf{B}$ is the magnetic field,

$\mathbf{J} \times \mathbf{B}$ is the Lorentz force per unit volume.

Ohm's Law (in moving conducting fluid):

$$\mathbf{J} = \sigma(\mathbf{E} + \mathbf{u} \times \mathbf{B}), \tag{2.13}$$

where:

σ is the electrical conductivity,

$\mathbf{E}$ is the electric field,

$\mathbf{u} \times \mathbf{B}$ is the electromotive force due to fluid motion.

Magnetic Induction Equation (if the magnetic field is time-dependent):

$$\frac{\partial \mathbf{B}}{\partial t} = \nabla \times (\mathbf{u} \times \mathbf{B}) + \eta \nabla^2 \mathbf{B}, \tag{2.14}$$

where $\eta = \frac{1}{\mu_0 \sigma}$ is the magnetic diffusivity and μ_0 is the magnetic permeability of free space.

2.4.7 Viscoelastic Fluids

"Viscoelastic fluids are those that exhibit both viscous and elastic characteristics when undergoing deformation. These fluids have memory effects, meaning the stress depends not only on the current strain but also on the history of deformation."[30]

2.4.8 Buoyancy forces

"The buoyant force is the net vertical force exerted on a body by the surrounding fluid. It is equal to the weight of the fluid displaced by the body."[31]

2.5 Spaces

2.5.1 Function Spaces

"A function space is a set of functions that share common properties and are subject to certain conditions, such as continuity, differentiability, or integrability, and are typically equipped with a norm or inner product that turns them into vector spaces." [32]

2.5.2 Hilbert Spaces

"A Hilbert space is a complete inner product space; that is, a vector space equipped with an inner product such that the norm induced by this inner product makes the space complete." [32]

2.6 Dimensionless Numbers

2.6.1 Prandtl Number

The **Prandtl number** is a dimensionless quantity that describes the relative importance of momentum diffusivity (viscous effects) to thermal diffusivity in a fluid. It provides insight into the relationship between heat conduction and convection within the fluid. The mathematical definition of the Prandtl number is given by

$$Pr = \frac{\nu}{\alpha} = \frac{\mu c_p}{k}, \tag{2.15}$$

where,

$\nu = \frac{\mu}{\rho}$ is the kinematic viscosity (m^2/s),
$\alpha = \frac{k}{\rho c_p}$ is the thermal diffusivity (m^2/s),
μ is the dynamic viscosity $(Pa \cdot s)$,
c_p is the specific heat capacity at constant pressure $(J/kg \cdot K)$,

k is the thermal conductivity $(W/m \cdot K)$,

ρ is the fluid density (kg/m^3).

The Prandtl number classifies heat transfer behavior in fluids:

- For $Pr \ll 1$, thermal diffusivity dominates over momentum diffusivity, typical in liquid metals where heat conduction is highly efficient.
- For $Pr \approx 1$, momentum and thermal diffusivities are comparable, as seen in gases like air.
- For $Pr \gg 1$, momentum diffusivity is dominant, characteristic of oils and highly viscous fluids where heat conduction is relatively slow.

In engineering and scientific applications, the Prandtl number plays a crucial role in analyzing heat transfer performance in convection processes, influencing thermal boundary layer development. It is widely used in fluid dynamics, aerodynamics, and heat exchanger design, ensuring efficient thermal management in industrial and environmental systems.

2.6.2 Grashof Number

The **Grashof number** is a dimensionless parameter that quantifies the relative significance of buoyancy forces to viscous forces in a fluid flow. It is a fundamental criterion in natural convection, where fluid motion arises due to temperature-induced density variations rather than external mechanical forces. The mathematical expression for the Grashof number is given by

$$Gr = \frac{g\beta\Delta T L^3}{\nu^2}, \tag{2.16}$$

where,

g is the gravitational acceleration (m/s^2),

β is the thermal expansion coefficient (K^{-1}),

ΔT represents the temperature difference (K),

L is the characteristic length (m), and

ν is the kinematic viscosity of the fluid (m^2/s).

A higher Grashof number indicates stronger buoyancy-driven flow, leading to more pronounced natural convection effects. When Gr is relatively low, viscous forces suppress buoyancy-induced motion, resulting in negligible convection. In engineering and scientific applications, the Grashof number is particularly useful in analyzing heat transfer in systems such as electronic cooling, atmospheric convection, thermal insulation, and industrial heat exchangers. It also plays a crucial role in determining the transition from laminar to turbulent flow in natural convection, typically occurring when Gr exceeds 10^9.

2.6.3 Reynolds Number

The **Reynolds number** is a dimensionless quantity that characterizes the flow regime of a fluid by comparing inertial forces to viscous forces. It plays a crucial role in determining whether a flow is laminar, transitional, or turbulent. The mathematical expression for the Reynolds number is given by:

$$Re = \frac{\rho U L}{\mu} = \frac{U L}{\nu}, \tag{2.17}$$

where:

ρ is the fluid density (kg/m^3),

U is the characteristic velocity of the fluid (m/s),

L is the characteristic length (m),

μ is the dynamic viscosity $(Pa \cdot s)$,

$\nu = \frac{\mu}{\rho}$ is the kinematic viscosity (m^2/s).

The Reynolds number serves as a key criterion for predicting flow behavior:

- For lower Reynolds numbers (typically $Re < 2000$ in internal flows), the fluid motion is generally laminar, exhibiting a smooth and stable profile with minimal disturbances.

- Within an intermediate Reynolds number range (approximately $2000 < Re < 4000$), the flow enters a transitional phase where instabilities may develop, and the behavior becomes sensitive to disturbances or boundary effects.
- At higher Reynolds numbers (usually $Re > 4000$ in pipe flow scenarios), the flow tends to become turbulent, marked by irregular fluctuations, chaotic motion, and enhanced mixing.

In engineering and scientific applications, the Reynolds number is widely used to analyze aerodynamics, pipeline flows, and heat transfer mechanisms. It is fundamental in designing efficient fluid transport systems, optimizing flow conditions in industrial processes, and understanding natural fluid dynamics in environmental systems.

2.6.4 Hartmann Number

The **Hartmann number** (Ha) is a dimensionless parameter that quantifies the influence of a magnetic field on the flow of an electrically conducting fluid, such as liquid metals or plasmas. It represents the ratio of electromagnetic forces to viscous forces within the fluid and plays a crucial role in magnetohydrodynamics (MHD). The mathematical definition of the Hartmann number is given by:

$$Ha = \frac{BL}{\sqrt{\mu\rho\nu}}, \tag{2.18}$$

where:

B is the applied magnetic field strength (T),
L is the characteristic length scale (m),
μ is the dynamic viscosity ($Pa \cdot s$),
ρ is the fluid density (kg/m^3),
ν is the kinematic viscosity (m^2/s).

The **Hartmann number** governs the behavior of MHD flows:

- For lower Hartmann numbers, viscous forces dominate, and the magnetic field has a minimal effect on the fluid motion.
- For higher Hartmann numbers, the Lorentz force becomes significant, suppressing velocity fluctuations and leading to a more stabilized flow.

In engineering and physics, the Hartmann number is widely used to analyze MHD systems, including plasma containment in fusion reactors, liquid metal cooling in nuclear reactors, and electromagnetic flow control in industrial applications. It plays a crucial role in optimizing heat transfer and fluid stability under the influence of a magnetic field.

2.6.5 Forchheimer number

The **Forchheimer number** (Fr) is a dimensionless parameter used to characterize the significance of non-linear inertial effects in porous media flow. It represents the ratio of inertial forces to viscous forces and is particularly important in high-velocity flow through porous structures, where Darcy's law alone is insufficient to describe the fluid behavior. The Forchheimer number is mathematically defined as:

$$Fr = \frac{\rho U L}{\mu}, \tag{2.19}$$

The **Forchheimer number** determines the **regime of flow** in porous media:

- For $Fr \ll 1$, the flow is dominated by viscous effects and follows Darcy's law.
- For $Fr \gg 1$, inertial effects become significant, leading to deviations from Darcy's law and requiring the Forchheimer correction term in the momentum equation.

The **Forchheimer correction** is widely used in engineering applications, such as groundwater flow, petroleum reservoir simulations, and heat transfer enhancement

in porous media. It provides a more accurate representation of fluid movement in high-velocity and high-porosity conditions where non-linearity cannot be ignored.

2.6.6 Porosity Number

Porosity (λ) is a dimensionless parameter that quantifies the fraction of void spaces within a porous medium relative to its total volume. It plays a crucial role in fluid flow, heat transfer, and mass transport in porous structures, such as soils, rocks, and industrial filters. The mathematical definition of porosity is given by

$$\lambda = \frac{V_v}{V_t}, \tag{2.20}$$

where,

V_v is the volume of void spaces (m^3),

V_t is the total volume of the porous medium (m^3).

Porosity values range between **0 and 1** with:

- **High porosity** ($\lambda \approx 1$) indicating a highly permeable structure, common in sand and gravel.
- **Low porosity** ($\lambda \approx 0$) signifying a compact material, such as dense rock or concrete.

Porosity influences the permeability of a medium, affecting the movement of fluids through porous structures. In engineering and geophysics, it is essential for modeling oil reservoirs, groundwater transport, and heat exchangers in porous media applications.

2.7 Governing Laws of Flow Dynamics

2.7.1 The Continuity Equation

The continuity equation is a fundamental principle in fluid mechanics that ensures the conservation of mass in a fluid flow system. It states that the rate of mass entering a control volume must be equal to the rate of mass leaving it, provided there

are no sources or sinks. This equation is applicable to both compressible and incompressible flows. The general form of the continuity equation for a compressible fluid is given by:

$$\frac{\partial \rho}{\partial t} + \nabla \cdot (\rho \mathbf{V}) = 0, \tag{2.21}$$

where:

ρ is the fluid density (kg/m^3),

$\mathbf{V} = (u, v, w)$ is the velocity vector with components in the x, y, z directions,

$\nabla \cdot (\rho \mathbf{V})$ represents the divergence of mass flux,

$\frac{\partial \rho}{\partial t}$ is the local rate of change of density over time.

For an incompressible fluid, where the density remains constant, the equation simplifies to:

$$\nabla \cdot \mathbf{V} = \frac{\partial u}{\partial x} + \frac{\partial v}{\partial y} + \frac{\partial w}{\partial z} = 0. \tag{2.22}$$

This implies that the net volume flux into any control volume is zero. Using the divergence theorem, the differential form can be integrated over a control volume V with a control surface S, leading to,

$$\frac{d}{dt} \int_V \rho \, dV + \int_S \rho \mathbf{V} \cdot d\mathbf{S} = 0. \tag{2.23}$$

This states that the rate of change of mass inside the control volume equals the net flux of mass across its boundaries.

The continuity equation, along with the Navier-Stokes equations, forms the foundation of computational fluid dynamics (CFD) and is widely used in real-world engineering and scientific applications.

2.7.2 The Momentum Equation

The conservation of momentum equation is a fundamental principle in fluid mechanics, derived from Newton's Second Law of Motion. It states that the rate of change of momentum in a control volume is equal to the sum of external forces acting on the fluid. This equation plays a crucial role in analyzing fluid dynamics and is the foundation of the Navier-Stokes equations.

The general form of the momentum equation for a control volume is given by:

$$\frac{\partial(\rho \mathbf{V})}{\partial t} + \nabla \cdot (\rho \mathbf{V} \otimes \mathbf{V}) = -\nabla p + \nabla \cdot \boldsymbol{\tau} + \rho \mathbf{g}, \tag{2.24}$$

For an incompressible, Newtonian fluid, the equation simplifies to the Navier-Stokes equation:

$$\rho \left(\frac{\partial \mathbf{V}}{\partial t} + \mathbf{V} \cdot \nabla \mathbf{V} \right) = -\nabla p + \mu \nabla^2 \mathbf{V} + \rho \mathbf{g}, \tag{2.25}$$

where μ is the dynamic viscosity of the fluid.

The momentum equation accounts for:

- **Convective term** ($\mathbf{V} \cdot \nabla \mathbf{V}$): Describes momentum transport due to fluid motion.
- **Pressure gradient** ($-\nabla p$): Represents the force due to pressure differences.
- **Viscous forces** ($\nabla \cdot \boldsymbol{\tau}$ or $\mu \nabla^2 \mathbf{V}$): Describes internal resistance due to viscosity.
- **Body forces** ($\rho \mathbf{g}$): Includes gravitational and other long-range forces.

Using the Reynolds Transport Theorem, the integral form for a control volume V with surface S is given by:

$$\frac{d}{dt} \int_V \rho \mathbf{V} dV + \int_S \rho \mathbf{V} (\mathbf{V} \cdot d\mathbf{S}) = \int_S \mathbf{T} dS + \int_V \rho \mathbf{g} dV \tag{2.26}$$

where **T** represents the surface forces acting on the fluid.

The conservation of momentum equation, along with the continuity equation and energy equation, forms the foundation of computational fluid dynamics (CFD) and fluid mechanics research.

2.7.3 The Energy Equation

The conservation of energy equation is a fundamental principle in fluid mechanics, derived from the First Law of Thermodynamics. It states that the total energy of a fluid system remains constant unless acted upon by external forces such as heat transfer or work done by external forces. This equation plays a crucial role in analyzing thermal and mechanical energy interactions in fluid flow. The general form of the energy equation for a control volume is given by

$$\frac{\partial}{\partial t}(\rho e) + \nabla \cdot (\rho e \mathbf{V}) = -\nabla \cdot \mathbf{q} + \Phi + \rho \mathbf{V} \cdot \mathbf{g}, \tag{2.27}$$

where,

e is the specific energy (internal, kinetic, and potential energy per unit mass),

$\mathbf{q}$ is the heat flux vector, representing heat conduction,

Φ represents viscous dissipation, converting mechanical energy into internal energy,

$\rho \mathbf{V} \cdot \mathbf{g}$ accounts for energy transfer due to gravitational forces.

For an incompressible, Newtonian fluid, the equation simplifies to:

$$\rho C_p \left(\frac{\partial T}{\partial t} + \mathbf{V} \cdot \nabla T \right) = \kappa \nabla^2 T + \Phi, \tag{2.28}$$

where, C_p is the specific heat at constant pressure, T is the temperature, and k is the thermal conductivity of the fluid. The energy equation accounts for:

- **Convective transport** ($\mathbf{V} \cdot \nabla T$): Movement of thermal energy due to bulk fluid motion.
- **Conduction** ($\nabla^2 T$): Heat transfer due to molecular interactions.
- **Viscous dissipation** (Φ): Conversion of kinetic energy into thermal energy.
- **External work** ($\rho \mathbf{V} \cdot \mathbf{g}$): Energy added or removed due to external forces.

Using the Reynolds Transport Theorem, the integral form for a control volume V with surface S is given by:

$$\frac{d}{dt}\int_V \rho e dV + \int_S \rho e \mathbf{V} \cdot d\mathbf{S} = \int_S \mathbf{q} \cdot dS + \int_V \Phi dV + \int_V \rho \mathbf{V} \cdot \mathbf{g} dV. \tag{2.29}$$

This equation expresses the balance of energy within a control volume, considering

heat conduction, work done by body forces, and dissipation effects.

The conservation of energy equation, alongside the continuity equation and momentum equation, forms the foundation of computational fluid dynamics (CFD) and thermal-fluid analysis.

2.8 Heat Transfer Phenomenon

Heat and mass transfer are fundamental processes in engineering and natural systems. These phenomena govern energy and material transport and play a crucial role in various industrial and environmental applications. Below are the primary mechanisms through which heat and mass transfer occur.

2.8.1 Conduction

Conduction is the process of heat transfer through a stationary medium, such as a solid or a non-moving fluid, due to molecular vibrations and free electron

movement. This mode of heat transfer is governed by Fourier's law:

$$q = -k\nabla T, \tag{2.30}$$

where, q is the heat flux, k is the thermal conductivity, and ∇T represents the temperature gradient. Conduction is significant in applications such as heat exchangers, insulation materials, and solid structures.

2.8.2 Convection

Convection refers to heat transfer due to the movement of a fluid. It is further classified into,natural and forced convection.

- **Natural (free) convection**: Occurs due to buoyancy forces induced by temperature variations within the fluid.
- **Forced convection**: Occurs when an external force, such as a fan, pump, or wind, drives the fluid motion.

The rate of convective heat transfer is described by Newton's law of cooling:

$$q = h(T_s - T_\infty), \tag{2.31}$$

where, h is the convective heat transfer coefficient, T_s is the surface temperature, and T_∞ is the ambient fluid temperature.

2.8.3 Radiation

Radiation is the transfer of heat through electromagnetic waves. The energy emitted is governed by the Stefan-Boltzmann law:

$$Q = \sigma\varepsilon AT^4, \tag{2.32}$$

where, σ is the Stefan-Boltzmann constant, ε is the emissivity of the surface, A is the surface area, and T is the absolute temperature.

2.9 Porous Media

Porous media refer to materials that contain a network of interconnected voids or pores, allowing the flow of fluids such as gases or liquids through them. These media are prevalent in both natural and engineered systems, including soil, biological tissues, packed bed reactors, geothermal reservoirs, and fuel cells. The study of porous media is essential in fields such as fluid mechanics, heat transfer, petroleum engineering, hydrogeology, and biomedical engineering. The complexity of flow and transport phenomena in porous media arises from the interaction between the solid matrix and the fluid, requiring specialized mathematical models to describe their behavior accurately.

The governing equations in porous media are modifications of classical conservation laws. The continuity equation remains valid, ensuring mass conservation. However, the momentum equation is modified to account for resistance due to the porous matrix. In low-velocity regimes, Darcy's law governs fluid flow, expressing a linear relationship between the pressure gradient and velocity, where permeability dictates the ease of flow. For higher velocities, the Forchheimer term is added to capture inertial effects, making the equation nonlinear. Similarly, the energy equation must consider effective thermal properties such as heat capacity and conductivity, which depend on the porosity and material composition of both the solid and fluid phases. In cases where the solid and fluid phases have distinct temperatures, a dual-phase energy model is required, introducing additional heat transfer terms that account for interactions between the phases.

The significance of porous media extends across various engineering and scientific applications. In petroleum engineering, understanding fluid flow through porous rock formations is critical for oil and gas extraction. In hydrogeology, the movement of water through soil and aquifers determines groundwater availability and contamination transport. Biomedical engineering relies on porous media principles for modeling blood flow in tissues and drug delivery through porous membranes. In energy systems, porous structures play a key role in optimizing heat exchangers, improving fuel cell efficiency, and enhancing thermal energy storage. Due to

the vast range of applications, researchers continually develop advanced numerical methods and experimental techniques to analyze and optimize flow and heat transfer within porous structures, leading to innovations in engineering design and environmental sustainability.

2.10 Darcy Forchheimer Porous Flow

The Darcy-Forchheimer model describes fluid flow through porous media by incorporating both viscous and inertial effects. It extends Darcy's law by adding a non-linear Forchheimer term to account for high-velocity flow resistance. This model is essential for applications like packed bed reactors, geothermal systems, and filtration processes.A detailed explanation of each part is provided below.

2.10.1 Darcy's Law

Darcy's law is a fundamental equation that describes the flow of a fluid through a porous medium. It was formulated by Henry Darcy in 1856 based on experimental observations of water flow through sand filters. The law establishes a linear relationship between the fluid velocity and the pressure gradient under laminar flow conditions. Mathematically, it is expressed as:

$$\mathbf{V} = -\frac{K}{\mu}\nabla P, \tag{2.33}$$

where,

$\mathbf{V}$	is the velocity (or specific discharge) [m/s],
K	is the permeability of the porous medium [m^2],
μ	is the dynamic viscosity of the fluid [Pa·s],
∇P	is the pressure gradient [Pa/m].

The law is valid only for low Reynolds number flow, where inertial effects are negligible.The porous structure is assumed to have uniform properties. For high-velocity flows, Darcy's law is extended by adding a Forchheimer term to account for inertial effects, leading to the Darcy-Forchheimer equation.

2.10.2 Forchheimer's Law

Forchheimer's law is an extension of Darcy's law, which accounts for the inertial effects in fluid flow through porous media. While Darcy's law assumes a linear relationship between velocity and pressure gradient, it is valid only for slow (laminar) flow. However, at higher velocities, inertial effects become significant due to flow acceleration and turbulence within the pores, leading to deviations from Darcy's linear behavior. Forchheimer introduced an additional quadratic correction term to capture these effects, resulting in the Darcy-Forchheimer equation,

$$\mathbf{V} = -\frac{K}{\mu}\nabla P - \beta\rho|\mathbf{V}|\mathbf{V}, \tag{2.34}$$

where,

- K is the permeability of the porous medium [m^2],
- μ is the dynamic viscosity of the fluid [Pa·s],
- β is the Forchheimer coefficient, which depends on the porosity and structure of the medium,
- ρ is the fluid density [$\mathrm{kg/m}^3$],
- $\mathbf{V}$ is the Darcy velocity [m/s],
- ∇P is the pressure gradient [Pa/m].

Unlike Darcy's law, Forchheimer's model captures deviations from linearity at high flow rates. The quadratic term represents **energy losses** due to inertial effects within the porous medium. Used in systems where flow speeds exceed the Darcy regime, such as packed bed reactors, porous heat exchangers, and geothermal reservoirs.

Forchheimer's correction is crucial in real-world engineering applications where simple Darcy's law fails to predict flow accurately, making it essential for porous media flow analysis under turbulent or transition regimes.

Chapter 3

Fundamentals of the Finite Element Method

3.1 Introduction

The accurate numerical analysis of fluid flow and heat transfer problems requires robust computational techniques. Among these, the Finite Element Method (FEM) has emerged as a powerful tool for solving complex engineering and physics-based problems. FEM provides a systematic approach to discretizing partial differential equations (PDEs) over a given domain, enabling efficient numerical approximation of solutions.

The chapter is structured as follows:

First, we provide a brief overview of FEM fundamentals, followed by a discussion of various FEM techniques commonly used in computational fluid dynamics (CFD) and heat transfer problems.

Next, we present the mathematical formulation of the concerned problem, including the governing equations, boundary conditions, and non-dimensionalization. Finally, we outline the numerical implementation using Two-Level Galerkin FEM, which ensures a stable and accurate solution framework.

3.2 Formulation of FEM Model

The formulation of the FEM is based on four fundamental approaches: direct approach, Variational approach, weighted residual approach, and energy balance approach. The direct approach is primarily used for simple structural problems, where equilibrium equations are formulated directly. The variational approach relies on the principle of minimum potential energy to derive the governing equations, making it widely applicable in solid mechanics. The weighted residual approach, including the Galerkin method, minimizes the residual error over the domain to obtain an approximate solution. Lastly, the energy balance approach is based on the principles of energy conservation and is commonly used in thermal and fluid mechanics problems. These approaches serve as the foundation for assembling the element stiffness matrix and force vector in FEM analysis.

3.2.1 Weighted Residual Method

The Weighted Residual Method (WRM) is a fundamental approach in the formulation of the FEM used to approximate the solutions of differential equations governing physical phenomena. The method is based on minimizing the residual error that arises when an approximate solution does not exactly satisfy the governing equation over the entire domain. The idea is to ensure that the residual, when weighted by a set of test functions, is minimized to achieve the best possible approximation.

Mathematically, if a differential equation is expressed as:

$$\mathcal{L}(u) = f, \quad \text{in } \Omega,$$

where $\mathcal{L}$ is the differential operator, u is the unknown function, and f is a given source term, an approximate solution u_h generally does not satisfy the equation exactly, resulting in a residual R:

$$R = \mathcal{L}(u_h) - f.$$

In WRM, the residual is forced to be orthogonal to a set of weight functions w_i over the domain Ω:

$$\int_\Omega w_i R \, d\Omega = 0, \quad i = 1, 2, \ldots, N,$$

where, w_i are carefully chosen functions to ensure stability and accuracy of the solution. Different choices of weight functions lead to various WRM techniques, including: Collocation Method, where weight functions are Dirac delta functions, ensuring the residual is zero at discrete points. Subdomain Method, where the residual is minimized over subdomains of Ω. Least Squares, which minimizes the squared residual over the entire domain. Galerkin Method, where the weight functions are chosen to be the same as the shape functions used to approximate u_h, making it one of the most widely used methods in FEM. More among these, the Galerkin method is particularly significant in FEM as it ensures consistency with the weak form of the governing equation, leading to symmetric and stable system matrices. The Weighted Residual Method provides a systematic framework for deriving finite element formulations and is widely applied in structural mechanics, fluid dynamics, and heat transfer problems.

In the finite element formulation, the discretized system of equations obtained using WRM is generally represented in matrix form as:

$$[A]\{U\} = \{F\},$$

where, $[A]$ is the global stiffness matrix (or system matrix), $\{U\}$ is the nodal unknown vector (such as displacement, temperature, or velocity), and $\{F\}$ is the global force (or load) vector. More here this equation forms the basis for solving FEM problems, where $[A]$ is assembled from individual element contributions, and boundary conditions are applied before solving for $\{U\}$. The solution of this system provides an approximation to the original differential equation while maintaining numerical stability and accuracy. The stiffness matrix $[A]$ is assembled from the contributions of individual elements using the principle of summation over all elements:

$$[A] = \sum_{e=1}^{n_e} [A]^e. \tag{3.1}$$

Similarly, the force vector is assembled as:

$$\{F\} = \sum_{e=1}^{n_e} \{F\}^e, \tag{3.2}$$

where, n_e is the total number of elements, and $[A]^e$ and $\{F\}^e$ are the element-wise stiffness matrices and force vectors, respectively. This summation process ensures that local element contributions are correctly integrated into the global system, maintaining consistency with the overall domain behavior.Moreover, this summation-based approach is a fundamental aspect of FEM, ensuring that the system accurately represents the physical problem being modeled. Once the system equations are assembled, appropriate boundary conditions are applied before solving for the unknown nodal values.

3.2.2 Example(One- Dimensional Problem)

Consider the differential equation:

$$\frac{d^2u}{dx^2} + x = 0, \quad \text{for } 0 \leq x \leq 1, \tag{3.3}$$

with boundary conditions:

$$u(0) = 0, \quad u(1) = 0. \tag{3.4}$$

Approximate Solution Form: We assume a trial solution that satisfies the boundary conditions:

$$u(x) = a_1 x(1 - x). \tag{3.5}$$

Here, a_1 is an unknown coefficient to be determined.

Residual Formulation: Substituting the assumed solution into the differential equation:

$$R(x) = \frac{d^2}{dx^2}[a_1 x(1 - x)] + x. \tag{3.6}$$

Computing the derivatives:

$$\frac{du}{dx} = a_1(1 - 2x), \tag{3.7}$$

$$\frac{d^2u}{dx^2} = -2a_1. \tag{3.8}$$

Thus, the residual becomes:

$$R(x) = -2a_1 + x. \tag{3.9}$$

Applying the Galerkin Method: The Galerkin method enforces:

$$\int_0^1 R(x)W(x)\,dx = 0, \tag{3.10}$$

where, the weight function is chosen as the same form as the trial function:

$$W(x) = x(1-x). \tag{3.11}$$

Thus, we have:

$$\int_0^1 (-2a_1 + x)x(1-x)\,dx = 0. \tag{3.12}$$

Solving for a_1 Expanding the integral:

$$-2a_1 \int_0^1 x(1-x)\,dx + \int_0^1 x^2(1-x)\,dx = 0. \tag{3.13}$$

Computing the integrals:

$$\int_0^1 x(1-x)\,dx = \frac{1}{6}, \tag{3.14}$$

$$\int_0^1 x^2(1-x)\,dx = \frac{1}{12}. \tag{3.15}$$

Thus, the equation simplifies to:

$$-2a_1 \times \frac{1}{6} + \frac{1}{12} = 0. \tag{3.16}$$

Solving for a_1:

$$a_1 = \frac{1}{4}. \tag{3.17}$$

Final Approximate Solution: Thus, the approximate solution is:

$$u(x) = \frac{1}{4}x(1-x). \tag{3.18}$$

3.3 Galerkin Finite Element Method

The Galerkin Finite Element Method (GFEM) is a widely used numerical technique for solving partial differential equations encountered in engineering and applied sciences. The method systematically transforms a continuous problem into a discrete system, making it computationally feasible. This section provides an in-depth discussion of GFEM, covering domain discretization, weak formulation, basis function selection, discretization, assembly, and solution of the global system, along with error estimation and convergence analysis.

Discretized Domain: To apply GFEM, the physical domain Ω is partitioned into a finite number of non-overlapping subdomains called finite elements. This process is known as mesh generation, and the quality of the mesh significantly impacts accuracy and computational efficiency. The nodes within these elements serve as reference points for approximating the solution. The choice of element type (linear, quadratic, etc.) plays a crucial role in the accuracy of the method.

Strong Form to Weak Form Transformation: A general linear second-order PDE in its strong form is given by:

$$\mathcal{L}u = f, \quad \text{in } \Omega, \tag{3.19}$$

where $\mathcal{L}$ is a differential operator, u is the unknown function, and f is a given source term.

To relax differentiability constraints, the weak form is obtained by multiplying the equation by a test function W and integrating over the domain:

$$\int_{\Omega} W(\mathcal{L}u - f)\, dx = 0. \tag{3.20}$$

Applying integration by parts transfers derivatives from u to W, ensuring a weaker continuity requirement and making the formulation more suitable for numerical implementation.

Approximate Function Space and Selection of Basis Functions: The exact solution u belongs to an infinite-dimensional function space. GFEM approximates this solution using a finite-dimensional subspace spanned by basis functions $\phi_i(x)$. The test functions in GFEM are chosen to be the same as the basis functions, a principle known as the Galerkin method:

$$W_i = \phi_i. \tag{3.21}$$

Galerkin Discretization and Representation of Approximate Solution: The approximate solution u_h is expressed as:

$$u_h = \sum_{i=1}^{N} a_i \phi_i(x), \tag{3.22}$$

where a_i, are unknown coefficients. Substituting this into the weak form leads to the discretized system:

$$\sum_{j=1}^{N} a_j \int_\Omega \phi_i \mathcal{L} \phi_j \, dx = \int_\Omega \phi_i f \, dx, \quad \forall i. \tag{3.23}$$

This forms a linear system $\mathbf{Ka} = \mathbf{F}$, where $\mathbf{K}$ is the stiffness matrix, $\mathbf{a}$ is the coefficient vector, and $\mathbf{F}$ is the force vector.

Local Element Formulation and Global System Assembly: The weak form integral is computed over individual elements before assembling the global system. The local stiffness matrix and load vector for an element e are:

$$K_{ij}^e = \int_{\Omega^e} \phi_i \mathcal{L} \phi_j \, dx, \quad F_i^e = \int_{\Omega^e} \phi_i f \, dx. \tag{3.24}$$

These local contributions are summed to construct the global system.

Boundary Conditions and System Solution: The boundary conditions modify the final system and can be of following two types

i) **Dirichlet conditions:** Enforced by prescribing values of u_h at boundary nodes.

ii) **Neumann conditions:** Incorporated naturally in the weak formulation.

Solving $\mathbf{Ka} = \mathbf{F}$ gives the coefficients a_i, reconstructing the approximate solution.

Error Estimation and Convergence Analysis: Accuracy depends on mesh resolution, basis function order, and numerical integration techniques. The error is measured using the L_2 norm:

$$\|u - u_h\|_{L_2} = \left(\int_\Omega |u - u_h|^2 \, dx \right)^{1/2}. \tag{3.25}$$

Refinement techniques such as h-refinement (reducing element size) and p-refinement (increasing polynomial degree) improve accuracy.

Conclusion The GFEM provides a structured approach to solving PDEs, balancing computational efficiency with accuracy. Through domain discretization, weak formulation, and systematic assembly, GFEM remains a cornerstone of numerical simulation in scientific and engineering applications.

3.3.1 Example(Two-Dimensional Problem)

We solve the steady-state heat conduction equation in a 2D rectangular plate:

$$-\nabla \cdot (k \nabla T) = Q \quad \text{in } \Omega, \tag{3.26}$$

where, $T(x, y)$ is the temperature field, k is the thermal conductivity (assumed constant), and more here $Q(x, y)$ is a heat source term.

The Boundary Conditions are

- $T = 0$, on the left and right edges.
- $\dfrac{\partial T}{\partial n} = 0$, (insulated) on the top and bottom edges.

The domain is a rectangular plate:

$$\Omega = \{(x, y) \mid 0 \leq x \leq 1, \ 0 \leq y \leq 1\}. \tag{3.27}$$

Weak Formulation Multiplying by a test function $v(x, y)$ and integrating over Ω:

$$\int_{\Omega} (-k\nabla^2 T)v \, d\Omega = \int_{\Omega} Qv \, d\Omega. \tag{3.28}$$

Applying integration by parts (Green's theorem):

$$\int_{\Omega} k\nabla T \cdot \nabla v \, d\Omega - \int_{\partial\Omega} k(\nabla T \cdot \mathbf{n})v \, d\Gamma = \int_{\Omega} Qv \, d\Omega. \tag{3.29}$$

Since, Neumann boundary condition gives $\frac{\partial T}{\partial n} = 0$, the boundary integral in equation (3.29) vanishes.

$\Rightarrow$

$$\int_{\Omega} k\nabla T \cdot \nabla v \, d\Omega = \int_{\Omega} Qv \, d\Omega. \tag{3.30}$$

Finite Element Approximation: Approximating T using finite element basis functions:

$$T_h = \sum_{i=1}^{N} T_i \phi_i(x, y), \tag{3.31}$$

with basis functions $\phi_i(x, y)$ (also know as hat functions). The Galerkin formulation becomes:

$$\sum_{i=1}^{N} T_i \int_{\Omega} k\nabla\phi_i \cdot \nabla\phi_j \, d\Omega = \int_{\Omega} Q\phi_j \, d\Omega, \quad \forall j = 1, 2, 3...N \tag{3.32}$$

This gives the system:

$$\boldsymbol{KT} = \boldsymbol{F}, \tag{3.33}$$

where, $K_{ij} = \int_{\Omega} k\nabla\phi_i \cdot \nabla\phi_j \, d\Omega$ is a stiffness metrix, $F_j = \int_{\Omega} Q\phi_j \, d\Omega$ is the load vector and $T = [T_1, T_2, ..., T_N]$ is the unknown temperature vector.

Mesh Generation and Discretization: The domain is discretized into triangular elements with linear shape functions. For each element:

$$\phi_i(x, y) = a_i + b_i x + c_i y. \tag{3.34}$$

Assembly of Global System: After computing local element matrices, we assemble the global system:

$$\boldsymbol{KT} = \boldsymbol{F}. \tag{3.35}$$

Solving the System We solve:

$$\boldsymbol{KT} = \boldsymbol{F}, \tag{3.36}$$

using numerical solvers such as Direct methods (Gaussian elimination) and Iterative methods (Conjugate Gradient, Multigrid).

Chapter 4

Mathematical Modeling of a Two-Dimensional Higher-Order Darcy-Forchheimer Flow in Porous Media

4.1 Problem Description

In this study, we investigate the flow and heat transfer characteristics within a lid-driven rectangular domain with three semicircular heated boundaries along the bottom wall. The computational domain consists of a rectangular enclosure, where all boundaries are stationary and subjected to no-slip boundary conditions (i.e, $u = v = 0$), except for the top horizontal wall, on which a uniform horizontal velocity of $u = 1$ is imposed, while maintaining $v = 0$, as illustrated in Fig 4.1. The physical setup consists of a closed rectangular fluid domain filled in a porous medium. The top wall is adiabatic, meaning that it does not allow any heat transfer through it. At the bottom boundary of the domain, there are three semicircular heat sources with diameter, denoted by d. These semicircular elements maintain a uniform temperature that is higher than the temperature of the vertical walls. The entire system is influenced by gravity acting in the vertical y- direction.

This geometrical configuration is of significant interest in the study of convective heat transfer, particularly in applications involving porous enclosures, thermal management systems, and microscale fluidic devices.

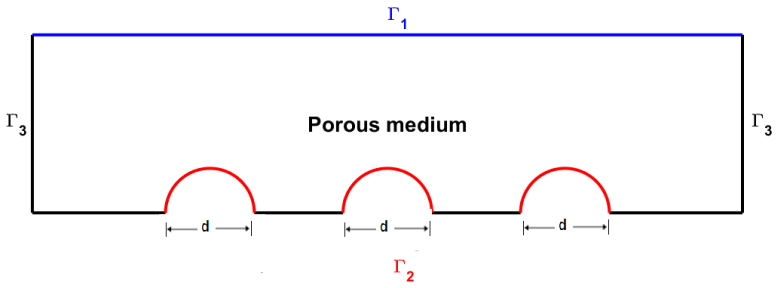

FIGURE 4.1: Schematic representation of the problem domain.

4.1.1 Dimensional Form of the Governing Equations

On account of the above discussion, now we are able to describe dimensional form of the governing equations for the proposed problem. For a two-dimensional flow field with constant fluid density, the dimensional form of the continuity equation in component form is given by:

$$\frac{\partial u}{\partial x}+\frac{\partial v}{\partial y}=0$$

The x-component of the momentum equation is given by [33]

$$\begin{aligned}\frac{\partial u}{\partial t}+u\frac{\partial u}{\partial x}+v\frac{\partial u}{\partial y}=\frac{1}{\rho}\Bigg[&-\frac{\partial p}{\partial x}+\left(\mu+\alpha_1\frac{\partial}{\partial t}\right)\left(\left(2\frac{\partial^2 u}{\partial x^2}+\frac{\partial^2 v}{\partial x\partial y}+\frac{\partial^2 u}{\partial y^2}\right)-\frac{\varphi}{K}u\right)\\&+\alpha_1\frac{\partial}{\partial x}\left[2\left(u\frac{\partial^2 u}{\partial x^2}+v\frac{\partial^2 u}{\partial x\partial y}\right)+\left(\frac{\partial v}{\partial x}\right)^2-\left(\frac{\partial u}{\partial y}\right)^2\right]\\&+\alpha_1\frac{\partial}{\partial y}\Bigg[(u\frac{\partial^2 v}{\partial x^2}+v\frac{\partial^2 v}{\partial x\partial y}+u\frac{\partial^2 u}{\partial x\partial y}+v\frac{\partial^2 u}{\partial y^2}-\frac{\partial u}{\partial x}\frac{\partial v}{\partial x}+\frac{\partial v}{\partial x}\frac{\partial v}{\partial y}\\&+\frac{\partial u}{\partial x}\frac{\partial u}{\partial y}-\frac{\partial u}{\partial y}\frac{\partial v}{\partial y})-\left(\frac{C_F\rho\varphi}{\sqrt{K}}u^2\right)\Bigg]\\&+\Big(-\sigma B_0^2u+\rho g_x(\beta_0)(\theta-\theta_0)\Big).\end{aligned}\tag{4.1}$$

The y-component of momentum equation is given by

$$\begin{aligned}
&\frac{\partial v}{\partial t}+u\frac{\partial v}{\partial x}+v\frac{\partial v}{\partial y}=\frac{1}{\rho}\\
&\left[-\frac{\partial p}{\partial y}+\left(\mu+\alpha_1\frac{\partial}{\partial t}\right)\left(\left(2\frac{\partial^2 v}{\partial y^2}+\frac{\partial^2 u}{\partial x\partial y}+\frac{\partial^2 v}{\partial x^2}\right)-\frac{\varphi}{K}v\right)\right.\\
&+\alpha_1\frac{\partial}{\partial x}\left[\left(u\frac{\partial^2 v}{\partial x^2}+u\frac{\partial^2 u}{\partial x\partial y}\right)+v\frac{\partial^2 u}{\partial y^2}+v\frac{\partial^2 v}{\partial y\partial x}+\frac{\partial u}{\partial x}\frac{\partial u}{\partial y}-\frac{\partial u}{\partial y}\frac{\partial v}{\partial y}\right.\\
&\left.-\frac{\partial v}{\partial x}\frac{\partial u}{\partial x}+\frac{\partial v}{\partial y}\frac{\partial v}{\partial x}\right]+\alpha_1\frac{\partial}{\partial y}\left[\left(2u\frac{\partial^2 v}{\partial x\partial y}+2v\frac{\partial^2 v}{\partial y^2}+(\frac{\partial u}{\partial y})^2\right.\right.\\
&\left.\left.+4(\frac{\partial v}{\partial y})^2-4\frac{\partial^2 v}{\partial y^2}-(\frac{\partial v}{\partial x})^2\right)-\left(\frac{C_F\rho\varphi}{\sqrt{K}}v^2\right)\right]\\
&\left.+\left(-\sigma B_0^2 v+\rho g_y(\beta_0)(\theta-\theta_0)\right)\right. .
\end{aligned}\tag{4.2}$$

The Energy equation is given as

$$\frac{\partial \theta}{\partial t}+u\frac{\partial \theta}{\partial x}+v\frac{\partial \theta}{\partial y}=\frac{k}{\rho C_p}\left(\frac{\partial^2 \theta}{\partial x^2}+\frac{\partial^2 \theta}{\partial y^2}\right). \tag{4.3}$$

The associated conditions of the problem on the computational domain in Fig 4.1 are described as follows:

- On the left wall (Γ_3) of the domain:

$$u=0, \quad v=0, \quad \text{and} \quad \theta=\theta_c. \tag{4.4}$$

- On the right wall (Γ_3) of the domain:

$$u=v=0, \quad \text{and} \quad \theta=\theta_c. \tag{4.5}$$

- On the bottom wall (Γ_2)

$$u=v=0, \quad \text{and} \quad \theta=\theta_c, \quad \text{on flatted boundary} \tag{4.6}$$

and

$$u=v=0, \quad \text{and} \quad \theta=100, \quad \text{on circular heater.} \tag{4.7}$$

- On the top wall (Γ_1) of the domain:

$$v = 0, \quad \theta = \theta_c, \quad \text{and} \quad u = 1. \tag{4.8}$$

To non-dimensionlize equations (4.1) -(4.3) let us define the following transformations.

Let

$$\hat{x} = \frac{x}{L}, \quad \hat{y} = \frac{y}{L}, \quad \hat{u} = \frac{u}{u_0}, \quad \hat{v} = \frac{v}{u_0}, \quad \hat{t} = \frac{u_0}{L}t, \quad \text{and} \quad P = \frac{p}{\rho u_0^2}. \tag{4.9}$$

4.2 Conversion of the Dimensional Equations into Dimensionless form

To convert equations (4.1)-(4.3) into the dimensionless form, certain derivatives are calculated which have been shown here in this sub-section.

- $\hat{x} = \dfrac{x}{L} \quad \Rightarrow \quad \dfrac{\partial \hat{x}}{\partial x} = \dfrac{1}{L}.$
- $\hat{y} = \dfrac{y}{L} \quad \Rightarrow \quad \dfrac{\partial \hat{y}}{\partial y} = \dfrac{1}{L}.$
- $\hat{u} = \dfrac{u}{u_0} \quad \Rightarrow \quad u = u_0\hat{u}.$
- $\hat{v} = \dfrac{v}{u_0} \quad \Rightarrow \quad v = u_0\hat{v}.$
- $\hat{t} = \dfrac{u_0}{L}t \quad \Rightarrow \quad \dfrac{\partial \hat{t}}{\partial t} = \dfrac{u_0}{L}.$

- $\dfrac{\partial u}{\partial t} = \dfrac{\partial u}{\partial \hat{t}}\dfrac{\partial \hat{t}}{\partial t} = \dfrac{\partial}{\partial \hat{t}}(u)\dfrac{\partial}{\partial t}(t) = \dfrac{\partial}{\partial \hat{t}}(u_0\hat{u})\dfrac{u_0}{L} = u_0\dfrac{\partial \hat{u}}{\partial \hat{t}}\dfrac{u_0}{L} = \dfrac{u_0^2}{L}\dfrac{\partial \hat{u}}{\partial \hat{t}}.$
- $\dfrac{\partial v}{\partial t} = \dfrac{\partial v}{\partial \hat{t}}\dfrac{\partial \hat{t}}{\partial t} = \dfrac{\partial}{\partial \hat{t}}(v)\dfrac{\partial}{\partial t}(t) = \dfrac{\partial}{\partial \hat{t}}(u_0\hat{v})\dfrac{u_0}{L} = u_0\dfrac{\partial \hat{v}}{\partial \hat{t}}\dfrac{u_0}{L} = \dfrac{u_0^2}{L}\dfrac{\partial \hat{v}}{\partial \hat{t}}.$
- $\dfrac{\partial u}{\partial x} = \dfrac{\partial u}{\partial \hat{x}}\dfrac{\partial \hat{x}}{\partial x} = \dfrac{\partial}{\partial \hat{x}}(u)\dfrac{\partial}{\partial x}(\hat{x}) = \dfrac{\partial}{\partial \hat{x}}(u_0\hat{u})\dfrac{1}{L} = \dfrac{u_0}{L}\dfrac{\partial \hat{u}}{\partial \hat{x}}.$
- $\dfrac{\partial u}{\partial y} = \dfrac{\partial u}{\partial \hat{y}}\dfrac{\partial \hat{y}}{\partial y} = \dfrac{\partial}{\partial \hat{y}}(u)\dfrac{\partial}{\partial y}(\hat{y}) = \dfrac{\partial}{\partial \hat{y}}(u_0\hat{u})\dfrac{1}{L} = \dfrac{u_0}{L}\dfrac{\partial \hat{u}}{\partial \hat{y}}.$

- $\dfrac{\partial v}{\partial x} = \dfrac{\partial v}{\partial \hat{x}}\dfrac{\partial \hat{x}}{\partial x} = \dfrac{\partial}{\partial \hat{x}}(v)\dfrac{\partial}{\partial x}(\hat{x}) = \dfrac{\partial}{\partial \hat{x}}(u_0\hat{v})\dfrac{1}{L} = \dfrac{u_0}{L}\dfrac{\partial \hat{v}}{\partial \hat{x}}.$
- $\dfrac{\partial v}{\partial y} = \dfrac{\partial v}{\partial \hat{y}}\dfrac{\partial \hat{y}}{\partial y} = \dfrac{\partial}{\partial \hat{y}}(v)\dfrac{\partial}{\partial y}(\hat{y}) = \dfrac{\partial}{\partial \hat{y}}(u_0\hat{v})\dfrac{1}{L} = \dfrac{u_0}{L}\dfrac{\partial \hat{v}}{\partial \hat{y}}.$

- $\left(\dfrac{\partial u}{\partial y}\right)^2 = \left(\dfrac{u_o}{L}\dfrac{\partial \hat{u}}{\partial \hat{y}}\right)^2 = \dfrac{u_o^2}{L^2}\left(\dfrac{\partial \hat{u}}{\partial \hat{y}}\right)^2.$
- $\left(\dfrac{\partial v}{\partial x}\right)^2 = \left(\dfrac{u_o}{L}\dfrac{\partial \hat{v}}{\partial \hat{x}}\right)^2 = \dfrac{u_o^2}{L^2}\left(\dfrac{\partial \hat{v}}{\partial \hat{x}}\right)^2.$
- $\left(\dfrac{\partial v}{\partial y}\right)^2 = \left(\dfrac{u_o}{L}\dfrac{\partial \hat{v}}{\partial \hat{y}}\right)^2 = \dfrac{u_o^2}{L^2}\left(\dfrac{\partial \hat{v}}{\partial \hat{y}}\right)^2.$

- $\dfrac{\partial^2 u}{\partial x^2} = \dfrac{\partial}{\partial x}\left(\dfrac{\partial u}{\partial x}\right) = \dfrac{\partial}{\partial x}\left(\dfrac{u_o}{L}\dfrac{\partial \hat{u}}{\partial \hat{x}}\right) = \dfrac{\partial}{\partial x}\left(\dfrac{u_o}{L}\dfrac{\partial \hat{u}}{\partial \hat{x}}\right) = \dfrac{u_o}{L^2}\dfrac{\partial^2 \hat{u}}{\partial \hat{x}^2}.$
- $\dfrac{\partial^2 u}{\partial y^2} = \dfrac{\partial}{\partial y}\left(\dfrac{\partial u}{\partial y}\right) = \dfrac{\partial}{\partial y}\left(\dfrac{u_o}{L}\dfrac{\partial \hat{u}}{\partial \hat{y}}\right) = \dfrac{1}{L}\left(\dfrac{u_o}{L}\dfrac{\partial \hat{u}}{\partial \hat{y}}\right) = \dfrac{u_o}{L^2}\dfrac{\partial^2 \hat{u}}{\partial \hat{y}^2}.$
- $\dfrac{\partial^2 v}{\partial x^2} = \dfrac{\partial}{\partial x}\left(\dfrac{\partial v}{\partial x}\right) = \dfrac{\partial}{\partial x}\left(\dfrac{u_o}{L}\dfrac{\partial \hat{v}}{\partial \hat{x}}\right) = \dfrac{1}{L}\left(\dfrac{u_o}{L}\dfrac{\partial \hat{v}}{\partial \hat{x}}\right) = \dfrac{u_o}{L^2}\dfrac{\partial^2 \hat{v}}{\partial \hat{x}^2}.$
- $\dfrac{\partial^2 v}{\partial y^2} = \dfrac{\partial}{\partial y}\left(\dfrac{\partial v}{\partial y}\right) = \dfrac{\partial}{\partial y}\left(\dfrac{u_o}{L}\dfrac{\partial \hat{v}}{\partial \hat{y}}\right) = \dfrac{1}{L}\left(\dfrac{u_o}{L}\dfrac{\partial \hat{v}}{\partial \hat{y}}\right) = \dfrac{u_o}{L^2}\dfrac{\partial^2 \hat{v}}{\partial \hat{y}^2}.$
- $\dfrac{\partial^2 u}{\partial x \partial y} = \dfrac{\partial}{\partial x}\left(\dfrac{\partial u}{\partial y}\right) = \dfrac{1}{L}\dfrac{\partial}{\partial \hat{x}}\left(\dfrac{u_o}{L}\dfrac{\partial \hat{u}}{\partial \hat{y}}\right) = \dfrac{u_o}{L^2}\dfrac{\partial^2 \hat{u}}{\partial \hat{x}\partial \hat{y}}.$
- $\dfrac{\partial^2 v}{\partial x \partial y} = \dfrac{\partial}{\partial x}\left(\dfrac{\partial v}{\partial y}\right) = \dfrac{1}{L}\dfrac{\partial}{\partial \hat{x}}\left(\dfrac{u_o}{L}\dfrac{\partial \hat{v}}{\partial \hat{y}}\right) = \dfrac{u_o}{L^2}\dfrac{\partial^2 \hat{v}}{\partial \hat{x}\partial \hat{y}}.$
- $u\dfrac{\partial u}{\partial x} = (u_o\hat{u})\dfrac{u_o}{L}\dfrac{\partial \hat{u}}{\partial \hat{x}} = \dfrac{u_o^2}{L}\hat{u}\dfrac{\partial \hat{u}}{\partial \hat{x}}.$
- $v\dfrac{\partial u}{\partial y} = (u_o\hat{v})\dfrac{u_o}{L}\dfrac{\partial \hat{u}}{\partial \hat{y}} = \dfrac{u_o^2}{L}\hat{v}\dfrac{\partial \hat{u}}{\partial \hat{y}}.$
- $u\dfrac{\partial v}{\partial x} = (u_o\hat{u})\dfrac{u_o}{L}\dfrac{\partial \hat{v}}{\partial \hat{x}} = \dfrac{u_o^2}{L}\hat{u}\dfrac{\partial \hat{v}}{\partial \hat{x}}.$

- $v\dfrac{\partial v}{\partial y} = (u_o\hat{v})\dfrac{u_o}{L}\dfrac{\partial \hat{v}}{\partial \hat{y}} = \dfrac{u_o^2}{L}\hat{v}\dfrac{\partial \hat{v}}{\partial \hat{y}}.$
- $u\dfrac{\partial^2 u}{\partial x^2} = (u_o\hat{u})\dfrac{u_o}{L^2}\dfrac{\partial^2 \hat{u}}{\partial \hat{x}^2} = \dfrac{u_o^2}{L^2}\hat{u}\dfrac{\partial^2 \hat{u}}{\partial \hat{x}^2},$
- $u\dfrac{\partial^2 v}{\partial x^2} = (u_o\hat{u})\dfrac{u_o}{L^2}\dfrac{\partial^2 \hat{v}}{\partial \hat{x}^2} = \dfrac{u_o^2}{L^2}\hat{u}\dfrac{\partial^2 \hat{v}}{\partial \hat{x}^2}.$

- $v\dfrac{\partial^2 u}{\partial y^2} = (u_o\hat{v})\dfrac{u_o}{L^2}\dfrac{\partial^2 \hat{u}}{\partial \hat{y}^2} = \dfrac{u_o^2}{L^2}\hat{v}\dfrac{\partial^2 \hat{u}}{\partial \hat{y}^2}.$
- $v\dfrac{\partial^2 v}{\partial y^2} = (u_o\hat{v})\dfrac{u_o}{L^2}\dfrac{\partial^2 \hat{v}}{\partial \hat{y}^2} = \dfrac{u_o^2}{L^2}\hat{v}\dfrac{\partial^2 \hat{v}}{\partial \hat{y}^2}.$
- $v\dfrac{\partial^2 u}{\partial x \partial y} = (u_o\hat{v})\dfrac{u_o}{L^2}\dfrac{\partial^2 \hat{u}}{\partial \hat{x}\partial \hat{y}} = \dfrac{u_o^2}{L^2}\hat{v}\dfrac{\partial^2 \hat{u}}{\partial \hat{x}\partial \hat{y}}.$
- $v\dfrac{\partial^2 v}{\partial x \partial y} = (u_o\hat{v})\dfrac{u_o}{L^2}\dfrac{\partial^2 \hat{v}}{\partial \hat{x}\partial \hat{y}} = \dfrac{u_o^2}{L^2}\hat{v}\dfrac{\partial^2 \hat{v}}{\partial \hat{x}\partial \hat{y}}.$
- $u\dfrac{\partial^2 u}{\partial x \partial y} = (u_o\hat{u})\dfrac{u_o}{L^2}\dfrac{\partial^2 \hat{u}}{\partial \hat{x}\partial \hat{y}} = \dfrac{u_o^2}{L^2}\hat{u}\dfrac{\partial^2 \hat{u}}{\partial \hat{x}\partial \hat{y}}.$
- $u\dfrac{\partial^2 v}{\partial x \partial y} = (u_o\hat{u})\dfrac{u_o}{L^2}\dfrac{\partial^2 \hat{v}}{\partial \hat{x}\partial \hat{y}} = \dfrac{u_o^2}{L^2}\hat{u}\dfrac{\partial^2 \hat{v}}{\partial \hat{x}\partial \hat{y}}.$
- $\dfrac{\partial u}{\partial x}\dfrac{\partial v}{\partial x} = \dfrac{u_o}{L}\dfrac{\partial \hat{u}}{\partial \hat{x}}\dfrac{u_o}{L}\dfrac{\partial \hat{v}}{\partial \hat{x}} = \dfrac{u_o^2}{L^2}\dfrac{\partial \hat{u}}{\partial \hat{x}}\dfrac{\partial \hat{v}}{\partial \hat{x}}.$
- $\dfrac{\partial u}{\partial y}\dfrac{\partial v}{\partial y} = \dfrac{u_o}{L}\dfrac{\partial \hat{u}}{\partial \hat{y}}\dfrac{u_o}{L}\dfrac{\partial \hat{v}}{\partial \hat{y}} = \dfrac{u_o^2}{L^2}\dfrac{\partial \hat{u}}{\partial \hat{y}}\dfrac{\partial \hat{v}}{\partial \hat{y}}.$
- $\dfrac{\partial u}{\partial x}\dfrac{\partial u}{\partial y} = \dfrac{u_o}{L}\dfrac{\partial \hat{u}}{\partial \hat{x}}\dfrac{u_o}{L}\dfrac{\partial \hat{u}}{\partial \hat{y}} = \dfrac{u_o^2}{L^2}\dfrac{\partial \hat{u}}{\partial \hat{x}}\dfrac{\partial \hat{u}}{\partial \hat{y}}.$
- $\dfrac{\partial v}{\partial x}\dfrac{\partial v}{\partial y} = \dfrac{u_o}{L}\dfrac{\partial \hat{v}}{\partial \hat{x}}\dfrac{u_o}{L}\dfrac{\partial \hat{v}}{\partial \hat{y}} = \dfrac{u_o^2}{L^2}\dfrac{\partial \hat{v}}{\partial \hat{x}}\dfrac{\partial \hat{v}}{\partial \hat{y}}.$
- $\hat{\theta} = \dfrac{\theta - \theta_o}{\theta_o} \quad \Rightarrow \quad \theta = \theta_o + \theta_o\hat{\theta} = \theta_o(1+\hat{\theta}).$
- $\dfrac{\partial \theta}{\partial t} = \dfrac{\partial}{\partial t}(\theta) = \dfrac{\partial}{\partial \hat{t}}\dfrac{\partial \hat{t}}{\partial t}(\theta) = \dfrac{\partial}{\partial \hat{t}}\dfrac{u_o}{L}(\theta) = \dfrac{u_o}{L}\dfrac{\partial}{\partial \hat{t}}(\theta_o + \theta_o\hat{\theta}) = \dfrac{u_o}{L}\theta_o\dfrac{\partial \hat{\theta}}{\partial \hat{t}}.$
- $\rho(C_p)\dfrac{\partial \theta}{\partial t} = \rho(C_p)\dfrac{\mu}{\rho L^2}\theta_o\dfrac{\partial \hat{\theta}}{\partial \hat{t}} = \dfrac{(C_p)\mu}{L^2}\theta_o\dfrac{\partial \hat{\theta}}{\partial \hat{t}}.$
- $\dfrac{\partial \theta}{\partial x} = \dfrac{\partial}{\partial x}(\theta) = \dfrac{\partial}{\partial \hat{x}}\dfrac{\partial \hat{x}}{\partial x}(\theta) = \dfrac{\partial}{\partial \hat{x}}\dfrac{1}{L}(\theta) = \dfrac{1}{L}\dfrac{\partial}{\partial \hat{x}}(\theta_o + \theta_o\hat{\theta}) = \dfrac{1}{L}\theta_o\dfrac{\partial \hat{\theta}}{\partial \hat{x}} = \dfrac{\theta_o}{L}\dfrac{\partial \hat{\theta}}{\partial \hat{x}}.$
- $\dfrac{\partial^2 \theta}{\partial x^2} = \dfrac{\partial}{\partial y}\left(\dfrac{\partial \theta}{\partial y}\right) = \dfrac{\partial}{\partial \hat{x}}\dfrac{\partial}{\partial \hat{x}}\left(\dfrac{\theta_o\hat{\theta}}{L}\right) = \dfrac{\partial}{\partial \hat{x}}\dfrac{1}{L}\left(\dfrac{\theta_o}{L}\dfrac{\partial \hat{\theta}}{\partial \hat{x}}\right) = \dfrac{\theta_o}{L^2}\dfrac{\partial^2 \hat{\theta}}{\partial \hat{x}^2}.$
- $\dfrac{\partial \theta}{\partial y} = \dfrac{\partial}{\partial y}(\theta) = \dfrac{\partial}{\partial \hat{y}}\dfrac{\partial \hat{y}}{\partial y}(\theta) = \dfrac{\partial}{\partial \hat{y}}\dfrac{1}{L}(\theta) = \dfrac{1}{L}\dfrac{\partial}{\partial \hat{y}}(\theta_o + \theta_o\hat{\theta}) = \dfrac{1}{L}\theta_o\dfrac{\partial \hat{\theta}}{\partial \hat{y}} = \dfrac{\theta_o}{L}\dfrac{\partial \hat{\theta}}{\partial \hat{y}}.$
- $\dfrac{\partial^2 \theta}{\partial y^2} = \dfrac{\partial}{\partial y}\left(\dfrac{\partial \theta}{\partial y}\right) = \dfrac{\partial}{\partial \hat{y}}\dfrac{\partial \hat{y}}{\partial y}\left(\dfrac{\theta_o\hat{\theta}}{L}\right) = \dfrac{\partial}{\partial \hat{y}}\dfrac{1}{L}\left(\dfrac{\theta_o}{L}\dfrac{\partial \hat{\theta}}{\partial \hat{y}}\right) = \dfrac{\theta_o}{L^2}\dfrac{\partial^2 \hat{\theta}}{\partial \hat{y}^2}.$

Equation (4.1) becomes:

$$\frac{\partial u}{\partial t}+u\frac{\partial u}{\partial x}+v\frac{\partial u}{\partial y}=\frac{1}{\rho}\Bigg[-\frac{\partial p}{\partial x}+\left(\mu+\alpha_1\frac{\partial}{\partial t}\right)\left\{2\frac{\partial^2 u}{\partial x^2}+\left(\frac{\partial^2 v}{\partial x\partial y}+\frac{\partial^2 u}{\partial y^2}\right)-\frac{\varphi}{K}u\right\}\Bigg]$$
$$+\alpha_1\frac{\partial}{\partial x}\left[2\left(u\frac{\partial^2 u}{\partial x^2}+v\frac{\partial^2 u}{\partial x\partial y}\right)+\left(\frac{\partial v}{\partial x}\right)^2-\left(\frac{\partial u}{\partial y}\right)^2\right]$$
$$+\alpha_1\frac{\partial}{\partial y}\left[u\frac{\partial^2 v}{\partial x^2}+u\frac{\partial^2 u}{\partial x\partial y}+v\frac{\partial^2 v}{\partial x\partial y}+v\frac{\partial^2 u}{\partial y^2}-\frac{\partial v}{\partial x}\frac{\partial u}{\partial x}-\frac{\partial v}{\partial y}\frac{\partial v}{\partial x}-\frac{\partial u}{\partial x}\frac{\partial u}{\partial y}+\frac{\partial u}{\partial y}\frac{\partial v}{\partial y}\right]$$
$$-\left(\frac{c_F\rho\varphi}{\sqrt{K}}\right)u^2-\sigma B_0^2u+\rho g_x(\beta_\theta)(\theta-\theta_0). \quad (4.10)$$

$\Rightarrow$

$$\frac{u_o^2}{L}\frac{\partial\hat{u}}{\partial\hat{t}}+\frac{u_o^2}{L}\hat{u}\frac{\partial\hat{u}}{\partial\hat{x}}+\frac{u_o^2}{L}\hat{v}\frac{\partial\hat{u}}{\partial\hat{y}}=\frac{1}{\rho}\Bigg[-\frac{\partial p}{\partial x}+\left(\mu+\alpha_1\frac{\partial}{\partial\hat{t}}\frac{\partial\hat{t}}{\partial t}\right)\Bigg\{$$
$$2\frac{u_o}{L^2}\frac{\partial^2\hat{u}}{\partial\hat{x}^2}+\frac{u_o}{L^2}\frac{\partial^2\hat{v}}{\partial\hat{x}\partial\hat{y}}+\frac{u_o}{L^2}\frac{\partial^2\hat{u}}{\partial\hat{y}^2}-\frac{\varphi}{K}u_o\hat{u}\Bigg\}\Bigg]$$
$$+\alpha_1\frac{\partial}{\partial\hat{x}}\frac{\partial\hat{x}}{\partial x}\left[2\left(\frac{u_o^2}{L^2}\hat{u}\frac{\partial^2\hat{u}}{\partial\hat{x}^2}+\frac{u_o^2}{L^2}\hat{v}\frac{\partial^2\hat{u}}{\partial\hat{x}\partial\hat{y}}\right)+\frac{u_o^2}{L^2}\frac{\partial^2\hat{v}}{\partial\hat{x}^2}-\frac{u_o^2}{L^2}\frac{\partial^2\hat{u}}{\partial\hat{y}^2}\right]$$
$$+\alpha_1\frac{\partial}{\partial\hat{y}}\frac{\partial\hat{y}}{\partial y}\Bigg[\frac{u_o^2}{L^2}\hat{u}\frac{\partial^2\hat{v}}{\partial\hat{x}^2}+\frac{u_o^2}{L^2}\hat{u}\frac{\partial^2\hat{u}}{\partial\hat{x}\partial\hat{y}}+\frac{u_o^2}{L^2}\hat{v}\frac{\partial^2\hat{v}}{\partial\hat{x}\partial\hat{y}}+\frac{u_o^2}{L^2}\hat{v}\frac{\partial^2\hat{u}}{\partial\hat{y}^2}$$
$$-\frac{u_o^2}{L^2}\frac{\partial\hat{v}}{\partial\hat{x}}\frac{\partial\hat{u}}{\partial\hat{x}}+\frac{u_o^2}{L^2}\frac{\partial\hat{v}}{\partial\hat{y}}\frac{\partial\hat{v}}{\partial\hat{x}}+\frac{u_o^2}{L^2}\frac{\partial\hat{u}}{\partial\hat{x}}\frac{\partial\hat{u}}{\partial\hat{y}}-\frac{u_o^2}{L^2}\frac{\partial\hat{u}}{\partial\hat{y}}\frac{\partial\hat{v}}{\partial\hat{y}}\Bigg]$$
$$-\left(\frac{c_F\rho\varphi}{\sqrt{K}}\right)(u_o\hat{u})^2-\sigma B_o^2(u_o\hat{u}). \quad (4.11)$$

$\Rightarrow$

$$\frac{u_o^2}{L}\frac{\partial\hat{u}}{\partial\hat{t}}+\frac{u_o^2}{L}\hat{u}\frac{\partial\hat{u}}{\partial\hat{x}}+\frac{u_o^2}{L}\hat{v}\frac{\partial\hat{u}}{\partial\hat{y}}=\frac{1}{\rho}\Bigg[-\frac{\partial p}{\partial x}+\left(\mu+\alpha_1\frac{\partial}{\partial\hat{t}}\frac{u_o}{L}\right)\Bigg\{2\frac{u_o}{L^2}\frac{\partial^2\hat{u}}{\partial\hat{x}^2}+\frac{u_o}{L^2}\frac{\partial^2\hat{v}}{\partial\hat{x}\partial\hat{y}}$$
$$+\frac{u_o}{L^2}\frac{\partial^2\hat{u}}{\partial\hat{y}^2}\Bigg\}\Bigg]-\left(\mu+\alpha_1\frac{\partial}{\partial\hat{t}}\frac{u_o}{L}\right)\frac{\varphi}{K}u_o\hat{u}+\alpha_1\frac{\partial}{\partial\hat{x}}\frac{1}{L}\Bigg[2\frac{u_o^2}{L^2}\hat{u}\frac{\partial^2\hat{u}}{\partial\hat{x}^2}+\frac{u_o^2}{L^2}\hat{v}\frac{\partial^2\hat{u}}{\partial\hat{x}\partial\hat{y}}$$
$$+\frac{u_o^2}{L^2}\frac{\partial^2\hat{v}}{\partial\hat{x}^2}-\frac{u_o^2}{L^2}\frac{\partial^2\hat{u}}{\partial\hat{y}^2}\Bigg]+\alpha_1\frac{\partial}{\partial\hat{y}}\frac{1}{L}\Bigg[\frac{u_o^2}{L^2}\hat{u}\frac{\partial^2\hat{u}}{\partial\hat{x}^2}+\frac{u_o^2}{L^2}\hat{u}\frac{\partial^2\hat{u}}{\partial\hat{x}\partial\hat{y}}+\frac{u_o^2}{L^2}\hat{v}\frac{\partial^2\hat{v}}{\partial\hat{x}\partial\hat{y}}$$
$$+\frac{u_o^2}{L^2}\hat{v}\frac{\partial^2\hat{u}}{\partial\hat{y}^2}-\frac{u_o^2}{L^2}\frac{\partial\hat{v}}{\partial\hat{x}}\frac{\partial\hat{u}}{\partial\hat{x}}+\frac{u_o^2}{L^2}\frac{\partial\hat{v}}{\partial\hat{y}}\frac{\partial\hat{v}}{\partial\hat{x}}+\frac{u_o^2}{L^2}\frac{\partial\hat{u}}{\partial\hat{x}}\frac{\partial\hat{u}}{\partial\hat{y}}-\frac{u_o^2}{L^2}\frac{\partial\hat{u}}{\partial\hat{y}}\frac{\partial\hat{v}}{\partial\hat{y}}\Bigg]$$
$$-\left(\frac{c_F\rho\varphi}{\sqrt{K}}\right)(u_o\hat{u})^2-\sigma B_o^2(u_o\hat{u}). \quad (4.12)$$

$\Rightarrow$

$$\frac{u_o^2}{L}\left[\frac{\partial \hat{u}}{\partial \hat{t}}+\hat{u}\frac{\partial \hat{u}}{\partial \hat{x}}+\hat{v}\frac{\partial \hat{u}}{\partial \hat{y}}\right]=-\frac{1}{\rho}\frac{\partial p}{\partial \hat{x}}+\frac{1}{\rho}\left(\frac{u_o}{L^2}\mu+\alpha_1\frac{\partial}{\partial \hat{t}}\frac{u_o^2}{L^3}\right)\left[2\frac{\partial^2 \hat{u}}{\partial \hat{x}^2}+\frac{\partial^2 \hat{v}}{\partial \hat{x}\partial \hat{y}}+\frac{\partial^2 \hat{u}}{\partial \hat{y}^2}\right]$$
$$-\frac{1}{\rho}\left(u_o\mu+\alpha_1\frac{\partial}{\partial \hat{t}}\frac{u_o^2}{L}\right)\frac{\varphi}{K}\hat{u}+\frac{1}{\rho}\alpha_1\frac{\partial}{\partial \hat{x}}\left[\frac{u_o^2}{L^3}\left(2(\hat{u}\frac{\partial^2 \hat{u}}{\partial \hat{x}^2}+\hat{v}\frac{\partial^2 \hat{u}}{\partial \hat{x}\partial \hat{y}})\right.\right.$$
$$\left.+\frac{\partial^2 \hat{v}}{\partial \hat{x}^2}-\frac{\partial^2 \hat{u}}{\partial \hat{y}^2}\right)\Big]+\frac{1}{\rho}\alpha_1\frac{\partial}{\partial \hat{y}}\left[\frac{u_o^2}{L^3}\left(\hat{u}\frac{\partial^2 \hat{v}}{\partial \hat{x}^2}+\hat{u}\frac{\partial^2 \hat{u}}{\partial \hat{x}\partial \hat{y}}+\hat{v}\frac{\partial^2 \hat{v}}{\partial \hat{x}\partial \hat{y}}\right.\right.$$
$$\left.\left.+\hat{v}\frac{\partial^2 \hat{u}}{\partial \hat{y}^2}-\frac{\partial \hat{v}}{\partial \hat{x}}\frac{\partial \hat{u}}{\partial \hat{x}}+\frac{\partial \hat{v}}{\partial \hat{y}}\frac{\partial \hat{v}}{\partial \hat{x}}+\frac{\partial \hat{u}}{\partial \hat{x}}\frac{\partial \hat{u}}{\partial \hat{y}}-\frac{\partial \hat{u}}{\partial \hat{y}}\frac{\partial \hat{v}}{\partial \hat{y}}\right)\right]$$
$$-\frac{1}{\rho}\left(\frac{c_F\rho\varphi}{\sqrt{K}}\right)u_o^2\hat{u}^2-\sigma B_o^2(u_o\hat{u}). \tag{4.13}$$

$\Rightarrow$

$$\frac{\partial \hat{u}}{\partial \hat{t}}+\hat{u}\frac{\partial \hat{u}}{\partial \hat{x}}+\hat{v}\frac{\partial \hat{u}}{\partial \hat{y}}=-\frac{L}{u_o^2\rho_{nf}}\frac{\partial}{\partial \hat{x}}\frac{\partial \hat{x}}{\partial x}(p)+\frac{1}{\rho}\left(\frac{Lu_o}{u_o^2L^2}\mu+\alpha_1\frac{\partial}{\partial \hat{t}}\frac{u_o^2}{L^3}\frac{L}{u_o^2}\right)\Big[2\frac{\partial^2 \hat{u}}{\partial \hat{x}^2}+$$
$$\frac{\partial^2 \hat{v}}{\partial \hat{x}\partial \hat{y}}+\frac{\partial^2 \hat{u}}{\partial \hat{y}^2}\Big]-\frac{1}{\rho}\left(\frac{L}{u_o^2}u_o\mu+\alpha_1\frac{\partial}{\partial \hat{t}}\frac{Lu_o^2}{Lu_o^2}\right)\frac{\varphi}{K}\hat{u}+\frac{1}{\rho}\alpha_1\frac{\partial}{\partial \hat{x}}\left[\frac{u_o^2}{L^3}\frac{L}{u_o^2}\left(2(\hat{u}\frac{\partial^2 \hat{u}}{\partial \hat{x}^2}\right.\right.$$
$$\left.+\hat{v}\frac{\partial^2 \hat{u}}{\partial \hat{x}\partial \hat{y}})+\frac{\partial^2 \hat{v}}{\partial \hat{x}^2}-\frac{\partial^2 \hat{u}}{\partial \hat{y}^2}\right)\Big]+\frac{1}{\rho}\alpha_1\frac{\partial}{\partial \hat{y}}\left[\frac{u_o^2}{L^3}\frac{L}{u_o^2}\left(\hat{u}\frac{\partial^2 \hat{v}}{\partial \hat{x}^2}+\hat{u}\frac{\partial^2 \hat{u}}{\partial \hat{x}\partial \hat{y}}+\hat{v}\frac{\partial^2 \hat{u}}{\partial \hat{y}^2}\right.\right.$$
$$\left.\left.+\hat{v}\frac{\partial^2 \hat{v}}{\partial \hat{x}\partial \hat{y}}-\frac{\partial \hat{v}}{\partial \hat{x}}\frac{\partial \hat{u}}{\partial \hat{x}}+\frac{\partial \hat{v}}{\partial \hat{y}}\frac{\partial \hat{v}}{\partial \hat{x}}+\frac{\partial \hat{u}}{\partial \hat{x}}\frac{\partial \hat{u}}{\partial \hat{y}}-\frac{\partial \hat{u}}{\partial \hat{y}}\frac{\partial \hat{v}}{\partial \hat{y}}\right)\right]$$
$$-\frac{L}{u_o^2\rho}\left(\frac{c_F\rho\varphi}{\sqrt{K}}\right)u_o^2\hat{u}^2-\frac{L}{u_o^2}\sigma B_o^2(u_o\hat{u}). \tag{4.14}$$

$\Rightarrow$

$$\frac{\partial \hat{u}}{\partial \hat{t}}+\hat{u}\frac{\partial \hat{u}}{\partial \hat{x}}+\hat{v}\frac{\partial \hat{u}}{\partial \hat{y}}=-L\frac{\partial}{\partial \hat{x}}\left(\frac{p}{\rho u_o^2}\right)+\frac{1}{\rho}\left(\frac{1}{Lu_o}\mu+\alpha_1\frac{\partial}{\partial \hat{t}}\frac{1}{L^2}\right)\left[2\frac{\partial^2 \hat{u}}{\partial \hat{x}^2}+\frac{\partial^2 \hat{v}}{\partial \hat{y}\partial \hat{x}}+\frac{\partial^2 \hat{u}}{\partial \hat{y}^2}\right]$$
$$-\frac{1}{\rho}\left(\frac{L}{u_o}\mu+\alpha_1\frac{\partial}{\partial \hat{t}}\right)\frac{\varphi}{K}\hat{u}+\frac{1}{\rho}\alpha_1\frac{\partial}{\partial \hat{x}}\left[\frac{1}{L^2}\Big(2(\hat{u}\frac{\partial^2 \hat{u}}{\partial \hat{x}^2}+\hat{v}\frac{\partial^2 \hat{u}}{\partial \hat{x}\partial \hat{y}})\right.$$
$$\left.+\frac{\partial^2 \hat{v}}{\partial \hat{x}^2}-\frac{\partial^2 \hat{u}}{\partial \hat{y}^2}\Big)\right]+\frac{1}{\rho}\alpha_1\frac{\partial}{\partial \hat{y}}\left[\frac{1}{L^2}\Big(\hat{u}\frac{\partial^2 \hat{v}}{\partial \hat{x}^2}+\hat{u}\frac{\partial^2 \hat{u}}{\partial \hat{x}\partial \hat{y}}+\hat{v}\frac{\partial^2 \hat{u}}{\partial \hat{y}^2}\right.$$
$$\left.+\hat{v}\frac{\partial^2 \hat{v}}{\partial \hat{x}\partial \hat{y}}-\frac{\partial \hat{v}}{\partial \hat{x}}\frac{\partial \hat{u}}{\partial \hat{x}}+\frac{\partial \hat{v}}{\partial \hat{y}}\frac{\partial \hat{v}}{\partial \hat{x}}+\frac{\partial \hat{u}}{\partial \hat{x}}\frac{\partial \hat{u}}{\partial \hat{y}}-\frac{\partial \hat{u}}{\partial \hat{y}}\frac{\partial \hat{v}}{\partial \hat{y}}\Big)\right]$$
$$-\frac{L}{\rho}\left(\frac{c_F\rho\varphi}{\sqrt{K}}\right)\hat{u}^2-L\frac{\sigma B_o^2}{u_o}\hat{u}. \tag{4.15}$$

$\Rightarrow$

$$\frac{\partial \hat{u}}{\partial \hat{t}} + \hat{u}\frac{\partial \hat{u}}{\partial \hat{x}} + \hat{v}\frac{\partial \hat{u}}{\partial \hat{y}} = -\frac{\partial P}{\partial \hat{x}} + \left(\frac{1}{Lu_o\rho}\mu + \frac{\alpha_1}{\rho}\frac{\partial}{\partial \hat{t}}\frac{1}{L^2}\right)\left[2\frac{\partial^2 \hat{u}}{\partial \hat{x}^2} + \left(\frac{\partial^2 \hat{v}}{\partial \hat{x}\partial \hat{y}} + \frac{\partial^2 \hat{u}}{\partial \hat{y}^2}\right)\right]$$
$$- \left(\frac{L}{u_o}\frac{\mu}{\rho} + \frac{\alpha_1}{\rho}\frac{\partial}{\partial \hat{t}}\right)\frac{\varphi}{K}\hat{u} + \frac{\alpha_1}{\rho}\frac{1}{L^2}\frac{\partial}{\partial \hat{x}}\left[2\left(\hat{u}\frac{\partial^2 \hat{u}}{\partial \hat{x}^2} + \hat{v}\frac{\partial^2 \hat{u}}{\partial \hat{x}\partial \hat{y}}\right)\right.$$
$$\left. + \frac{\partial^2 \hat{v}}{\partial \hat{x}^2} - \frac{\partial^2 \hat{u}}{\partial \hat{y}^2}\right] + \frac{\alpha_1}{\rho}\frac{1}{L^2}\frac{\partial}{\partial \hat{y}}\left[\hat{u}\frac{\partial^2 \hat{v}}{\partial \hat{x}^2} + \hat{u}\frac{\partial^2 \hat{u}}{\partial \hat{x}\partial \hat{y}} + \hat{v}\frac{\partial^2 \hat{u}}{\partial \hat{y}^2} - \frac{\partial \hat{v}}{\partial \hat{x}}\frac{\partial \hat{u}}{\partial \hat{x}}\right.$$
$$\left. + \frac{\partial \hat{v}}{\partial \hat{y}}\frac{\partial \hat{v}}{\partial \hat{x}} + \frac{\partial \hat{u}}{\partial \hat{x}}\frac{\partial \hat{u}}{\partial \hat{y}} - \frac{\partial \hat{u}}{\partial \hat{y}}\frac{\partial \hat{v}}{\partial \hat{y}} + \hat{v}\frac{\partial^2 \hat{v}}{\partial \hat{x}\partial \hat{y}}\right]$$
$$- L\frac{1}{\rho}\left(\frac{c_F\rho\varphi}{\sqrt{K}}\right)\hat{u}^2 - \frac{L}{u_o}\sigma B_o^2\hat{u}. \tag{4.16}$$

$\Rightarrow$

$$\frac{\partial \hat{u}}{\partial \hat{t}} + \hat{u}\frac{\partial \hat{u}}{\partial \hat{x}} + \hat{v}\frac{\partial \hat{u}}{\partial \hat{y}} = -\frac{\partial P}{\partial \hat{x}} + \left(\frac{1}{Lu_o\rho}\mu + \frac{\alpha_1}{\rho}\frac{1}{L^2}\frac{\partial}{\partial \hat{t}}\right)\left[2\frac{\partial^2 \hat{u}}{\partial \hat{x}^2} + \frac{\partial^2 \hat{v}}{\partial \hat{x}\partial \hat{y}} + \frac{\partial^2 \hat{u}}{\partial \hat{y}^2}\right]$$
$$+ \frac{\alpha_1}{\rho}\frac{1}{L^2}\frac{\partial}{\partial \hat{x}}\left[2\left(\hat{u}\frac{\partial^2 \hat{u}}{\partial \hat{x}^2} + \hat{v}\frac{\partial^2 \hat{u}}{\partial \hat{x}\partial \hat{y}}\right) + \frac{\partial^2 \hat{v}}{\partial \hat{x}^2} - \frac{\partial^2 \hat{u}}{\partial \hat{y}^2}\right]$$
$$+ \frac{\alpha_1}{\rho}\frac{1}{L^2}\frac{\partial}{\partial \hat{y}}\left[\hat{u}\frac{\partial^2 \hat{v}}{\partial \hat{x}^2} + \hat{u}\frac{\partial^2 \hat{u}}{\partial \hat{x}\partial \hat{y}} + \hat{v}\frac{\partial^2 \hat{v}}{\partial \hat{x}\partial \hat{y}} + \hat{v}\frac{\partial^2 \hat{u}}{\partial \hat{y}^2}\right.$$
$$\left. - \frac{\partial \hat{v}}{\partial \hat{x}}\frac{\partial \hat{u}}{\partial \hat{x}} + \frac{\partial \hat{v}}{\partial \hat{y}}\frac{\partial \hat{v}}{\partial \hat{x}} + \frac{\partial \hat{u}}{\partial \hat{x}}\frac{\partial \hat{u}}{\partial \hat{y}} - \frac{\partial \hat{u}}{\partial \hat{y}}\frac{\partial \hat{v}}{\partial \hat{y}}\right]$$
$$- L\frac{1}{\rho}\left(\frac{c_F\rho\varphi}{\sqrt{K}}\right)\hat{u}^2 - \frac{L}{u_o}\sigma B_o^2\hat{u}. \tag{4.17}$$

$\Rightarrow$

$$\frac{\partial \hat{u}}{\partial \hat{t}} + \hat{u}\frac{\partial \hat{u}}{\partial \hat{x}} + \hat{v}\frac{\partial \hat{u}}{\partial \hat{y}} = -\frac{\partial P}{\partial \hat{x}} + \left(\frac{1}{Lu_o\rho}\mu + \gamma\frac{\partial}{\partial \hat{t}}\right)\left(2\frac{\partial^2 \hat{u}}{\partial \hat{x}^2} + \frac{\partial^2 \hat{v}}{\partial \hat{x}\partial \hat{y}} + \frac{\partial^2 \hat{u}}{\partial \hat{y}^2}\right)$$
$$- \left[\left(\frac{L}{u_o}\frac{\mu}{\rho}\frac{1}{L^2} + \gamma\frac{\partial}{\partial \hat{t}}\right)\lambda + \frac{L}{u_o}\sigma B_o^2\right]\hat{u} - L\left(\frac{c_F\varphi}{\sqrt{K}}\right)\hat{u}^2$$
$$+ \gamma\frac{\partial}{\partial \hat{x}}\left[2\left(\hat{u}\frac{\partial^2 \hat{u}}{\partial \hat{x}^2} + \hat{v}\frac{\partial^2 \hat{u}}{\partial \hat{x}\partial \hat{y}}\right) + \frac{\partial^2 \hat{v}}{\partial \hat{x}^2} - \frac{\partial^2 \hat{u}}{\partial \hat{y}^2}\right]$$
$$+ \gamma\frac{\partial}{\partial \hat{y}}\left[\hat{u}\frac{\partial^2 \hat{v}}{\partial \hat{x}^2} + \hat{u}\frac{\partial^2 \hat{u}}{\partial \hat{x}\partial \hat{y}} + \hat{v}\frac{\partial^2 \hat{v}}{\partial \hat{x}\partial \hat{y}} + \hat{v}\frac{\partial^2 \hat{u}}{\partial \hat{y}^2} - \frac{\partial \hat{v}}{\partial \hat{x}}\frac{\partial \hat{u}}{\partial \hat{x}}\right.$$
$$\left. + \frac{\partial \hat{v}}{\partial \hat{y}}\frac{\partial \hat{v}}{\partial \hat{x}} + \frac{\partial \hat{u}}{\partial \hat{x}}\frac{\partial \hat{u}}{\partial \hat{y}} - \frac{\partial \hat{u}}{\partial \hat{y}}\frac{\partial \hat{v}}{\partial \hat{y}}\right]. \tag{4.18}$$

$\Rightarrow$

$$\frac{\partial \hat{u}}{\partial \hat{t}} + \hat{u}\frac{\partial \hat{u}}{\partial \hat{x}} + \hat{v}\frac{\partial \hat{u}}{\partial \hat{y}} = -\frac{\partial P}{\partial \hat{x}} + \left(\frac{1}{Lu_o\rho}\mu + \gamma\frac{\partial}{\partial \hat{t}}\right)\left(\left[2\frac{\partial^2 \hat{u}}{\partial \hat{x}^2} + \frac{\partial^2 \hat{v}}{\partial \hat{x}\partial \hat{y}}\right] + \left(\frac{\partial^2 \hat{u}}{\partial \hat{y}^2}\right)\right) - \left[\left(\frac{1}{u_o}\frac{\mu}{\rho}\frac{1}{L} + \gamma\frac{\partial}{\partial \hat{t}}\right)\lambda + Ha\right]\hat{u} + \gamma\frac{\partial}{\partial \hat{x}}\left(2(\hat{u}\frac{\partial^2 \hat{u}}{\partial \hat{x}^2} + \hat{v}\frac{\partial^2 \hat{u}}{\partial \hat{x}\partial \hat{y}}) + \frac{\partial^2 \hat{v}}{\partial x^2} - \frac{\partial^2 \hat{u}}{\partial y^2}\right) + \gamma\frac{\partial}{\partial \hat{y}}\left(\hat{u}\frac{\partial^2 \hat{v}}{\partial \hat{x}^2} + \hat{u}\frac{\partial^2 \hat{u}}{\partial \hat{x}\partial \hat{y}} + \hat{v}\frac{\partial^2 \hat{v}}{\partial \hat{x}\partial \hat{y}} + \hat{v}\frac{\partial^2 \hat{u}}{\partial \hat{y}^2} - \frac{\partial \hat{v}}{\partial \hat{x}}\frac{\partial \hat{u}}{\partial \hat{x}} + \frac{\partial \hat{v}}{\partial \hat{y}}\frac{\partial \hat{v}}{\partial \hat{x}} + \frac{\partial \hat{u}}{\partial \hat{x}}\frac{\partial \hat{u}}{\partial \hat{y}} - \frac{\partial \hat{u}}{\partial \hat{y}}\frac{\partial \hat{v}}{\partial \hat{y}}\right) - F_r\hat{u}^2. \tag{4.19}$$

Equation (4.2) becomes:

$$\frac{\partial v}{\partial t} + u\frac{\partial v}{\partial x} + v\frac{\partial v}{\partial y} = \frac{1}{\rho}\left[-\frac{\partial p}{\partial y} + \left(\mu + \alpha_1\frac{\partial}{\partial t}\right)\left\{2\frac{\partial^2 v}{\partial y^2} + \left(\frac{\partial^2 u}{\partial x\partial y} + \frac{\partial^2 v}{\partial x^2}\right) - \frac{\varphi}{K}u\right\}\right] + \alpha_1\frac{\partial}{\partial y}\left[2\left(u\frac{\partial^2 v}{\partial x\partial y} + v\frac{\partial^2 v}{\partial y^2}\right) + (4)\left(\frac{\partial v}{\partial y}\right)^2 + \left(\frac{\partial u}{\partial y}\right)^2 - 4\frac{\partial^2 v}{\partial y^2} - \left(\frac{\partial v}{\partial x}\right)^2\right] + \alpha_1\frac{\partial}{\partial x}\left[u\frac{\partial^2 u}{\partial x\partial y} + u\frac{\partial^2 v}{\partial x^2} + v\frac{\partial^2 u}{\partial y^2} + v\frac{\partial^2 v}{\partial y\partial x} + \frac{\partial u}{\partial x}\frac{\partial u}{\partial y} - \frac{\partial u}{\partial y}\frac{\partial v}{\partial y} - \frac{\partial v}{\partial x}\frac{\partial u}{\partial x} + \frac{\partial v}{\partial y}\frac{\partial v}{\partial x}\right] - \left(\frac{c_F\rho\varphi}{\sqrt{K}}\right)v^2 - \sigma B_0^2 v + \rho g_y(\beta_\theta)(\theta - \theta_0). \tag{4.20}$$

$\Rightarrow$

$$\frac{u_o^2}{L}\frac{\partial \hat{u}}{\partial \hat{t}} + \frac{u_o^2}{L}\hat{u}\frac{\partial \hat{u}}{\partial \hat{x}} + \frac{u_o^2}{L}\hat{v}\frac{\partial \hat{u}}{\partial \hat{y}} = \frac{1}{\rho}\left[-\frac{\partial p}{\partial y} + \left(\mu + \alpha_1\frac{\partial}{\partial \hat{t}}\frac{\partial \hat{t}}{\partial t}\right)\left\{2\frac{u_o}{L^2}\frac{\partial^2 \hat{v}}{\partial \hat{y}^2} + \frac{u_o}{L^2}\left(\frac{\partial^2 \hat{u}}{\partial \hat{x}\partial \hat{y}} + \frac{\partial^2 \hat{v}}{\partial \hat{x}^2}\right) - \frac{\varphi}{K}u_o\hat{v}\right\}\right] + \alpha_1\frac{\partial}{\partial \hat{y}}\frac{\partial \hat{y}}{\partial y}\left[2\frac{u_o^2}{L^2}\left(\hat{u}\frac{\partial^2 \hat{v}}{\partial \hat{x}\partial \hat{y}} + \hat{v}\frac{\partial^2 \hat{v}}{\partial \hat{y}^2}\right) + \frac{u_o^2}{L^2}\left(\frac{\partial \hat{u}}{\partial \hat{y}}\right)^2 + 4\frac{u_o^2}{L^2}\left(\frac{\partial \hat{v}}{\partial \hat{y}}\right)^2 - 4\frac{u_o^2}{L^2}\frac{\partial^2 \hat{v}}{\partial \hat{y}^2} - \frac{u_o^2}{L^2}\left(\frac{\partial \hat{v}}{\partial \hat{x}}\right)^2\right] + \alpha_1\frac{\partial}{\partial \hat{x}}\frac{\partial \hat{x}}{\partial x}\left[\frac{u_o^2}{L^2}\hat{u}\frac{\partial^2 \hat{u}}{\partial \hat{x}\partial \hat{y}} + \frac{u_o^2}{L^2}\hat{v}\frac{\partial^2 \hat{u}}{\partial \hat{y}^2} + \frac{u_o^2}{L^2}\hat{u}\frac{\partial^2 \hat{v}}{\partial \hat{x}^2} + \frac{u_o^2}{L^2}\hat{v}\frac{\partial^2 \hat{v}}{\partial \hat{y}\partial \hat{x}} + \frac{u_o^2}{L^2}\frac{\partial \hat{u}}{\partial \hat{x}}\frac{\partial \hat{u}}{\partial \hat{y}} - \frac{u_o^2}{L^2}\frac{\partial \hat{u}}{\partial \hat{y}}\frac{\partial \hat{v}}{\partial \hat{y}} - \frac{u_o^2}{L^2}\frac{\partial \hat{v}}{\partial \hat{x}}\frac{\partial \hat{u}}{\partial \hat{x}} - \frac{u_o^2}{L^2}\frac{\partial \hat{v}}{\partial \hat{y}}\frac{\partial \hat{v}}{\partial \hat{x}}\right] - \left(\frac{c_F\rho\varphi}{\sqrt{K}}\right)(u_o\hat{v})^2 - \sigma B_o^2(u_o\hat{v}) + \rho g_y(\beta_\theta)(\theta_0 + \theta_0\hat{\theta} - \theta_0). \tag{4.21}$$

$$\Rightarrow$$

$$\frac{u_o^2}{L}\frac{\partial \hat{v}}{\partial \hat{t}} + \frac{u_o^2}{L}\hat{u}\frac{\partial \hat{v}}{\partial \hat{x}} + \frac{u_o^2}{L}\hat{v}\frac{\partial \hat{v}}{\partial \hat{y}} = \frac{1}{\rho}\Bigg[- \frac{\partial p}{\partial y} + \left(\mu + \alpha_1 \frac{\partial}{\partial \hat{t}}\frac{u_o}{L}\right)\Bigg\{2\frac{u_o}{L^2}\frac{\partial^2 \hat{v}}{\partial \hat{y}^2} + \frac{u_o}{L^2}\frac{\partial^2 \hat{u}}{\partial \hat{x}\partial \hat{y}}$$
$$+ \frac{u_o}{L^2}\frac{\partial^2 \hat{v}}{\partial \hat{x}^2} - \left(\mu + \alpha_1 \frac{\partial}{\partial \hat{t}}\frac{u_o}{L}\right)\frac{\varphi}{K}u_o\hat{v}\Bigg\}\Bigg] + \alpha_1 \frac{\partial}{\partial \hat{y}}\frac{1}{L}\Bigg[2\frac{u_o^2}{L^2}\hat{u}\frac{\partial^2 \hat{v}}{\partial \hat{x}\partial \hat{y}} + 2\frac{u_o^2}{L^2}\hat{v}\frac{\partial^2 \hat{v}}{\partial \hat{y^2}}$$
$$+ \frac{u_o^2}{L^2}\left(\frac{\partial \hat{u}}{\partial \hat{y}}\right)^2 + 4\frac{u_o^2}{L^2}\left(\frac{\partial \hat{v}}{\partial \hat{y}}\right)^2 - 4\frac{u_o}{L^2}\frac{\partial^2 \hat{v}}{\partial \hat{y}^2} - \frac{u_o^2}{L^2}\left(\frac{\partial \hat{v}}{\partial \hat{x}}\right)^2\Bigg] + \left(\alpha_1 \frac{\partial}{\partial \hat{x}}\frac{1}{L}\right)$$
$$\Bigg(\Bigg[\frac{u_o^2}{L^2}\hat{u}\frac{\partial^2 \hat{u}}{\partial \hat{x}\partial \hat{y}} + \frac{u_o^2}{L^2}\hat{u}\frac{\partial^2 \hat{v}}{\partial \hat{x^2}} + \frac{u_o^2}{L^2}\hat{v}\frac{\partial^2 \hat{v}}{\partial \hat{y}\partial \hat{x}} + \frac{u_o^2}{L^2}\hat{v}\frac{\partial^2 \hat{u}}{\partial \hat{y}^2}$$
$$+ \frac{u_o^2}{L^2}\frac{\partial \hat{u}}{\partial \hat{x}}\frac{\partial \hat{u}}{\partial \hat{y}} - \frac{u_o^2}{L^2}\frac{\partial \hat{u}}{\partial \hat{y}}\frac{\partial \hat{v}}{\partial \hat{y}} - \frac{u_o^2}{L^2}\frac{\partial \hat{v}}{\partial \hat{x}}\frac{\partial \hat{u}}{\partial \hat{x}} + \frac{u_o^2}{L^2}\frac{\partial \hat{v}}{\partial \hat{y}}\frac{\partial \hat{v}}{\partial \hat{x}}\Bigg]\Bigg)$$
$$- \left(\frac{c_F \rho \varphi}{\sqrt{K}}\right)(u_o\hat{v})^2 - \sigma B_o^2(u_o\hat{v}) + \rho g_y(\beta_\theta)(\theta_0\hat{\theta}). \tag{4.22}$$

$$\Rightarrow$$

$$\frac{u_o^2}{L}\left[\frac{\partial \hat{v}}{\partial \hat{t}} + \hat{u}\frac{\partial \hat{v}}{\partial \hat{x}} + \hat{v}\frac{\partial \hat{v}}{\partial \hat{y}}\right] = -\frac{1}{\rho}\frac{\partial p}{\partial \hat{y}} + \frac{1}{\rho}\left(\mu + \alpha_1 \frac{\partial}{\partial \hat{t}}\frac{u_o}{L}\right)\frac{u_0}{L^2}\left[2\frac{\partial^2 \hat{v}}{\partial \hat{y}^2} + \frac{\partial^2 \hat{u}}{\partial \hat{x}\partial \hat{y}} + \frac{\partial^2 \hat{v}}{\partial \hat{x}^2}\right]$$
$$- \frac{1}{\rho}\left(\mu + \alpha_1 \frac{\partial}{\partial \hat{t}}\frac{u_o}{L}\right)\frac{\varphi}{K}\hat{u}u_0 + \frac{\alpha_1 u_0^2}{\rho L^3}\frac{\partial}{\partial \hat{y}}\left[2\hat{u}\frac{\partial^2 \hat{v}}{\partial \hat{x}\partial \hat{y}} + 2\hat{v}\frac{\partial^2 \hat{v}}{\partial \hat{y}^2}\right.$$
$$\left. + \left(\frac{\partial \hat{u}}{\partial \hat{y}}\right)^2 + 4\left(\frac{\partial \hat{v}}{\partial \hat{y}}\right)^2 - \frac{4}{u_0}\frac{\partial^2 \hat{v}}{\partial \hat{y}^2} + \left(\frac{\partial \hat{v}}{\partial \hat{x}}\right)^2\right]$$
$$+ \frac{\alpha_1 u_0^2}{\rho L^3}\frac{\partial}{\partial \hat{x}}\left[\hat{u}\frac{\partial^2 \hat{v}}{\partial \hat{x}^2} + \hat{u}\frac{\partial^2 \hat{u}}{\partial \hat{x}\partial \hat{y}} + \hat{v}\frac{\partial^2 \hat{v}}{\partial \hat{x}\partial \hat{y}} + \hat{v}\frac{\partial^2 \hat{u}}{\partial \hat{y}^2}\right.$$
$$\left. + \frac{\partial \hat{u}}{\partial \hat{x}}\frac{\partial \hat{u}}{\partial \hat{y}} - \frac{\partial \hat{u}}{\partial \hat{y}}\frac{\partial \hat{v}}{\partial \hat{y}} - \frac{\partial \hat{v}}{\partial \hat{x}}\frac{\partial \hat{u}}{\partial \hat{x}} + \frac{\partial \hat{v}}{\partial \hat{y}}\frac{\partial \hat{v}}{\partial \hat{x}}\right]$$
$$- \frac{c_F \varphi}{\sqrt{K}}u_o^2\hat{u}^2 - \sigma B_o^2(u_o\hat{v}) + \rho g_y \beta_\theta \theta_0 \hat{\theta}. \tag{4.23}$$

$$\Rightarrow$$

$$\frac{{u_0}^2}{L}\left[\frac{\partial \hat{v}}{\partial \hat{t}} + \hat{u}\frac{\partial \hat{v}}{\partial \hat{x}} + \hat{v}\frac{\partial \hat{v}}{\partial \hat{y}}\right] = -\frac{1}{\rho}\frac{\partial p}{\partial y} + \frac{1}{\rho}\left(\frac{u_o}{L^2}\mu + \alpha_1 \frac{\partial}{\partial \hat{t}}\frac{u_o^2}{L^3}\right)\left[2\frac{\partial^2 \hat{v}}{\partial \hat{y}^2} + \frac{\partial^2 \hat{u}}{\partial \hat{x}\partial \hat{y}} + \frac{\partial^2 \hat{v}}{\partial \hat{x}^2}\right]$$
$$+ \frac{1}{\rho}\alpha_1 \frac{\partial}{\partial \hat{y}}\left[\frac{u_o^2}{L^3}\left(2\left(\hat{v}\frac{\partial^2 \hat{v}}{\partial \hat{y}^2} + \hat{u}\frac{\partial^2 \hat{v}}{\partial \hat{x}\partial \hat{y}}\right) + \left(\frac{\partial \hat{u}}{\partial \hat{y}}\right)^2 + 4\left(\frac{\partial \hat{v}}{\partial \hat{y}}\right)^2\right.\right.$$
$$\left.\left. - 4\frac{1}{u_0}\frac{\partial^2 \hat{v}}{\partial \hat{y}^2} - \left(\frac{\partial \hat{v}}{\partial \hat{x}}\right)^2\right)\Bigg] - \frac{1}{\rho}\left(u_o\mu + \alpha_1 \frac{\partial}{\partial \hat{t}}\frac{u_o^2}{L}\right)\frac{\varphi}{K}\hat{v}$$
$$+ \frac{1}{\rho}\alpha_1 \frac{\partial}{\partial \hat{x}}\left[\frac{u_o^2}{L^3}\left(\hat{u}\frac{\partial^2 \hat{v}}{\partial \hat{x}^2} + \hat{u}\frac{\partial^2 \hat{u}}{\partial \hat{x}\partial \hat{y}} + \hat{v}\frac{\partial^2 \hat{u}}{\partial \hat{y}^2} + \hat{v}\frac{\partial^2 \hat{v}}{\partial \hat{x}\partial \hat{y}} + \frac{\partial \hat{u}}{\partial \hat{x}}\frac{\partial \hat{u}}{\partial \hat{y}} - \frac{\partial \hat{u}}{\partial \hat{y}}\frac{\partial \hat{v}}{\partial \hat{y}}\right.\right.$$
$$\left.\left. - \frac{\partial \hat{v}}{\partial \hat{x}}\frac{\partial \hat{u}}{\partial \hat{x}} + \frac{\partial \hat{v}}{\partial \hat{y}}\frac{\partial \hat{v}}{\partial \hat{x}}\right)\Bigg] - \frac{1}{\rho}\left(\frac{c_F \rho \varphi}{\sqrt{K}}\right)u_o^2\hat{v}^2 - \sigma B_o^2(u_o\hat{v}) + \rho g_y(\beta_\theta)(\theta_0\hat{\theta}).$$

(4.24)

$$\Rightarrow$$

$$\begin{aligned}\frac{\partial \hat{v}}{\partial \hat{t}} + \hat{u}\frac{\partial \hat{v}}{\partial \hat{x}} + \hat{v}\frac{\partial \hat{v}}{\partial \hat{y}} &= -\frac{L}{u_0^2}\frac{1}{\rho}\frac{\partial}{\partial \hat{y}}\left(\frac{\partial \hat{y}}{\partial y}p\right) + \frac{1}{\rho}\left(\frac{1}{Lu_o}\mu + \alpha_1\frac{\partial}{\partial \hat{t}}\frac{1}{L^2}\right)\left[2\frac{\partial^2 \hat{v}}{\partial \hat{y}^2}\right.\\ &\left. + \frac{\partial^2 \hat{u}}{\partial \hat{y}\partial \hat{x}} + \frac{\partial^2 \hat{v}}{\partial \hat{x}^2}\right] - \frac{1}{\rho}\left(\frac{L}{u_o}\mu + \alpha_1\frac{\partial}{\partial \hat{t}}\right)\frac{\varphi}{K}\hat{v} + \frac{1}{\rho}\alpha_1\frac{\partial}{\partial \hat{y}}\left[\frac{1}{L^2}\Big(2\hat{v}\frac{\partial^2 \hat{v}}{\partial \hat{y}^2} + 2\hat{u}\frac{\partial^2 \hat{v}}{\partial \hat{x}\partial \hat{y}}\right.\\ &+ \left(\frac{\partial \hat{u}}{\partial \hat{y}}\right)^2 + 4\left(\frac{\partial \hat{v}}{\partial \hat{y}}\right)^2 - 4\frac{1}{u_0}\frac{\partial^2 \hat{v}}{\partial \hat{y}^2} - \left(\frac{\partial \hat{v}}{\partial \hat{x}}\right)^2\Big)\Big] + \frac{1}{\rho}\alpha_1\frac{\partial}{\partial \hat{x}}\left[\frac{1}{L^2}\Big(\hat{u}\frac{\partial^2 \hat{v}}{\partial \hat{x}^2} + \hat{u}\frac{\partial^2 \hat{u}}{\partial \hat{x}\partial \hat{y}}\right.\\ &\left. + \hat{v}\frac{\partial^2 \hat{u}}{\partial \hat{y}^2} + \hat{v}\frac{\partial^2 \hat{v}}{\partial \hat{x}\partial \hat{y}} - \frac{\partial \hat{v}}{\partial \hat{x}}\frac{\partial \hat{u}}{\partial \hat{x}} + \frac{\partial \hat{v}}{\partial \hat{y}}\frac{\partial \hat{v}}{\partial \hat{x}} + \frac{\partial \hat{u}}{\partial \hat{x}}\frac{\partial \hat{u}}{\partial \hat{y}} - \frac{\partial \hat{u}}{\partial \hat{y}}\frac{\partial \hat{v}}{\partial \hat{y}}\Big)\right]\\ &- \frac{L}{\rho u_0^2}\left(\frac{c_F\rho\varphi}{\sqrt{K}}\right)\hat{u}^2\hat{v}^2 - L\frac{\sigma B_o^2}{u_o}\hat{v} + \frac{L}{u_o^2}\rho g_y\beta_\theta\theta_0\hat{\theta}. \end{aligned} \tag{4.25}$$

$$\Rightarrow$$

$$\begin{aligned}\frac{\partial \hat{v}}{\partial \hat{t}} + \hat{u}\frac{\partial \hat{v}}{\partial \hat{x}} + \hat{v}\frac{\partial \hat{v}}{\partial \hat{y}} &= -L\frac{\partial}{\partial \hat{y}}\frac{1}{L}\left(\frac{P}{\rho u_o^2}\right) + \left(\frac{1}{Lu_o\rho}\mu + \frac{\alpha_1}{\rho}\frac{\partial}{\partial \hat{t}}\frac{1}{L^2}\right)\left[2\frac{\partial^2 \hat{v}}{\partial \hat{y}^2} + \left(\frac{\partial^2 \hat{u}}{\partial \hat{x}\partial \hat{y}}\right.\right.\\ &\left.\left. + \frac{\partial^2 \hat{v}}{\partial \hat{x}^2}\right) - \left(\frac{L}{u_o}\frac{\mu}{\rho} + \frac{\alpha_1}{\rho}\frac{\partial}{\partial \hat{t}}\right)\frac{\varphi}{K}\hat{u} + \frac{\alpha_1}{\rho}\frac{1}{L^2}\frac{\partial}{\partial \hat{y}}\left[2\left(\hat{v}\frac{\partial^2 \hat{u}}{\partial \hat{y}^2} + \hat{u}\frac{\partial^2 \hat{v}}{\partial \hat{x}\partial \hat{y}}\right)\right]\\ &+ \frac{\alpha_1}{\rho}\frac{1}{L^2}\left[\left(\frac{\partial \hat{u}}{\partial \hat{y}}\right)^2 + 4\left(\frac{\partial \hat{v}}{\partial \hat{y}}\right)^2 - \frac{4}{u_0}\frac{\partial^2 \hat{v}}{\partial \hat{y}^2} - \left(\frac{\partial \hat{v}}{\partial \hat{x}}\right)^2\right]\\ &+ \frac{\alpha_1}{\rho}\frac{1}{L^2}\frac{\partial}{\partial \hat{x}}\left(\hat{u}\frac{\partial^2 \hat{v}}{\partial \hat{x}^2} + \hat{u}\frac{\partial^2 \hat{u}}{\partial \hat{x}\partial \hat{y}} + \hat{v}\frac{\partial^2 \hat{u}}{\partial \hat{y}^2}\right)\\ &- \frac{\alpha_1}{\rho}\frac{1}{L^2}\frac{\partial}{\partial \hat{x}}\left(\frac{\partial \hat{v}}{\partial \hat{x}}\frac{\partial \hat{u}}{\partial \hat{x}} + \frac{\partial \hat{v}}{\partial \hat{y}}\frac{\partial \hat{v}}{\partial \hat{x}} + \frac{\partial \hat{u}}{\partial \hat{x}}\frac{\partial \hat{u}}{\partial \hat{y}} - \frac{\partial \hat{u}}{\partial \hat{y}}\frac{\partial \hat{v}}{\partial \hat{y}} + \hat{v}\frac{\partial^2 \hat{v}}{\partial \hat{x}\partial \hat{y}}\right)\\ &- L\frac{1}{\rho}\left(\frac{c_F\rho\varphi}{\sqrt{K}}\right)\hat{v}^2 - \frac{L}{u_o}\sigma B_o^2\hat{v} + \frac{\frac{L^3\rho g_y(\beta_\theta)\theta_0}{\nu^2}}{\frac{u_0^2L^2}{\nu^2}}\hat{\theta}. \end{aligned} \tag{4.26}$$

$$\Rightarrow$$

$$\begin{aligned}\frac{\partial \hat{v}}{\partial \hat{t}} + \hat{u}\frac{\partial \hat{v}}{\partial \hat{x}} + \hat{v}\frac{\partial \hat{v}}{\partial \hat{y}} &= -\frac{\partial P}{\partial \hat{y}} + \left(\frac{1}{Lu_o\rho}\mu + \frac{\alpha_1}{\rho}\frac{\partial}{\partial \hat{t}}\frac{1}{L^2}\right)\left(2\frac{\partial^2 \hat{v}}{\partial \hat{y}^2} + \frac{\partial^2 \hat{u}}{\partial \hat{x}\partial \hat{y}} + \frac{\partial^2 \hat{v}}{\partial \hat{x}^2}\right)\\ &- \left(\frac{L}{u_o}\frac{\mu}{\rho} + \frac{\alpha_1}{\rho}\frac{\partial}{\partial \hat{t}}\right)\frac{\varphi}{K}\hat{v} + \frac{\alpha_1}{\rho}\frac{1}{L^2}\frac{\partial}{\partial \hat{y}}\left(2\hat{v}\frac{\partial^2 \hat{v}}{\partial \hat{y}^2} + 2\hat{u}\frac{\partial^2 \hat{v}}{\partial \hat{x}\partial \hat{y}}\right.\\ &\left. + \left(\frac{\partial \hat{u}}{\partial y}\right)^2 + 4\left(\frac{\partial \hat{v}}{\partial y}\right)^2 - \frac{4}{u_0}\frac{\partial^2 \hat{v}}{\partial y^2} + \left(\frac{\partial \hat{v}}{\partial x}\right)^2\right)\\ &+ \frac{\alpha_1}{\rho}\frac{1}{L^2}\frac{\partial}{\partial \hat{x}}\left(\hat{u}\frac{\partial^2 \hat{v}}{\partial \hat{x}^2} + \hat{u}\frac{\partial^2 \hat{u}}{\partial \hat{x}\partial \hat{y}} + \hat{v}\frac{\partial^2 \hat{v}}{\partial \hat{x}\partial \hat{y}} + \hat{v}\frac{\partial^2 \hat{u}}{\partial \hat{y}^2}\right.\\ &\left. - \frac{\partial \hat{v}}{\partial \hat{x}}\frac{\partial \hat{u}}{\partial \hat{x}} + \frac{\partial \hat{v}}{\partial \hat{y}}\frac{\partial \hat{v}}{\partial \hat{x}} + \frac{\partial \hat{u}}{\partial \hat{x}}\frac{\partial \hat{u}}{\partial \hat{y}} - \frac{\partial \hat{u}}{\partial \hat{y}}\frac{\partial \hat{v}}{\partial \hat{y}}\right) - L\frac{1}{\rho}\left(\frac{c_F\rho\varphi}{\sqrt{K}}\right)\hat{v}^2\\ &- \frac{L}{u_o}\sigma B_o^2\hat{v} + \frac{G_r}{Re^2}\hat{\theta}. \end{aligned} \tag{4.27}$$

$$\Rightarrow$$

$$\begin{aligned}\frac{\partial \hat{v}}{\partial \hat{t}}+\hat{u}\frac{\partial \hat{v}}{\partial \hat{x}}+\hat{v}\frac{\partial \hat{v}}{\partial \hat{y}} &= -\frac{\partial P}{\partial \hat{y}}+\left(\frac{1}{Lu_o\rho}\mu+\frac{\alpha}{\rho}\frac{\partial}{\partial \hat{t}}\frac{1}{L^2}\right)\left(2\frac{\partial^2 \hat{v}}{\partial \hat{y}^2}+\frac{\partial^2 \hat{u}}{\partial \hat{x}\partial \hat{y}}+\frac{\partial^2 \hat{v}}{\partial \hat{x}^2}\right)\\ &-\left(\frac{L}{u_o}\frac{\mu}{\rho}\frac{1}{L^2}+\frac{\alpha}{\rho}\frac{\partial}{\partial \hat{t}}\frac{1}{L^2}\right)L^2\left(\frac{\varphi}{k}\right)\hat{v}-\frac{L}{u_o}\sigma B_o^2\hat{v}\\ &+\frac{\alpha_1}{\rho L^2}\frac{\partial}{\partial \hat{y}}\left(2\hat{v}\frac{\partial^2 \hat{v}}{\partial \hat{y}^2}+2\hat{u}\frac{\partial^2 \hat{v}}{\partial \hat{x}\partial \hat{y}}+\left(\frac{\partial \hat{u}}{\partial y}\right)^2+4\left(\frac{\partial \hat{v}}{\partial y}\right)^2\right)\\ &-\frac{\alpha_1}{\rho L^2}\frac{\partial}{\partial \hat{y}}\left(\frac{4}{u_0}\frac{\partial^2 \hat{v}}{\partial y^2}+\left(\frac{\partial \hat{v}}{\partial x}\right)^2\right)+\frac{\alpha_1}{\rho L^2}\frac{\partial}{\partial \hat{x}}\left(\hat{u}\frac{\partial^2 \hat{v}}{\partial \hat{x}^2}\right.\\ &+\hat{u}\frac{\partial^2 \hat{u}}{\partial \hat{x}\partial \hat{y}}+\hat{v}\frac{\partial^2 \hat{v}}{\partial \hat{x}\partial \hat{y}}+\hat{v}\frac{\partial^2 \hat{u}}{\partial \hat{y}^2}-\frac{\partial \hat{v}}{\partial \hat{x}}\frac{\partial \hat{u}}{\partial \hat{x}}+\frac{\partial \hat{v}}{\partial \hat{y}}\frac{\partial \hat{v}}{\partial \hat{x}}\\ &\left.+\frac{\partial \hat{u}}{\partial \hat{x}}\frac{\partial \hat{u}}{\partial \hat{y}}-\frac{\partial \hat{u}}{\partial \hat{y}}\frac{\partial \hat{v}}{\partial \hat{y}}\right)-L\left(\frac{c_F\varphi}{\sqrt{K}}\right)\hat{v}^2+\frac{G_r}{Re^2}\hat{\theta}. \end{aligned} \tag{4.28}$$

$$\Rightarrow$$

$$\begin{aligned}\frac{\partial \hat{v}}{\partial \hat{t}}+\hat{u}\frac{\partial \hat{v}}{\partial \hat{x}}+\hat{v}\frac{\partial \hat{v}}{\partial \hat{y}} &= -\frac{\partial P}{\partial \hat{y}}+\left(\frac{1}{Re}+\gamma\frac{\partial}{\partial \hat{t}}\right)\left[2\frac{\partial^2 \hat{v}}{\partial \hat{y}^2}+\frac{\partial^2 \hat{u}}{\partial \hat{x}\partial \hat{y}}+\frac{\partial^2 \hat{v}}{\partial \hat{x}^2}\right]\\ &-\left[\left(\frac{1}{Re}+\gamma\frac{\partial}{\partial \hat{t}}\right)\lambda+Ha\right]\hat{v}\\ &+\gamma\frac{\partial}{\partial \hat{y}}\left(2\left(\hat{v}\frac{\partial^2 \hat{v}}{\partial \hat{y}^2}+\hat{u}\frac{\partial^2 \hat{v}}{\partial \hat{x}\partial \hat{y}}\right)+\left(\frac{\partial \hat{u}}{\partial y}\right)^2+4\left(\frac{\partial \hat{v}}{\partial y}\right)^2-\frac{4}{u_0}\frac{\partial^2 \hat{v}}{\partial y^2}\right.\\ &\left.-(\frac{\partial \hat{v}}{\partial x})^2\right)+\gamma\frac{\partial}{\partial \hat{x}}\left(\hat{u}\frac{\partial^2 \hat{v}}{\partial \hat{x}^2}+\hat{u}\frac{\partial^2 \hat{u}}{\partial \hat{x}\partial \hat{y}}+\hat{v}\frac{\partial^2 \hat{v}}{\partial \hat{x}\partial \hat{y}}+\hat{v}\frac{\partial^2 \hat{u}}{\partial \hat{y}^2}-\frac{\partial \hat{v}}{\partial \hat{x}}\frac{\partial \hat{u}}{\partial \hat{x}}\right.\\ &\left.+\frac{\partial \hat{v}}{\partial \hat{y}}\frac{\partial \hat{v}}{\partial \hat{x}}+\frac{\partial \hat{u}}{\partial \hat{x}}\frac{\partial \hat{u}}{\partial \hat{y}}-\frac{\partial \hat{u}}{\partial \hat{y}}\frac{\partial \hat{v}}{\partial \hat{y}}\right)\\ &-F_r\hat{u}^2+\frac{G_r}{Re^2}\hat{\theta}. \end{aligned} \tag{4.29}$$

Now Equation (4.3) becomes:

$$\frac{\partial \theta}{\partial t}+u\frac{\partial \theta}{\partial x}+v\frac{\partial \theta}{\partial y}=\frac{k}{\rho C_p}\left(\frac{\partial^2 \theta}{\partial x^2}+\frac{\partial^2 \theta}{\partial y^2}\right), \tag{4.30}$$

$$\Rightarrow \frac{u_0}{L}\theta_0\frac{\partial \hat{\theta}}{\partial \hat{t}}+u_0\hat{u}\frac{\theta_0}{L}\frac{\partial \hat{\theta}}{\partial \hat{x}}+u_0\hat{v}\frac{\theta_0}{L}\frac{\partial \hat{\theta}}{\partial \hat{y}}=\frac{k}{\rho C_p}\left(\frac{\theta_0}{L^2}\frac{\partial^2 \hat{\theta}}{\partial \hat{x}^2}+\frac{\theta_0}{L^2}\frac{\partial^2 \hat{\theta}}{\partial \hat{y}^2}\right), \tag{4.31}$$

$$\Rightarrow \frac{u_0}{L}\theta_0\left(\frac{\partial \hat{\theta}}{\partial t}+\hat{u}\frac{\partial \hat{\theta}}{\partial \hat{x}}+\hat{v}\frac{\partial \hat{\theta}}{\partial \hat{y}}\right)=\frac{\theta_0}{L^2}\frac{k}{\rho C_p}\left(\frac{\partial^2 \hat{\theta}}{\partial \hat{x}^2}+\frac{\partial^2 \hat{\theta}}{\partial \hat{y}^2}\right), \tag{4.32}$$

$$\Rightarrow u_0\left(\frac{\partial \hat{\theta}}{\partial t}+\hat{u}\frac{\partial \hat{\theta}}{\partial \hat{x}}+\hat{v}\frac{\partial \hat{\theta}}{\partial \hat{y}}\right)=\frac{1}{L}\frac{k}{\rho C_p}\left(\frac{\partial^2 \hat{\theta}}{\partial \hat{x}^2}+\frac{\partial^2 \hat{\theta}}{\partial \hat{y}^2}\right), \tag{4.33}$$

$$\Rightarrow \left(\frac{\partial \hat{\theta}}{\partial t} + \hat{u}\frac{\partial \hat{\theta}}{\partial \hat{x}} + \hat{v}\frac{\partial \hat{\theta}}{\partial \hat{y}}\right) = \frac{\mu}{Lu_0\rho}\frac{k}{\mu C_p}\left(\frac{\partial^2 \hat{\theta}}{\partial \hat{x}^2} + \frac{\partial^2 \hat{\theta}}{\partial \hat{y}^2}\right), \tag{4.34}$$

$$\Rightarrow \left(\frac{\partial \hat{\theta}}{\partial t} + \hat{u}\frac{\partial \hat{\theta}}{\partial \hat{x}} + \hat{v}\frac{\partial \hat{\theta}}{\partial \hat{y}}\right) = \frac{1}{RePr}\left(\frac{\partial^2 \hat{\theta}}{\partial \hat{x}^2} + \frac{\partial^2 \hat{\theta}}{\partial \hat{y}^2}\right). \tag{4.35}$$

For convenience, we can ignore the hats on the variables, and after some simple manipulations, we arrive at:

$$\begin{aligned}\frac{\partial u}{\partial t} + u\frac{\partial u}{\partial x} + v\frac{\partial u}{\partial y} &= -\frac{\partial P}{\partial x} + \left(\frac{1}{\mathrm{Re}} + \gamma\frac{\partial}{\partial t}\right)\left[2\frac{\partial^2 u}{\partial x^2} + \left(\frac{\partial^2 v}{\partial x \partial y} + \frac{\partial^2 u}{\partial y^2}\right)\right] \\ &- \left[\left(\frac{1}{Re} + \gamma\frac{\partial}{\partial t}\right)\lambda + Ha\right]u + \gamma\frac{\partial}{\partial x}\left[2\left(u\frac{\partial^2 u}{\partial x^2} + v\frac{\partial^2 u}{\partial x \partial y}\right) + \frac{\partial^2 v}{\partial x^2} - \frac{\partial^2 u}{\partial y^2}\right] \\ &+ \gamma\frac{\partial}{\partial y}\left[\left(u\frac{\partial^2 v}{\partial x^2} + u\frac{\partial^2 u}{\partial x \partial y} + v\frac{\partial^2 v}{\partial x \partial y} + v\frac{\partial^2 u}{\partial y^2} - \frac{\partial v}{\partial x}\frac{\partial u}{\partial x} + \frac{\partial v}{\partial y}\frac{\partial v}{\partial x}\right.\right. \\ &\left.\left. + \frac{\partial u}{\partial x}\frac{\partial u}{\partial y} - \frac{\partial u}{\partial y}\frac{\partial v}{\partial y}\right)\right] - Fru^2.\end{aligned} \tag{4.36}$$

$$\begin{aligned}\frac{\partial v}{\partial t} + u\frac{\partial v}{\partial x} + v\frac{\partial v}{\partial y} &= -\frac{\partial P}{\partial y} + \left(\frac{1}{\mathrm{Re}} + \gamma\frac{\partial}{\partial t}\right)\left[2\frac{\partial^2 v}{\partial y^2} + \left(\frac{\partial^2 u}{\partial x \partial y} + \frac{\partial^2 v}{\partial x^2}\right)\right] \\ &- \left[\left(\frac{1}{\mathrm{Re}} + \gamma\frac{\partial}{\partial t}\right)\lambda + Ha\right]v + \gamma\frac{\partial}{\partial x}\left[\left(u\frac{\partial^2 u}{\partial x \partial y} + u\frac{\partial^2 v}{\partial x^2} + v\frac{\partial^2 u}{\partial y^2}\right.\right. \\ &+ \left.\left. v\frac{\partial^2 v}{\partial x \partial y} + \frac{\partial u}{\partial x}\frac{\partial u}{\partial y} - \frac{\partial u}{\partial y}\frac{\partial v}{\partial y} - \frac{\partial v}{\partial x}\frac{\partial u}{\partial x} + \frac{\partial v}{\partial y}\frac{\partial v}{\partial x}\right)\right] \\ &+ \gamma\frac{\partial}{\partial y}\left[\left(2u\frac{\partial^2 v}{\partial x \partial y} + \left(\frac{\partial u}{\partial y}\right)^2 + 2v\frac{\partial^2 v}{\partial y^2} + 4\left(\frac{\partial v}{\partial y}\right)^2 - 4\frac{1}{u_o}\frac{\partial^2 v}{\partial y^2} - \left(\frac{\partial v}{\partial x}\right)^2\right)\right] \\ &- F_r v^2 + \frac{G_r}{\mathrm{Re}^2}\theta.\end{aligned} \tag{4.37}$$

$$\frac{\partial \theta}{\partial t} + u\frac{\partial \theta}{\partial x} + v\frac{\partial \theta}{\partial y} = \frac{1}{\mathrm{Re}\,\mathrm{Pr}}\left(\frac{\partial^2 \theta}{\partial x^2} + \frac{\partial^2 \theta}{\partial y^2}\right). \tag{4.38}$$

4.3 Dimensionless Governing Equations

In the absence of viscous elasticity, $\gamma = 0$ the model reduces to the following set of transformed dimensionless equations

$$\frac{\partial u}{\partial t}+u\frac{\partial u}{\partial x}+v\frac{\partial u}{\partial y}=-\frac{\partial P}{\partial x}+\frac{1}{Re}\left[2\frac{\partial^2 u}{\partial x^2}+\left(\frac{\partial^2 v}{\partial x\partial y}+\frac{\partial^2 u}{\partial y^2}\right)\right]-\left(\frac{\lambda}{Re}+Ha\right)u-F_r u^2, \tag{4.39}$$

$$\frac{\partial v}{\partial t}+u\frac{\partial v}{\partial x}+v\frac{\partial v}{\partial y}=-\frac{\partial P}{\partial y}+\frac{1}{Re}\left[2\frac{\partial^2 v}{\partial y^2}+\left(\frac{\partial^2 u}{\partial x\partial y}+\frac{\partial^2 v}{\partial x^2}\right)\right]-\left[\frac{\lambda}{Re}+Ha\right]v - Frv^2+\frac{Gr}{Re^2}\theta, \tag{4.40}$$

and

$$\frac{\partial \theta}{\partial t}+u\frac{\partial \theta}{\partial x}+v\frac{\partial \theta}{\partial y}=\frac{1}{Re\,Pr}\left(\frac{\partial^2 \theta}{\partial x^2}+\frac{\partial^2 \theta}{\partial y^2}\right), \tag{4.41}$$

where the parameters are defined as follows:

$$\lambda=\frac{L^2\varphi}{K},\quad Ha=\frac{L}{u_0}\sigma B_0^2,\quad Fr=\frac{LC_f\varphi}{\sqrt{K}},\quad Re=\frac{u_0 L}{\nu},\quad Gr=\frac{L^3\rho g(\beta_\theta)\theta_0}{\nu^2},\quad Pr=\frac{\mu C_p}{k}. \tag{4.42}$$

The associated dimensionless boundary conditions are as follows:

- On the left wall (Γ_3) of the domain

$$u=v=0,\quad \text{and}\quad \theta=0. \tag{4.43}$$

- On the right wall (Γ_3) of the domain

$$u=v=0,\quad \text{and}\quad \theta=0. \tag{4.44}$$

- On the bottom portions (Γ_2) of the domain

$$u=v=0,\quad \text{and}\quad \theta=0,\quad \text{on flatted boundary} \tag{4.45}$$

- On the bottom portions (Γ_2) of the domain

$$\text{and}\quad u=v=0,\quad \text{and}\quad \theta=100.\quad \text{on circular heater} \tag{4.46}$$

- On the top wall (Γ_1) of the domain

$$u = 1, v = 0 \quad \text{and} \quad \theta = 100. \tag{4.47}$$

4.3 Finite Element Formulation and Numerical Procedure

The Galerkin Finite Element Method GFEM is employed to numerically solve the nonlinear coupled PDEs from equation (4.39) to (4.41) along with their corresponding boundary conditions (4.43) to (4.47). The strong form of the equations is then converted into the weak form by multiplying the PDEs with test functions, followed by integration over the entire domain. Finally, a set of approximate trial functions, defined over specific subdomains, is utilized to obtain an approximate numerical solution. The main steps of the methodology are outlined as follows:

4.3.1 Strong Form of The Governing Equations

The set of governing PDEs from equation. (4.39) to (4.41) are initially known as strong form which are re-written as

$$\frac{\partial u}{\partial t} + u\frac{\partial u}{\partial x} + v\frac{\partial u}{\partial y} = -\frac{\partial P}{\partial x} + a_1\left[2\frac{\partial^2 u}{\partial x^2} + \left(\frac{\partial^2 u}{\partial x \partial y} + \frac{\partial^2 u}{\partial y^2}\right)\right] - d_2 u - a_3 u^2, \tag{4.48}$$

$$\frac{\partial v}{\partial t} + u\frac{\partial v}{\partial x} + v\frac{\partial v}{\partial y} = \frac{\partial P}{\partial y} + a_4\left[2\frac{\partial^2 v}{\partial y^2} + \left(\frac{\partial^2 v}{\partial x \partial y} + \frac{\partial^2 v}{\partial x^2}\right)\right] - a_5 v - a_6 v^2 + a_7\theta, \tag{4.49}$$

and

$$\frac{\partial \theta}{\partial t} + u\frac{\partial \theta}{\partial x} + v\frac{\partial \theta}{\partial y} = a_8\left(\frac{\partial^2 \theta}{\partial x^2} + \frac{\partial^2 \theta}{\partial y^2}\right) + Q, \tag{4.50}$$

where $Q,$ is the source function and the parameters $\mathrm{a}_1, a_2, \ldots, a_8$ are given as:

$$a_1 = a_4 = \frac{1}{Re}, \quad a_2 = a_5 = \left[\frac{\lambda}{Re} + Ha\right], \quad a_3 = a_6 = F_r,$$
$$a_7 = \frac{Gr}{Re^2} \quad \text{and} \quad a_8 = \frac{1}{RePr}. \tag{4.51}$$

4.3.2 Weak/Variational Formulation

The weak formulation is a fundamental variational approach used to transform differential equations into an integral form. This transformation is achieved by multiplying the governing equations with suitable test functions and integrating over the entire computational domain.

To establish the weak formulation, it is essential to define appropriate function spaces and corresponding test functions. Let $\mathbf{W}$ and Q represent the test function spaces for different governing equations, where $\mathbf{W} = [H_1(\Omega)]$ corresponds to velocity and temperature fields, while $Q = L_2(\Omega)$ is associated with the pressure field. Furthermore, let $\tilde{\phi}$ be a test function such that $\tilde{\phi} \in \mathbf{W}$.

In the weak formulation of PDEs, the solutions and corresponding test functions are sought within suitable Hilbert spaces that ensure the well-posedness of the variational problem. In this study, we consider the function spaces $L^2(\Omega)$ and $H^1(\Omega)$, which are commonly employed in the finite element method for modeling fluid flow and heat transfer problems.

The space $L^2(\Omega)$ consists of all square-integrable functions over a domain $\Omega \subset \mathbb{R}^n$. Formally, it is defined as:

$$L^2(\Omega) = \left\{ \tilde{\phi} : \Omega \to \mathbb{R} \;\middle|\; \int_\Omega |\tilde{\phi}(x)|^2 \, dx < \infty \right\}.$$

This is a Hilbert space equipped with the inner product:

$$(u, \tilde{\phi})_{L^2(\Omega)} = \int_\Omega u(x)\tilde{\phi}(x) \, dx,$$

and the associated norm:

$$\|\tilde{\phi}\|_{L^2(\Omega)} = \left(\int_\Omega |\tilde{\phi}(x)|^2 \, dx \right)^{1/2}.$$

The space $L^2(\Omega)$ is typically used to define scalar fields such as pressure, which do not require differentiability in the weak formulation. The Sobolev space $H^1(\Omega)$ includes functions in $L^2(\Omega)$ whose first-order weak derivatives are also in $L^2(\Omega)$. It is defined as:

$$H^1(\Omega) = \left\{ \tilde{\phi} \in L^2(\Omega) \;\middle|\; \frac{\partial \tilde{\phi}}{\partial x_i} \in L^2(\Omega),\ i = 1, 2, \ldots, n \right\}.$$

This space is also a Hilbert space, with the inner product:

$$(u, \tilde{\phi})_{H^1(\Omega)} = \int_\Omega u(x)\tilde{\phi}(x) \, dx + \int_\Omega \nabla u(x) \cdot \nabla \tilde{\phi}(x) \, dx,$$

and corresponding norm:

$$\|\tilde{\phi}\|_{H^1(\Omega)} = \left(\|\tilde{\phi}\|^2_{L^2(\Omega)} + \|\nabla \tilde{\phi}\|^2_{L^2(\Omega)} \right)^{1/2}.$$

The space $H^1(\Omega)$ is used for fields such as velocity and temperature that appear with first derivatives in the governing equations.

In multiphysics problems involving vector fields, such as velocity and temperature, we define the test and trial function space as:

$$W = [H^1(\Omega)]$$

while scalar fields such as pressure belong to:

$$Q = L^2(\Omega).$$

These spaces form the foundation of the weak formulation employed in this work and ensure the compatibility and stability of the finite element discretization [32, 34, 35]. The variational formulation is obtained by multiplying the momentum and energy equations with the test function $\tilde{w}$ and integrating over the domain Ω. The

weak formulation of the governing PDEs from equation (4.39) to (4.41) is presented below. The weak form for x-component of momentum equation (4.39) is derived by multiply with test function $\tilde{\phi}$ first and then integrate over the computational domain,

$$\int \left(\frac{\partial u}{\partial t} + u\frac{\partial u}{\partial x} + v\frac{\partial u}{\partial y}\right)\tilde{\phi}\, d\Omega = -\int \frac{\partial p}{\partial x}\,\tilde{\phi}\, d\Omega + \frac{1}{Re}\int 2\frac{\partial^2 u}{\partial x^2}\,\tilde{\phi}\, d\Omega + \frac{1}{Re}\int \frac{\partial^2 v}{\partial x \partial y}\,\tilde{\phi}\, d\Omega + \frac{1}{Re}\int \frac{\partial^2 u}{\partial y^2}\,\tilde{\phi}\, d\Omega - \int \left(\frac{\lambda}{Re} + Ha\right) u\,\tilde{\phi}\, d\Omega - \int Fr|u|u\,\tilde{\phi}\, d\Omega.\ \forall \tilde{\phi} \in W \tag{4.52}$$

$$\int \frac{\partial u}{\partial t}\,\tilde{\phi}\, d\Omega + \int u\frac{\partial u}{\partial x}\,\tilde{\phi}\, d\Omega + \int v\frac{\partial u}{\partial y}\,\tilde{\phi}\, d\Omega = -\int \frac{\partial p}{\partial x}\,\tilde{\phi}\, d\Omega + \frac{1}{Re}\int 2\frac{\partial^2 u}{\partial x^2}\,\tilde{\phi}\, d\Omega + \frac{1}{Re}\int \frac{\partial^2 u}{\partial y^2}\,\tilde{\phi}\, d\Omega + \frac{1}{Re}\int \frac{\partial^2 v}{\partial x \partial y}\,\tilde{\phi}\, d\Omega - \left(\frac{\lambda}{Re} + Ha\right)\int u\,\tilde{\phi}\, d\Omega - Fr\int |u|u\,\tilde{\phi}\, d\Omega.\quad \forall \tilde{\phi} \in W \tag{4.53}$$

$$\int \frac{\partial u}{\partial t}\,\tilde{\phi}\, d\Omega + \int u\frac{\partial u}{\partial x}\,\tilde{\phi}\, d\Omega + \int v\frac{\partial u}{\partial y}\,\tilde{\phi}\, d\Omega = -\int \frac{\partial P}{\partial x}\,\tilde{\phi}\, d\Omega + \frac{2}{Re}\int \frac{\partial}{\partial x}\left(\frac{\partial u}{\partial x}\right)\tilde{\phi}\, d\Omega + \int \frac{\partial}{\partial x}\frac{\partial v}{\partial y}\,\tilde{\phi}\, d\Omega + \int \frac{\partial}{\partial y}\frac{\partial u}{\partial y}\,\tilde{\phi}\, d\Omega - \left(\frac{\lambda}{Re} + Ha\right)\int u\,\tilde{\phi}\, d\Omega - F_r\int |u|u\,\tilde{\phi}\, d\Omega.\quad \forall \tilde{\phi} \in W \tag{4.54}$$

$$\int \frac{\partial u}{\partial t}\,\tilde{\phi}\, d\Omega + \int u\frac{\partial u}{\partial x}\,\tilde{\phi}\, d\Omega + \int v\frac{\partial u}{\partial y}\,\tilde{\phi}\, d\Omega = -\int \frac{\partial P}{\partial x}\,\tilde{\phi}\, d\Omega + \frac{2}{Re}\left\{\tilde{\phi}\int \frac{\partial}{\partial x}\left(\frac{\partial u}{\partial x}\right) d\Omega - \int \frac{\partial \tilde{\phi}}{\partial x}\frac{\partial u}{\partial x}\, d\Omega\right\} + \left\{\tilde{\phi}\int \frac{\partial}{\partial x}\frac{\partial v}{\partial y}\, d\Omega - \int \frac{\partial \tilde{\phi}}{\partial x}\frac{\partial v}{\partial y}\, d\Omega\right\} + \left\{\tilde{\phi}\int \frac{\partial}{\partial x}\frac{\partial u}{\partial y}\, d\Omega - \int \frac{\partial \tilde{\phi}}{\partial y}\frac{\partial u}{\partial y}\, d\Omega\right\} - \left(\frac{\lambda}{Re} + H_a\right)\int u\,\tilde{\phi}\, d\Omega - F_r|u|\int u\,\tilde{\phi}\, d\Omega.\quad \forall \tilde{\phi} \in W \tag{4.55}$$

$$\int \frac{\partial u}{\partial t}\,\tilde{\phi}\,d\Omega + \int u\frac{\partial u}{\partial x}\,\tilde{\phi}\,d\Omega + \int v\frac{\partial u}{\partial y}\,\tilde{\phi}\,d\Omega = -\int \frac{\partial P}{\partial x}\,\tilde{\phi}\,d\Omega + \frac{2}{Re}\left\{\tilde{\phi}\frac{\partial u}{\partial x} - \int \frac{\partial \tilde{\phi}}{\partial x}\frac{\partial u}{\partial x}\,d\Omega\right\} + \left\{\tilde{\phi}\frac{\partial v}{\partial y} - \int \frac{\partial \tilde{\phi}}{\partial x}\frac{\partial v}{\partial y}\,d\Omega\right\} + \left\{\tilde{\phi}\frac{\partial u}{\partial y} - \int \frac{\partial \tilde{\phi}}{\partial x}\frac{\partial u}{\partial y}\,d\Omega\right\} - \left(\frac{\lambda}{Re} + H_a\right)\int u\,\tilde{\phi}\,d\Omega - F_r|u|\int u\,\tilde{\phi}\,d\Omega. \tag{4.56}$$

$$\int \frac{\partial u}{\partial t}\,\tilde{\phi}\,d\Omega + \int u\frac{\partial u}{\partial x}\,\tilde{\phi}\,d\Omega + \int v\frac{\partial u}{\partial y}\,\tilde{\phi}\,d\Omega = -\int \frac{\partial P}{\partial x}\,\tilde{\phi}\,d\Omega + \frac{2}{Re}\tilde{\phi}\frac{\partial u}{\partial x} - \frac{2}{Re}\int \frac{\partial \tilde{\phi}}{\partial x}\frac{\partial u}{\partial x}\,d\Omega + \tilde{\phi}\frac{\partial v}{\partial y} - \int \frac{\partial \tilde{\phi}}{\partial x}\frac{\partial v}{\partial y}\,d\Omega + \tilde{\phi}\frac{\partial u}{\partial y} - \int \frac{\partial \tilde{\phi}}{\partial x}\frac{\partial u}{\partial y}\,d\Omega - \left(\frac{\lambda}{Re} + H_a\right)\int u\,\tilde{\phi}\,d\Omega - F_r\int |u|u\,\tilde{\phi}\,d\Omega. \tag{4.57}$$

$$\int \frac{\partial u}{\partial t}\,\tilde{\phi}\,d\Omega + \int u\frac{\partial u}{\partial x}\,\tilde{\phi}\,d\Omega + \int v\frac{\partial u}{\partial y}\,\tilde{\phi}\,d\Omega = -\int \frac{\partial P}{\partial x}\,\tilde{\phi}\,d\Omega - \frac{2}{Re}\int \frac{\partial \tilde{\phi}}{\partial x}\frac{\partial u}{\partial x}\,d\Omega - \int \frac{\partial \tilde{\phi}}{\partial x}\frac{\partial v}{\partial y}\,d\Omega - \int \frac{\partial \tilde{\phi}}{\partial x}\frac{\partial u}{\partial y}\,d\Omega - \left(\frac{\lambda}{Re} + H_a\right)\int u\,\tilde{\phi}\,d\Omega - F_r|u|\int u\,\tilde{\phi}\,d\Omega + \underbrace{\left\{\frac{2}{Re}\tilde{\phi}\frac{\partial u}{\partial x}\right\}}_{\longrightarrow 0} + \underbrace{\left\{\tilde{\phi}\frac{\partial v}{\partial y} + \tilde{\phi}\frac{\partial u}{\partial y}\right\}}_{\longrightarrow 0}. \tag{4.58}$$

Let us start with the identity:

$$-\frac{\partial}{\partial x}\left(P\tilde{\phi}\right)+P\frac{\partial\tilde{\phi}}{\partial x}=-\frac{\partial P}{\partial x}\tilde{\phi}. \tag{4.59}$$

Integrating over the domain Ω, we get:

$$\int_{\Omega}-\frac{\partial}{\partial x}\left(P\tilde{\phi}\right)d\Omega+\int_{\Omega}P\frac{\partial\tilde{\phi}}{\partial x}\,d\Omega=-\int_{\Omega}\frac{\partial P}{\partial x}\tilde{\phi}\,d\Omega. \tag{4.60}$$

This implies to:

$$-\int_{\Omega}\frac{\partial}{\partial x}\left(P\tilde{\phi}\right)d\Omega+\int_{\Omega}P\frac{\partial\tilde{\phi}}{\partial x}\,d\Omega=-\int_{\Omega}\frac{\partial P}{\partial x}\tilde{\phi}\,d\Omega. \tag{4.61}$$

Using the divergence theorem, the first term vanishes under appropriate boundary conditions, yielding:

$$\int_{\Omega}P\frac{\partial\tilde{\phi}}{\partial x}\,d\Omega=-\int_{\Omega}\frac{\partial P}{\partial x}\tilde{\phi}\,d\Omega. \tag{4.62}$$

Now, equation (4.58) becomes, which is weak form for x-compnent of momentum equation (4.39)

$$\begin{aligned}\int\frac{\partial u}{\partial t}\tilde{\phi}\,d\Omega+\int u\frac{\partial u}{\partial x}\tilde{\phi}\,d\Omega+\int v\frac{\partial u}{\partial y}\tilde{\phi}\,d\Omega=p\int\frac{\partial\tilde{\phi}}{\partial x}\,d\Omega-\frac{2}{Re}\int\frac{\partial\tilde{\phi}}{\partial x}\frac{\partial u}{\partial x}\,d\Omega\\-\int\frac{\partial\tilde{\phi}}{\partial x}\frac{\partial v}{\partial y}\,d\Omega-\int\frac{\partial\tilde{\phi}}{\partial x}\frac{\partial u}{\partial y}\,d\Omega\\-\left(\frac{\lambda}{Re}+H_a\right)\int u\,\tilde{\phi}\,d\Omega-\int F_r|u|u\,\tilde{\phi}\,d\Omega.\end{aligned} \tag{4.63}$$

Similarly, the weak form for y-component of momentum equation is obtained by multiplying the equation (4.40) with the test function $\tilde{\phi}$, then integrate it over the entire computational domain.

$$\begin{aligned}\int\left(\frac{\partial v}{\partial t}+u\frac{\partial v}{\partial x}+v\frac{\partial v}{\partial y}\right)\tilde{\phi}\,d\Omega=-\int\frac{\partial p}{\partial y}\tilde{\phi}\,d\Omega+\frac{1}{Re}\int 2\frac{\partial^2 v}{\partial y^2}\tilde{\phi}\,d\Omega\\+\frac{1}{Re}\int\frac{\partial^2 u}{\partial x\partial y}\tilde{\phi}\,d\Omega+\frac{1}{Re}\int\frac{\partial^2 v}{\partial x^2}\tilde{\phi}\,d\Omega\\-\int\left(\frac{\lambda}{Re}+Ha\right)v\,\tilde{\phi}\,d\Omega-\int Fr|v|v\,\tilde{\phi}\,d\Omega\\+\int\frac{Gr}{R_e^2}\theta\tilde{\phi}\,d\Omega.\end{aligned} \tag{4.64}$$

This is the weak formulation of the y-component of the momentum equation (4.40) and is expressed as

$$\int \frac{\partial v}{\partial t}\tilde{\phi}\, d\Omega + \int u\frac{\partial v}{\partial x}\tilde{\phi}\, d\Omega + \int v\frac{\partial u}{\partial y}\tilde{\phi}\, d\Omega = p\int \frac{\partial \tilde{\phi}}{\partial y}d\Omega - \frac{2}{Re}\int \frac{\partial v}{\partial y}\frac{\partial \tilde{\phi}}{\partial y}\, d\Omega + \int \frac{\partial u}{\partial y}\frac{\partial \tilde{\phi}}{\partial x}\, d\Omega - \frac{1}{Re}\int \left(\frac{\partial v}{\partial x}\frac{\partial \tilde{\phi}}{\partial x}\right) d\Omega - \left(\frac{\lambda}{Re} + Ha\right)\int v\tilde{\phi}\, d\Omega. - \int Fv|v|\tilde{\phi}\, d\Omega + \frac{Gr}{R_e^2}\int \theta\tilde{\phi}\, d\Omega. \quad (4.65)$$

Following the similiar procedure the energy equation (4.41) is multiplied by the test function $\tilde{\phi}$ and integrated over the whole computaional domain results in

$$\int \left(\frac{\partial \theta}{\partial t} + u\frac{\partial \theta}{\partial x} + v\frac{\partial \theta}{\partial y}\right)\tilde{\phi} d\Omega = \left(\frac{1}{RePr}\right)\int \left(\frac{\partial^2 \theta}{\partial x^2} + \frac{\partial^2 \theta}{\partial y^2}\right)\tilde{\phi} d\Omega. \quad (4.66)$$

$\Longrightarrow$

$$\int \frac{\partial \theta}{\partial t}\tilde{\phi} d\Omega + \int u\frac{\partial \theta}{\partial x}\phi\tilde{d}\Omega + \int v\frac{\partial \theta}{\partial y}\tilde{\phi} d\Omega = \left(\frac{1}{RePr}\right)\left(\int \frac{\partial^2 \theta}{\partial x^2}\tilde{\phi} d\Omega + \int \frac{\partial^2 \theta}{\partial y^2}\tilde{\phi} d\Omega\right). \quad (4.67)$$

$\Longrightarrow$

$$\int \frac{\partial \theta}{\partial t}\tilde{\phi} d\Omega + \int u\frac{\partial \theta}{\partial x}\phi\tilde{d}\Omega + \int v\frac{\partial \theta}{\partial y}\tilde{\phi} d\Omega = \left(\frac{1}{RePr}\right)\int \frac{\partial}{\partial x}(\frac{\partial \theta}{\partial x})\tilde{\phi} d\Omega + \left(\frac{1}{RePr}\right)\int \frac{\partial}{\partial y}(\frac{\partial \theta}{\partial y})\tilde{\phi} d\Omega. \quad (4.68)$$

$\Longrightarrow$

$$\int \frac{\partial \theta}{\partial t}\tilde{\phi} d\Omega + \int u\frac{\partial \theta}{\partial x}\phi\tilde{d}\Omega + \int v\frac{\partial \theta}{\partial y}\tilde{\phi} d\Omega = \left(\frac{1}{RePr}\right)\left\{\tilde{\phi}\frac{\partial \theta}{\partial x} - \int \frac{\partial \tilde{\phi}}{\partial x}\frac{\partial \theta}{\partial x}\tilde{\phi} d\Omega\right\} + \left(\frac{1}{RePr}\right)\left\{\tilde{\phi}\frac{\partial \theta}{\partial y} - \int \frac{\partial \tilde{\phi}}{\partial y}\frac{\partial \theta}{\partial y}\tilde{\phi} d\Omega\right\}. \quad (4.69)$$

$$\Longrightarrow \int \frac{\partial \theta}{\partial t}\tilde{\phi} d\Omega + \int u\frac{\partial \theta}{\partial x}\phi\tilde{d}\Omega + \int v\frac{\partial \theta}{\partial y}\tilde{\phi} d\Omega = -\frac{1}{RePr}\int \left[\frac{\partial \theta}{\partial x}\frac{\partial \tilde{\phi}}{\partial x} + \frac{\partial \theta}{\partial y}\frac{\partial \tilde{\phi}}{\partial y}\right] d\Omega. \quad (4.70)$$

Thus, we get

$$\int \frac{\partial \theta}{\partial t}\tilde{\phi}d\Omega + \int u\frac{\partial \theta}{\partial x}\phi\tilde{d}\Omega + \int v\frac{\partial \theta}{\partial y}\tilde{\phi}d\Omega + \frac{1}{RePr}\int \left[\frac{\partial \theta}{\partial x}\frac{\partial \tilde{\phi}}{\partial x} + \frac{\partial \theta}{\partial y}\frac{\partial \tilde{\phi}}{\partial y}\right] d\Omega = 0. \tag{4.71}$$

4.4 Two-level Mixed Finite Element Method

In this section, we introduce the two-level mixed finite element method to approximate the solution of the governing equations. It is worthy to note that the Euclidean norm $|u|$ is not differentiable at zero. Therefore, let

$$|u|_\epsilon = \sqrt{|u|^2 + \epsilon^2}, \tag{4.72}$$

where ϵ is a small positive constant. For ϵ very small, it is shown in [36] that $|u|_\epsilon$ is a good approximation for $|u|$ and the partial derivatives of $|u|_\epsilon$ approximate the partial derivatives of $|u|$ very well. Particularly, $|u|_\epsilon - |u| < \epsilon$. Now consider the map defined by

$$f_\epsilon : \mathbb{R}^2 \to \mathbb{R}^2, \tag{4.73}$$

$$f_\epsilon(u) = |u|_\epsilon u. \tag{4.74}$$

This is further expanded as:

$$f_\epsilon(u) = \begin{bmatrix} f_{\epsilon,1}(u) \\ f_{\epsilon,2}(u) \end{bmatrix} = \begin{bmatrix} |u|_\epsilon u_1 \\ |u|_\epsilon u_2 \end{bmatrix}. \tag{4.75}$$

The Taylor series representation of $f_\epsilon(u)$ about $u_H \in \mathbb{R}^2$ is given by

$$f_\epsilon(u) = f_\epsilon(u_H) + Df_\epsilon(u_H)(u-u_H) + \frac{1}{2!}D^2 f_\epsilon(u_H)(u-u_H)^2 + \frac{1}{3!}D^3 f_\epsilon(\zeta_H)(u-u_H)^3 + \ldots, \tag{4.76}$$

where $\zeta_H = tu + (1-t)u_H$ for some $t \in [0,1]$ and $(u-u_H)^2$ is expressed as the Kronecker product $(u-u_H) \otimes (u-u_H)$. Precisely, $(u-u_H)^2$ is equal to

$$\Big[(u_1 - u_{H,1})^2, \quad (u_1 - u_{H,1})(u_2 - u_{H,2}), \quad (u_2 - u_{H,2})(u_1 - u_{H,1}), \quad (u_2 - u_{H,2})^2\Big]^T. \tag{4.77}$$

The first and second derivatives of f_ϵ are given by:

$$Df_\epsilon(u_H) = \begin{bmatrix} \frac{\partial f_{\epsilon,1}(u_H)}{\partial u_1} & \frac{\partial f_{\epsilon,1}(u_H)}{\partial u_2} \\ \frac{\partial f_{\epsilon,2}(u_H)}{\partial u_1} & \frac{\partial f_{\epsilon,2}(u_H)}{\partial u_2} \end{bmatrix}, \tag{4.78}$$

and

$$D^2 f_\epsilon(\zeta_H) = \begin{bmatrix} \frac{\partial^2 f_{\epsilon,1}(\zeta_H)}{\partial u_1^2} & \frac{\partial^2 f_{\epsilon,1}(\zeta_H)}{\partial u_1 \partial u_2} & \frac{\partial^2 f_{\epsilon,1}(\zeta_H)}{\partial u_2 \partial u_1} & \frac{\partial^2 f_{\epsilon,1}(\zeta_H)}{\partial u_1^2} \\ \frac{\partial^2 f_{\epsilon,2}(\zeta_H)}{\partial u_1^2} & \frac{\partial^2 f_{\epsilon,2}(\zeta_H)}{\partial u_1 \partial u_2} & \frac{\partial^2 f_{\epsilon,2}(\zeta_H)}{\partial u_2 u_1} & \frac{\partial^2 f_{\epsilon,2}(\zeta_H)}{\partial u_2^2} \end{bmatrix}. \tag{4.79}$$

In the next section, an overview of the two-level algorithm is given.

4.4.1 Two-level Algorithm

Let h and H denote the mesh sizes of the fine and coarse grids, respectively. The spaces $X_h \subset H_1(\Omega)$ and $X_H \subset H_1(\Omega)$ are used to approximate the velocity (or flux) field. Pressure approximations are handled in separate spaces $Q_h \subset L_2(\Omega)$ and $Q_H \subset L_2(\Omega)$ within the mixed finite element framework.

Let $X_H, X_h \subset X, M_H, M_h \subset M$ denote finite element spaces with $X_H \subset X_h, M_H \subset M_h$, with $H \gg h$.

Step 1. Solve the nonlinear system on a coarse mesh T_H with mesh size H: For all $(\tilde{\phi}_H, q_H) \in \{ X_H \times M_H \}$, find $(u_H, p_H) \in \{X_H \times M_H\}$ such that

$$U_H = (U_{1H}, U_{2H}).$$

Also, given that

$$|U|_\epsilon = \sqrt{|U|^2 + \epsilon^2},$$

and

$$|U_H| = \sqrt{U_{1H}^2 + U_{2H}^2}.$$

It follows that

$$|U_H|_\epsilon = \sqrt{U_{1H}^2 + U_{2H}^2 + \epsilon^2}.$$

Thus,

$$f_\epsilon(U_H) = |U_H|_\epsilon U_H,$$

which can be rewritten as

$$f_\epsilon(U_H) = \sqrt{U_{1H}^2 + U_{2H}^2 + \epsilon^2}(U_{1H}, U_{2H}).$$

Here, is non linear system on a coarse mesh:

$$\begin{aligned}
&\int \left(\frac{\partial U_{1H}}{\partial t}\tilde{\phi_{1H}} + U_{1H}\frac{\partial U_{1H}}{\partial x}\tilde{\phi_{1H}} + U_{2H}\frac{\partial U_{1H}}{\partial y}\tilde{\phi_{1H}} \right) dxdy = P\int \frac{\partial \tilde{\phi_{1H}}}{\partial x} dxdy \\
&- \left(\frac{1}{Re}\right)\left[\int \left(2\frac{\partial U_{1H}}{\partial x}\frac{\partial \tilde{\phi_{1H}}}{\partial x} + \frac{\partial U_{2H}}{\partial y}\frac{\partial \tilde{\phi_{1H}}}{\partial x} \quad + \frac{\partial U_{1H}}{\partial y}\frac{\partial \tilde{\phi_{1H}}}{\partial y} \right) dxdy \right] \\
&- \left(\frac{\lambda}{Re} + Ha\right)\int U_H\tilde{\phi_{1H}} dxdy - \int F_r U_{1H}\tilde{\phi_{1H}} \cdot \left(\sqrt{U_{1H}^2 + U_{2H}^2 + \epsilon^2}\right) dxdy,
\end{aligned} \tag{4.80}$$

$$\begin{aligned}
&\int \left(\frac{\partial U_{2H}}{\partial t}\tilde{\phi_{2H}} + U_{1H}\frac{\partial U_{2H}}{\partial x}\tilde{\phi_{2H}} + U_{2H}\frac{\partial U_{2H}}{\partial y}\tilde{\phi_{2H}} \right) dxdy = P\int \frac{\partial \tilde{\phi_{2H}}}{\partial y} dxdy \\
&- \left(\frac{1}{Re}\right)\left[\int \left(2\frac{\partial U_{2H}}{\partial y}\frac{\partial \tilde{\phi_{2H}}}{\partial y} + \frac{\partial U_{1H}}{\partial y}\frac{\partial \tilde{\phi_{2H}}}{\partial x} \quad + \frac{\partial U_{2H}}{\partial x}\frac{\partial \tilde{\phi_{2H}}}{\partial x} \right) dxdy \right] \\
&- \left(\frac{\lambda}{Re} + Ha\right)\int U_{2H}\tilde{\phi_{2H}} dxdy - \int F_r U_{2H}\tilde{\phi_{2H}} \cdot \left(\sqrt{U_{1H}^2 + U_{2H}^2 + \epsilon^2}\right) dxdy \\
&+ \frac{Gr}{Re^2}\int \theta\tilde{\phi_{2H}} dxdy,
\end{aligned} \tag{4.81}$$

and

$$\begin{aligned}
&\int \left(\frac{\partial \theta}{\partial t}\tilde{\phi_H} + u\frac{\partial \theta}{\partial x}\tilde{\phi_H} + v\frac{\partial \theta}{\partial y}\tilde{\phi_H} \right) dx\, dy \\
&= \left(\frac{1}{\mathrm{Re}\,\mathrm{Pr}}\right)\int \left(\frac{\partial \theta}{\partial x}\frac{\partial \tilde{\phi_H}}{\partial x} + \frac{\partial \theta}{\partial y}\frac{\partial \tilde{\phi_H}}{\partial y} \right) dx\, dy.
\end{aligned} \tag{4.82}$$

.

Step 2. Solve the linear system on a fine mesh T_h with mesh size h: For all $(\tilde{\phi_h}, q_h) \in X_h \times M_h$, find $(u_h, p_h) \in X_h \times M_h$ such that

The nonlinear term in the governing equation is given by the integral expression.

$$\int u_h|u_H|\tilde{\phi}\, dxdy. \tag{4.83}$$

Now, We expand $u_h|u_H|$ using a Taylor series around U_H.

$$u_h|u_H| = \left\{ |U_H|_e U_H + Df_e(U_H)[U_h - U_H] + \frac{1}{2!} Df_e^2(U_H)[U_h - U_H]^2 + ... \right\}. \tag{4.84}$$

$\Longrightarrow$

$$u_h|u_H| = \left\{ |U_H|_e U_H + Df_e(U_H)U_h - Df_e(U_H)U_H + \frac{1}{2!} D_e^2(U_H)[U_h - U_H]^2 + ... \right\}. \tag{4.85}$$

This expansion allows to express the function in terms of U_H and its derivatives.

$$\frac{\partial f_{\epsilon,i}(U_H)}{\partial u_j} = \left(U_i U_j + |U_H|_\epsilon^2\right) \delta_{ij} |U_H|_\epsilon^{-1}. \tag{4.86}$$

In (4.86), δ_{ij} denotes the Kronecker delta, defined as follows.

$$\delta_{ij} = \begin{cases} 1, & i = j, \\ 0, & i \neq j. \end{cases} \tag{4.87}$$

By evaluating the Jacobian matrix, the following matrix representation is obtained.

$$Df_\epsilon(U_H) = \begin{bmatrix} U_{1H}^2 + |U_H|_\epsilon^2 & 0 \\ 0 & U_{2H}^2 + |U_H|_\epsilon^2 \end{bmatrix}. \tag{4.88}$$

The second and third terms in the nonlinear part of the equation (4.63) and (4.65) are solved separately. After performing the matrix-vector multiplication, we get the resulting expression.

$$(Df_\epsilon(U_H)).(U_h) = \begin{bmatrix} (U_{1H}^2 + |U_H|_\epsilon^2)U_{1h} \\ (U_{2H}^2 + |U_H|_\epsilon^2)U_{2h} \end{bmatrix}, \tag{4.89}$$

$\Longrightarrow$

$$(Df_\epsilon(U_H)).(U_H) = \begin{bmatrix} (U_{1H}^2 + |U_H|_\epsilon^2)U_{1H} \\ (U_{2H}^2 + |U_H|_\epsilon^2)U_{2H} \end{bmatrix}. \tag{4.90}$$

The x-component of the equation is derived by simplifying the linearized terms as.

$$u_h|u_H| = \left\{ \sqrt{U_{1H}^2 + U_{2H}^2 + \epsilon^2}U_{1H} + (U_{1H}^2 + |U_H|_\epsilon^2)U_{1h} - (U_{1H}^2 + |U_H|_\epsilon^2)U_{1H} + ... \right\}. \tag{4.91}$$

or

$$u_h|u_H| = \left\{ \sqrt{U_{1H}^2 + U_{2H}^2 + \epsilon^2}U_{1H} + (U_{1H}^2)U_{1h} + (|U_H|_\epsilon^2)U_{1h} - (U_{1H}^3) + |U_H|_\epsilon^2 U_{1H} + ... \right\}. \tag{4.92}$$

Higher-order terms are ignored to obtain the following equation.

$$u_h|u_H| = \left\{ \sqrt{U_{1H}^2 + U_{2H}^2 + \epsilon^2}U_{1H} + (U_{1H}^2)U_{1h} + (|U_H|_\epsilon^2)U_{1h} - (U_{1H}^3) + |U_H|_\epsilon^2 U_{1H} \right\}. \tag{4.93}$$

The y-component of the equation is derived as follows:

$$u_h|u_H| = \left\{ \sqrt{U_{1H}^2 + U_{2H}^2 + \epsilon^2}U_{2H} + (U_{2H}^2 + |U_H|_\epsilon^2)U_{2h} - (U_{2H}^2 + |U_H|_\epsilon^2)U_{2H} + ... \right\}. \tag{4.94}$$

or

$$u_h|u_H| = \left\{ \sqrt{U_{1H}^2 + U_{2H}^2 + \epsilon^2}U_{2H} + (U_{2H}^2)U_{2h} + (|U_H|_\epsilon^2)U_{2h} - (U_{2H}^3) + |U_H|_\epsilon^2 U_{2H} + ... \right\}. \tag{4.95}$$

Ignoring higher-order terms, in equation (4.95) we get

$$u_h|u_H| = \left\{ \sqrt{U_{1H}^2 + U_{2H}^2 + \epsilon^2}U_{2H} + (U_{2H}^2)U_{2h} + (|U_H|_\epsilon^2)U_{2h} - (U_{2H}^3) + |U_H|_\epsilon^2 U_{2H} \right\}. \tag{4.96}$$

Finally, the system of equation for fine mesh is expressed as

$$\int \left(\frac{\partial u_{1h}}{\partial t}\tilde{\phi_{1h}} + u_{1h}\frac{\partial u_{1h}}{\partial x}\tilde{\phi_{1h}} + u_{2h}\frac{\partial u_{1h}}{\partial y}\tilde{\phi_{1h}} \right) dxdy$$
$$= P\int \frac{\partial \tilde{\phi_{1h}}}{\partial x}\,dxdy - \left(\frac{1}{Re}\right)\int \left(2\frac{\partial u_{1h}}{\partial x}\frac{\partial \tilde{\phi_{1h}}}{\partial x} + \frac{\partial u_{2h}}{\partial y}\frac{\partial \tilde{\phi_{1h}}}{\partial x} \right.$$
$$\left. + \frac{\partial u_{1h}}{\partial y}\frac{\partial \tilde{\phi_{1h}}}{\partial y} \right) dxdy - \left(\frac{\lambda}{Re} + Ha\right)\int u_{1h}\tilde{\phi_{1h}}\,dxdy$$
$$- \frac{Fr}{|U|_e}\int \sqrt{U_{1H}^2 + U_{2H}^2 + \epsilon^2}\,u_{1H}\tilde{\phi_{1h}}\,dxdy - \frac{Fr}{|U|_e}\int u_{1H}^2 U_{1h}\tilde{\phi_{1h}}\,dxdy$$
$$- \frac{Fr}{|U|_e}\int (\sqrt{(u_{1H}^2 + U_{2H}^2 + \epsilon^2)})^2 U_{1h}\tilde{\phi_{1h}}\,dxdy + \frac{Fr}{|U|_e}\int u_{1H}^3\tilde{\phi_{1h}}\,dxdy$$
$$+ \frac{Fr}{|U|_e}\int u_{1H}(|U|_e)^2\tilde{\phi_{1h}}\,dxdy, \tag{4.97}$$

$$\int \left(\frac{\partial u_{2h}}{\partial t}\tilde{\phi_{2h}} + u_{1h}\frac{\partial u_{2h}}{\partial x}\tilde{\phi_{2h}} + u_{2h}\frac{\partial u_{1h}}{\partial y}\tilde{\phi_{2h}} \right) dxdy$$
$$= P\int \frac{\partial \tilde{\phi_{2h}}}{\partial y}\,dxdy - \left(\frac{1}{Re}\right)\int \left(2\frac{\partial u_{2h}}{\partial y}\frac{\partial \tilde{\phi_{2h}}}{\partial y} + \frac{\partial u_{2h}}{\partial y}\frac{\partial \tilde{\phi_{2h}}}{\partial x} \right.$$
$$\left. + \frac{\partial u_{2h}}{\partial x}\frac{\partial \tilde{\phi_{2h}}}{\partial x} \right) dxdy - \left(\frac{\lambda}{Re} + Ha\right)\int u_{2h}\tilde{\phi_{2h}}\,dxdy$$
$$- Fr\int \sqrt{U_{1H}^2 + U_{2H}^2 + \epsilon^2}\,u_{2H}\tilde{\phi_{2h}}\,dxdy$$
$$- \frac{Fr}{|U|_e}\int (u_{2H}^2 u_{2h} + |u_H|_e{}^2 u_{2H})\tilde{\phi_{2h}}\,dxdy$$
$$- \frac{Fr}{|U|_e}\int (u_{2H}^3 + |U|_e{}^2 u_{2H})\tilde{\phi_{2h}}\,dxdy +$$
$$+ \frac{Gr}{R_e^2}\int \theta\tilde{\phi_{2h}}\,dxdy, \tag{4.98}$$

and

$$\int \left(\frac{\partial \theta}{\partial t}\tilde{\phi_h} + u_{1h}\frac{\partial \theta}{\partial x}\tilde{\phi_h} + u_{2h}\frac{\partial \theta}{\partial y}\tilde{\phi_h} \right) dxdy$$
$$= \left(\frac{1}{RePr}\right)\int \left(\frac{\partial \theta}{\partial x}\frac{\partial \tilde{\phi_h}}{\partial x} + \frac{\partial \theta}{\partial y}\frac{\partial \tilde{\phi_h}}{\partial y} \right) dxdy. \tag{4.99}$$

In the present work, numerical computations are performed using the open-source

finite element code FreeFEM++. The governing equations are discretized using the Mixed Finite Element Method (MFEM), and the resulting system of equations is assembled and solved within the FreeFEM++ framework. A time-marching algorithm is employed with a final simulation time of $T = 20$ and a uniform time step size of $\Delta t = 0.05$ is choosen, resulting in a total of 400 time steps. The computational domain is discretized using unstructured triangular elements. For the coarse mesh level, the domain consists of 1305 triangles and 721 vertices. On the fine mesh level, the domain is refined to 13334 triangles and 6884 vertices, ensuring enhanced resolution and improved accuracy in the solution. This meshing strategy enables precise evaluation of the flow, pressure, and temperature distributions across the domain.

4.5 Computational Results and Analysis

In this section, we share and discuss the numerical results. The boundary value problem, set up in its finite element form, as outlined earlier, has been solved using FreeFEM++. For these simulations, the dimensionless parameter values were thoughtfully chosen to reflect the physical significance of the problem.

In figure 4.2, the velocity profiles exhibit notable variations with changing values of the Grashof number. The selected values of the Grashof number in these simulations are $Gr = 0, Gr = 10, Gr = 30$ and $Gr = 40$. It is observed that at $Gr = 0$ where buoyant forces are absent, the velocity profile is smooth and subdued, indicating a flow dominated by viscous forces. As the Grashof number increases to $Gr = 10$, the buoyant forces begin to influence the flow, leading to moderate velocity peaks. With further increases to $Gr = 30$ and $Gr = 40$, the velocity profiles exhibit sharper gradients and more pronounced peaks, reflecting the dominance of buoyancy-driven convection.This transition highlights the strengthening of natural convection effects as the Grashof number increases.

In figure 4.3, the velocity profiles are presented with varying Prandtl numbers $Pr = 0.5, Pr = 2, Pr = 3.3, Pr = 7.3$. At lower Prandtl numbers, the velocity contours appear broader and more diffused, indicating that the upward fluid motion is more widely distributed. In contrast, as the Prandtl number increases, these

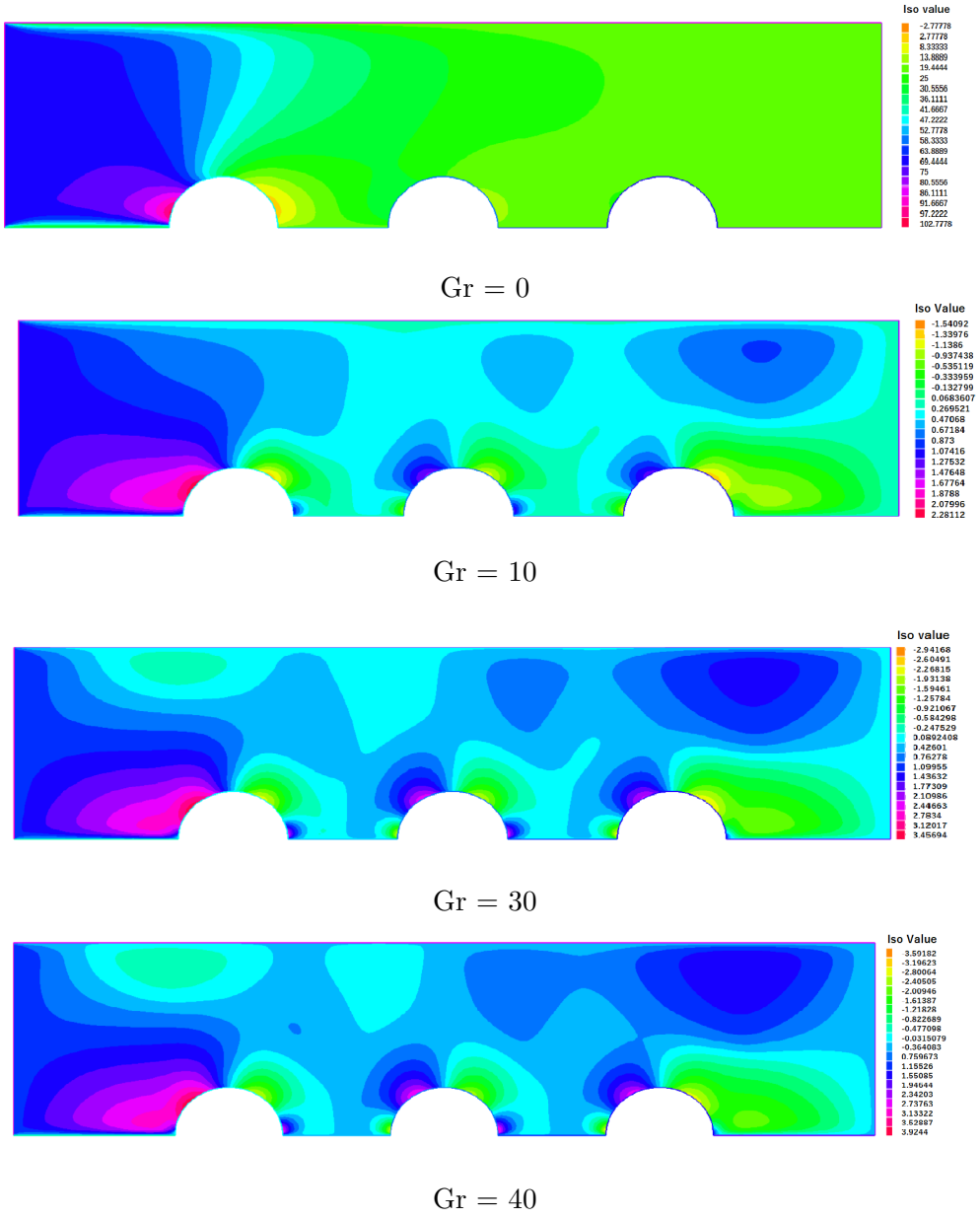

FIGURE 4.2: Velocity profiles with varying values of the Grashof Number (Gr). Other parameters used: $Fr = 100$, $Re = 1.5$, $Gr = 20.5$, $\lambda = 5.5$ and $Ha = 1.0$.

contours become more concentrated and tightly confined above the heaters. This demonstrates that fluid motion within the porous medium becomes more focused and vigorous, even though the overall circulatory flow pattern within the domain remains largely unchanged.

Figure 4.4, presents velocity contours corresponding to varying values of the material parameter Forchheimer number (Fr), with the simulations conducted for $Fr = 0$, 5, 20, 40, and 100. It is evident that as the Forchheimer number increases, the velocity within the domain progressively decreases. At lower Forchheimer values,

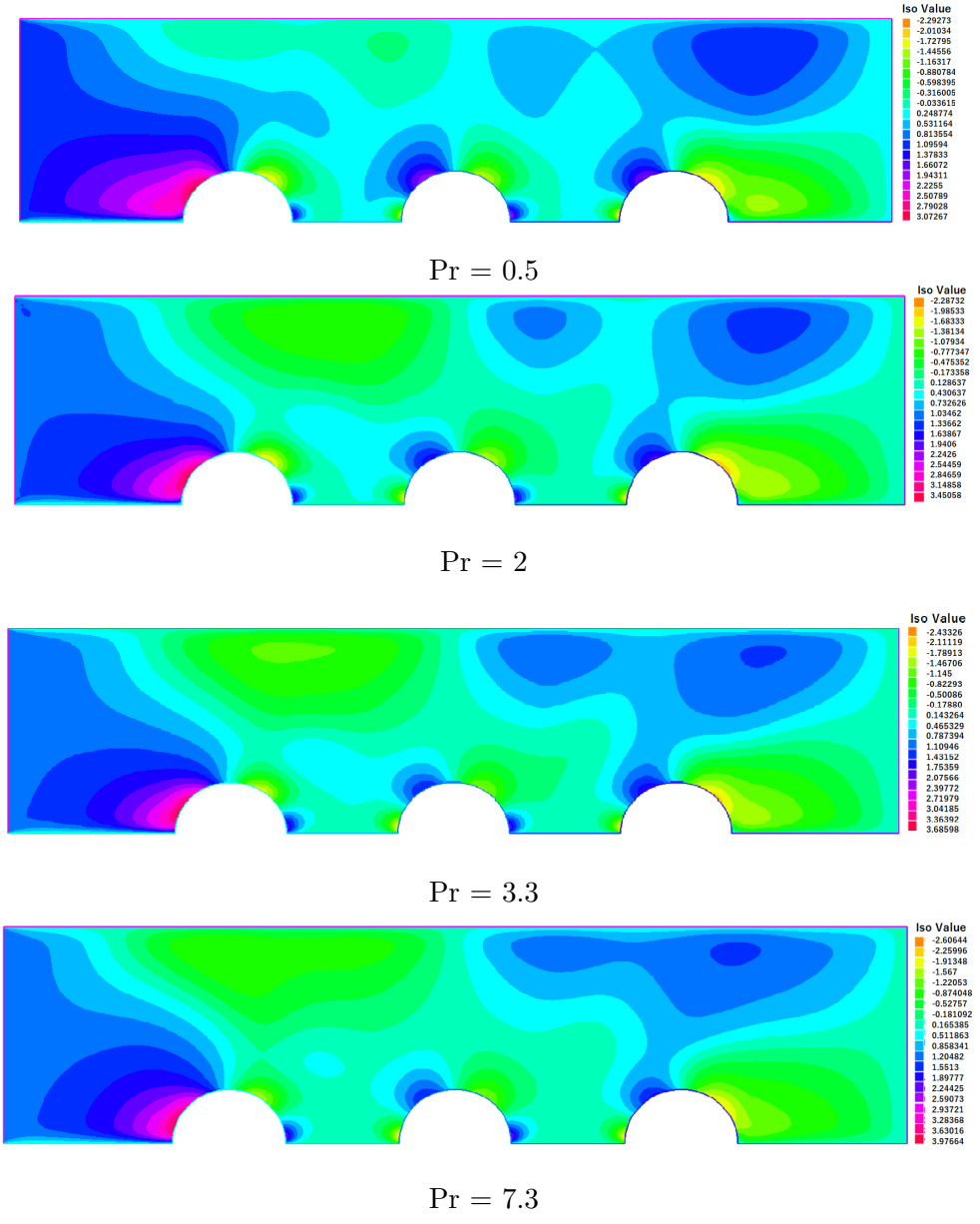

FIGURE 4.3: Velocity profiles with varying values of the Prandtle Number (Pr). Other parameters used: $Fr = 100$, $Re = 1.5$, $Pr = 0.1$, $\lambda = 5.5$ and $Ha = 1.0$.

the velocity contours exhibit a pronounced parabolic profile, indicating minimal resistance to the flow. However, with higher values of Fr, the non-linear drag effects become dominant, leading to a substantial suppression of velocity and a noticeable flattening of the velocity contours. The transition from a parabolic to a flatter profile highlights the increasing influence of the porous medium's resistance, ultimately reducing the flow intensity throughout the domain. This behavior underscores the significant role of the Forchheimer number in modulating flow dynamics within porous channels.

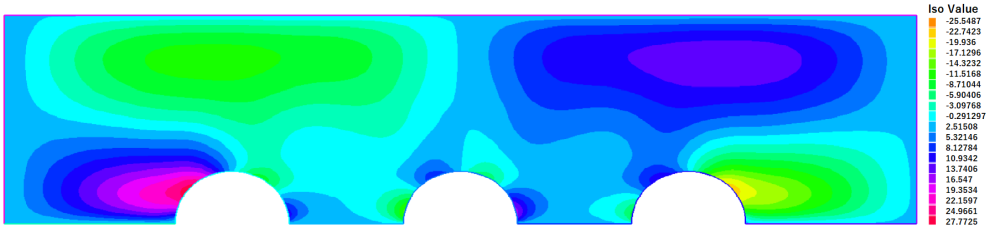

Fr = 0

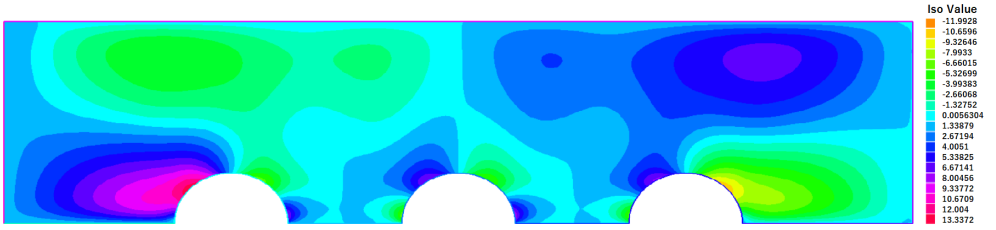

Fr = 05

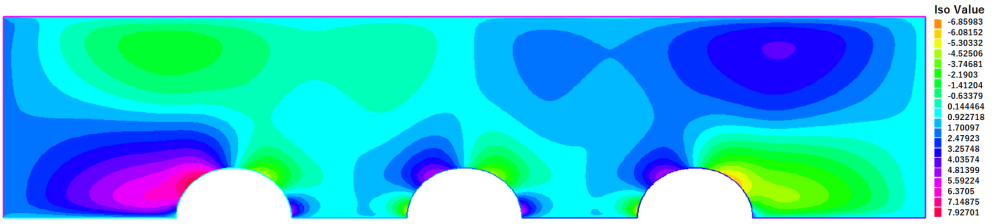

Fr = 20

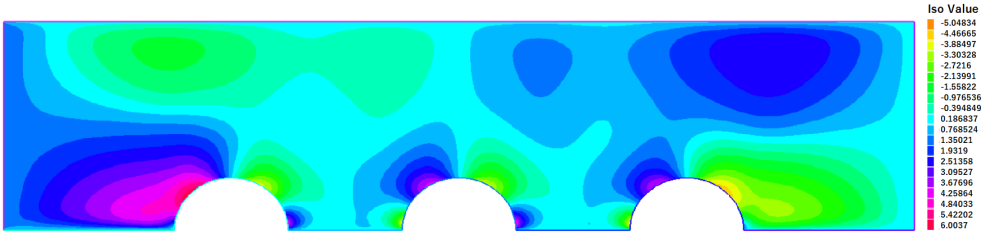

Fr = 40

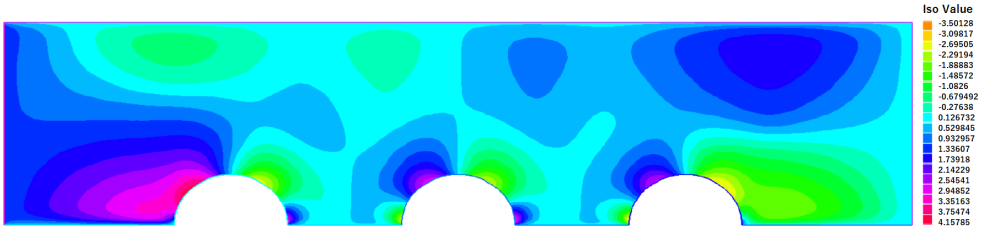

Fr = 100

FIGURE 4.4: Velocity profiles with varying values of the Forchheimer Number (Fr). Other parameters used: $Pr = 0.3$, $Re = 1.0$, $Gr = 20.5$, $\lambda = 5.5$ and $Ha = 1.0$

Figure 4.5, shows the velocity profiles for varying Reynolds numbers (Re) illustrate the transition of flow from a viscous-dominated laminar regime to an inertia-driven turbulent onset. At low Re (e.g. $Re = 1$), viscous forces dominate, resulting in smooth velocity profiles with steep gradients near the boundaries. As Re increases, the influence of inertial forces grows, leading to a rise in the central velocity and thinning of the boundary layers. Transitional behavior becomes evident at intermediate values of Re (for example $Re = 5$ and $Re = 7$), where the balance between viscous and inertial forces alters the flow structure. At higher Re (e.g. $Re = 10$), inertial forces strongly dominate, flattening the velocity in the core region and creating sharp gradients near the walls. These variations underscore the critical role of Re in determining the flow characteristics, from smooth laminar profiles to the onset of turbulence.

In Figure 4.6, the analysis of temperature profiles demonstrates the significant impact of the Prandtl number (Pr) on heat transfer characteristics. At low Prandtl numbers ($Pr = 0.5$), thermal diffusivity dominates, resulting in smooth and uniform temperature distributions with thicker thermal boundary layers. For moderate Prandtl numbers ($Pr = 2.0, 3.3$), the influence of momentum diffusivity increases, leading to sharper thermal gradients and thinner boundary layers. At high Prandtl numbers ($Pr = 7.3$), the momentum diffusivity strongly outweighs the thermal diffusivity, producing steep thermal gradients near the boundaries and highly localized heat transfer. These results highlight the critical role of Pr in shaping thermal boundary layer behavior and heat transfer efficiency.

Figure 4.7, shows the effect of different Forchheimer numbers on the temperature distribution within the channel. The Forchheimer number shows how much extra resistance is added to the flow in porous media due to inertial effects, on top of the normal Darcy drag. When $Fr = 0$, there is no additional resistance, so the flow follows Darcy's law only. In this case, the temperature spreads smoothly and widely through the channel, with gentle temperature changes, which means the heat is carried away well by the fluid. As Fr increases to 5, the extra resistance begins to slow the fluid more. This makes the heat build up closer to the obstacles, especially behind them. Because the fluid moves slower, it cannot carry heat away as easily, so hotter spots form and the temperature changes more sharply in

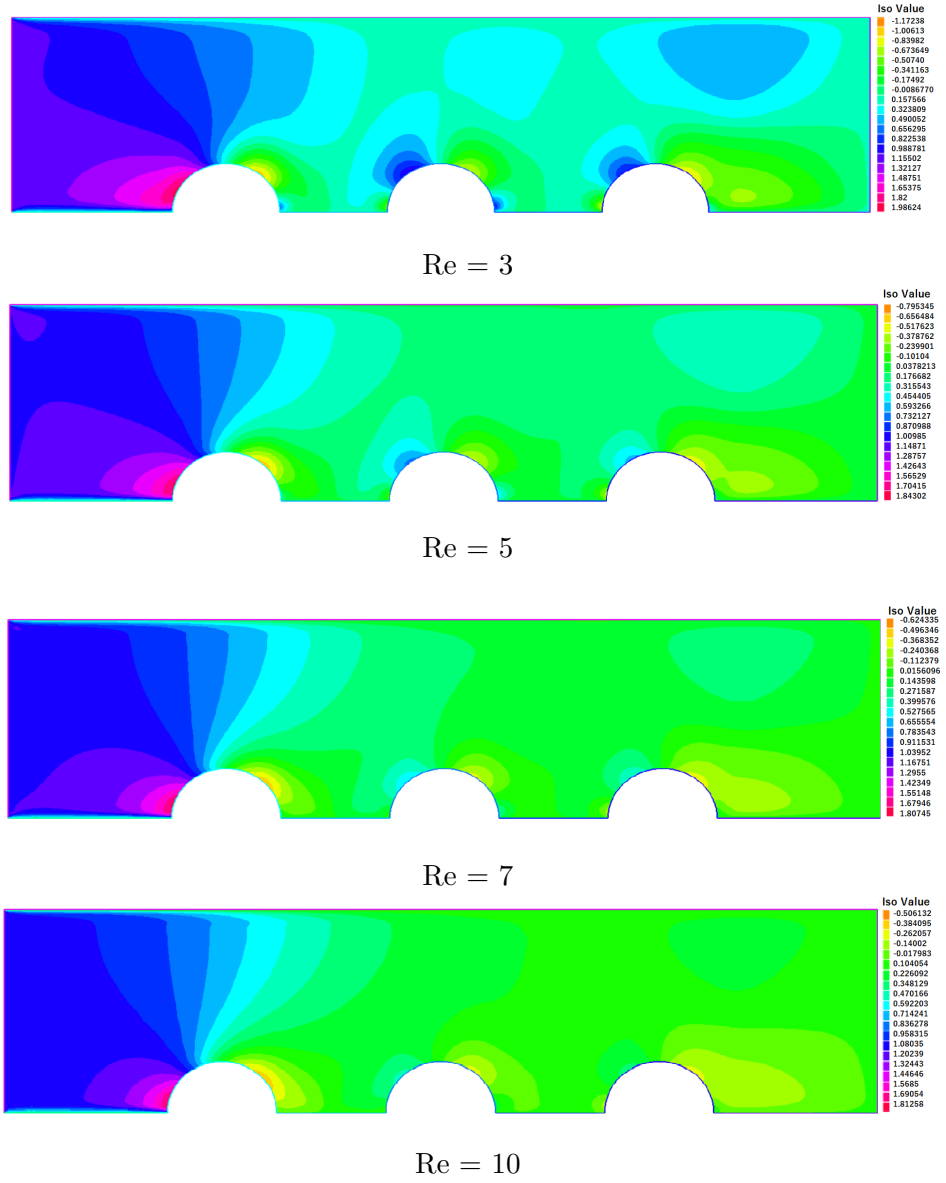

FIGURE 4.5: Velocity profiles with varying values of the Reynold Number (Re). Other parameters used: $Fr = 120$, $Pr = 0.3$, $Gr = 20.5$, $\lambda = 5.5$ and $Ha = 1.0$.

certain areas. At $Fr = 20$, this resistance is much stronger, so the flow slows down considerably and heat transfer becomes much less effective. As a result, very hot regions develop and the temperature pattern becomes uneven, with sharp changes near the obstacles. In summary, a higher Forchheimer number increases flow resistance, slows the fluid, and reduces how well heat is transported. This causes heat to gather in certain spots and makes the temperature inside the channel less uniform. Therefore, the Forchheimer number has a strong effect on how the flow and heat transfer behave in porous channels with obstacles.

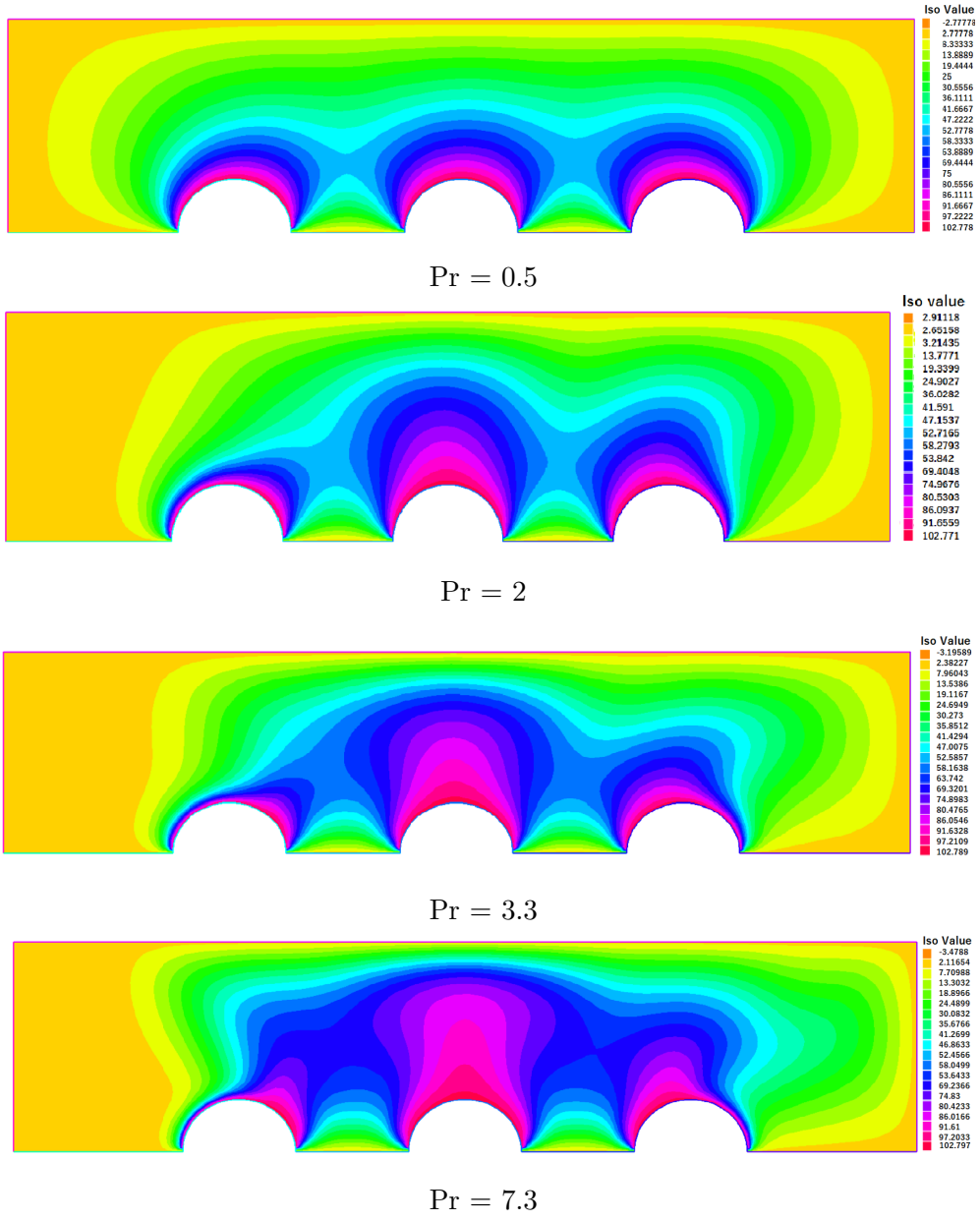

FIGURE 4.6: Temperature profiles with varying values of the Prandtl Number (Pr). Other parameters used: $Fr = 100$, $Re = 1.5$, $Gr = 20.5$, $\lambda = 5.5$ and $Ha = 1.0$.

Figure 4.8, shows how the Reynolds number changes the heat pattern inside the channel.At $Re = 10$, the flow is slow and smooth, so heat stays near the obstacles and spreads gently by conduction and weak convection.When Re rises to 30, the faster flow carries heat further downstream, stretching the warm areas and creating sharper temperature changes.

At $Re = 50$, convection is strong. Heat moves away quickly, forming long and clear warm trails behind the obstacles, and thinner warm layers near the surfaces. At $Re = 70$, the fluid's motion dominates heat transfer. The warm trails become

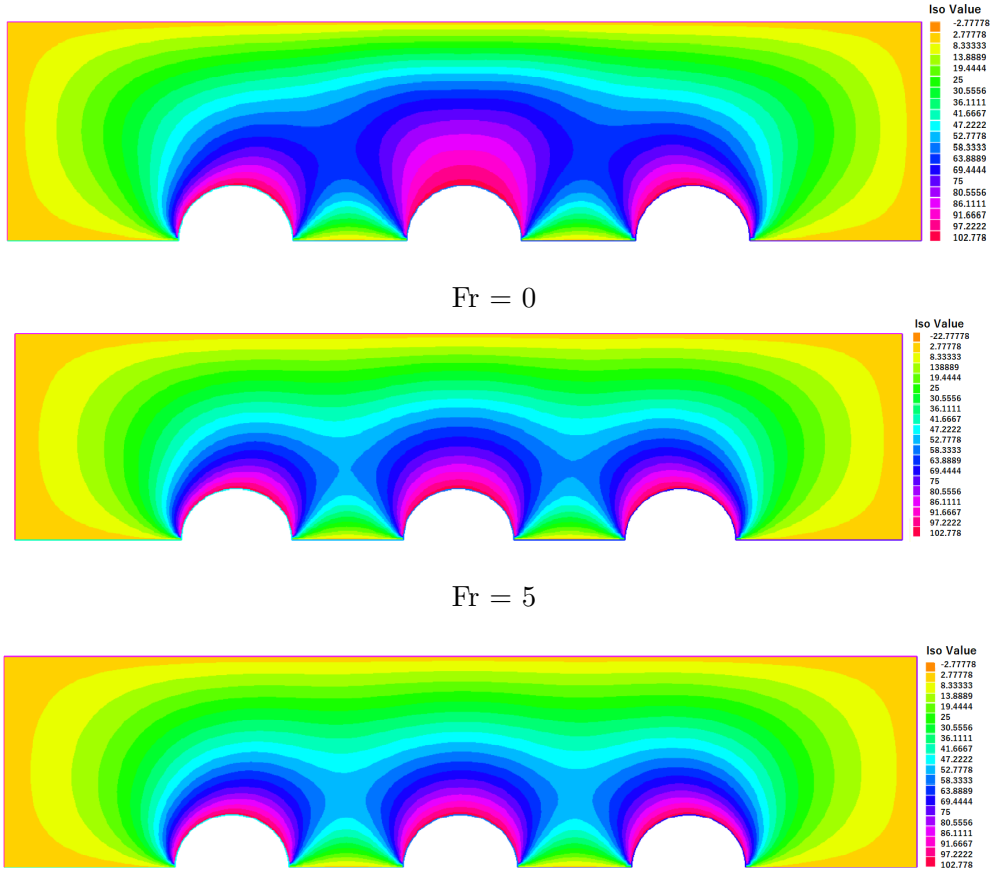

FIGURE 4.7: Temperature profiles with varying values of the Forchheimer number Number (Fr). Other parameters used: $Re = 1.0$, $Pr = 0.3$, $Gr = 20.5$, $\lambda = 5.5$ and $Ha = 1.0$..

very long and well-defined, with clear differences between cooler upstream zones and warmer downstream areas. Overall, as the Reynolds number increases, the flow sweeps heat away more effectively, leading to longer warm wakes, steeper temperature changes, and a heat pattern strongly shaped by the moving fluid.

Figure 4.9, shows how very low Reynolds numbers affect the temperature distribution in a channel with obstacles. At $Re = 1$, the flow is extremely slow, so heat spreads mainly by conduction. The temperature field is smooth, thick, and almost symmetrical around each obstacle. At $Re = 3$, the flow speed is slightly higher, but convection is still very weak. Heat still spreads mainly by diffusion, with barely any stretching of warm zones downstream. At $Re = 5$, the fluid moves a little faster, causing a tiny bit more downstream influence, but conduction remains dominant. Warm areas stay broad and uniform. At $Re = 7$, the highest in this low range, convection starts to show a minor effect. Still, heat mostly diffuses

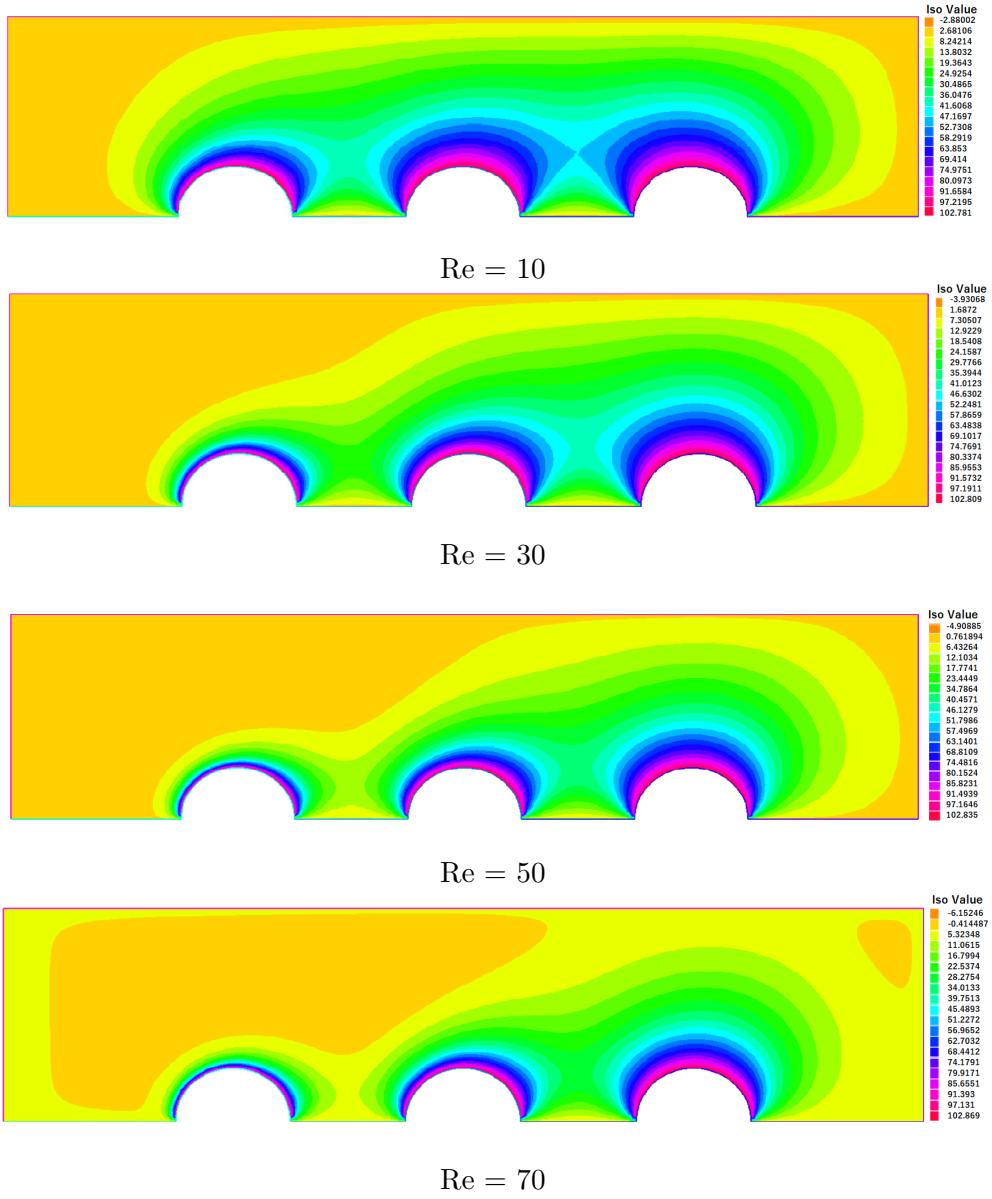

FIGURE 4.8: Temperature profiles with varying values of the Reynolds Number(Re). Other parameters used: $Fr = 120$, $Pr = 0.3$, $Gr = 20.5$, $\lambda = 5.5$ and $Ha = 1.0$.

smoothly around the obstacles with little sign of flow-driven transport. Overall, for these low Reynolds numbers, viscous forces overpower any inertial effects. As a result, heat transfer is ruled by conduction, with minimal help from convection. The temperature contours stay smooth and mostly symmetrical, showing that heat is not carried far by the flow.

In the present study, mesh independence analysis has been carried out to ensure the reliability and accuracy of the numerical results. The mesh is constructed based on two key geometric discretization parameters K and N. By varying these

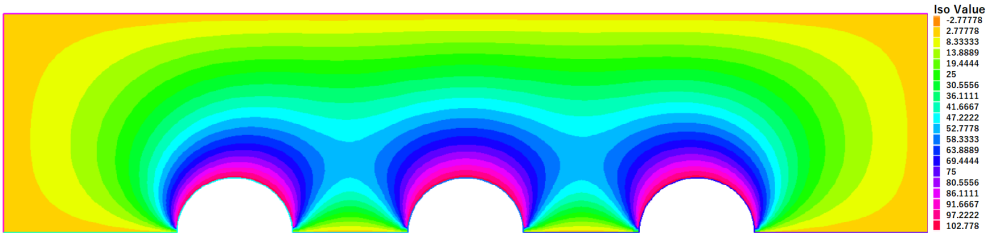

Re = 1

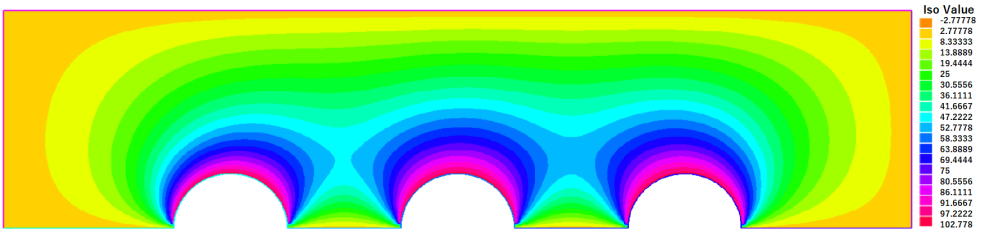

Re = 3

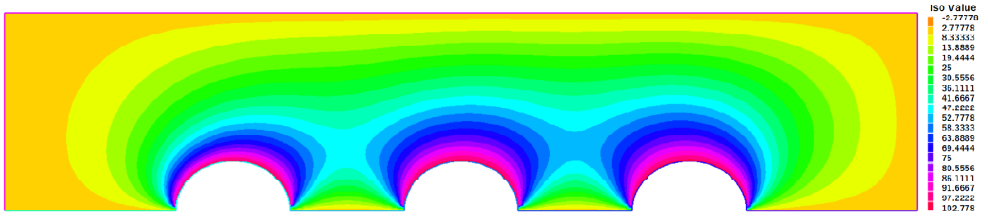

Re = 5

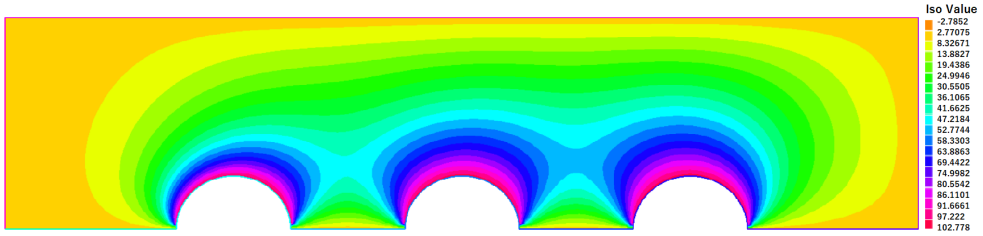

Re = 7

FIGURE 4.9: Temperature profiles with varying values of the lower Reynold Number (Re). Other parameters used: $Fr = 120, Pr = 0.3, Gr = 20.5, \lambda = 5.5$ and $Ha = 1.0$.

TABLE 4.1: Mesh independence analysis with maximum velocity magnitude

S No	Mesh (K,N)	No. of Triangles	No. of Vertices	Max $\|V\|$	Absolute Difference	Difference %
1	(2,5)	1303	720	2.51565	–	–
2	(2,7)	2565	1378	2.59874	0.08309	3.30%
3	(2,9)	4193	2219	2.60611	0.00737	0.28%
4	(2,11)	6281	3290	2.60592	0.00019	0.01%

parameters, a sequence of progressively finer meshes is generated, ranging from coarse to highly refined configurations.Each mesh configuration is characterized by a specific number of triangles, representing the discretized elements of the

computational domain, and vertices, which are the nodal points where the solution is approximated. Using FreeFEM++, an open-source finite element code, the maximum velocity magnitude within the domain is computed for each mesh setup. The variation in maximum velocity values across different mesh resolutions serves as a basis for evaluating mesh independence. Minimal changes in the results as the mesh is refined indicate that the numerical solution is stable and not significantly influenced by the mesh density, thereby confirming mesh-independent behavior.

Chapter 5

Conclusions and Future Work

In this research, we explored the flow and heat transfer characteristics through a porous medium governed by the Darcy-Forchheimer model. The geometry consists of a rectangular domain with three semicircular heaters connected beneath the bottom boundary, representing localized heat sources. We formulated a coupled nonlinear system of equations involving velocity, pressure, and temperature fields. The Finite Element Method (FEM) was employed in combination with a two-level algorithm to efficiently solve the problem with coarse and fine mesh discretizations. We analyzed the influence of key physical parameters, including the Darcy number, Forchheimer number, Reynolds number, Hartmann number, Prandtl number, and Grashof number. Detailed graphical results were obtained to illustrate their effects on the velocity profiles, temperature gradients. Mesh independence analysis was also performed with different four meshes. The influence of porosity was thoroughly investigated. This study contributes to the modeling of complex heat and fluid flow in porous domains. The main findings of this research is decribed as follows

- Increasing the Forchheimer number leads to a reduction in the fluid velocity due to enhanced inertial resistance in the porous medium.
- Higher Darcy number allows easier flow through the porous structure, resulting in increased velocity.

- Increase in the Hartmann number suppresses the velocity due to Lorentz force and this leads to a more uniform temperature distribution in the porous domain.
- The rise in the Grashof number enhances buoyancy-driven convection and significantly improves heat transfer near the heated regions.
- Higher Prandtl number reduces thermal diffusivity, causing sharper temperature gradients and more localized heating effects.
- Heater placement and shape (semicircles) creates strong localized convection, influencing overall heat distribution in the porous medium.

Several promising directions can be identified for future research. One of the possible future research direction is to extend the current steady-state model to unsteady (transient) flow conditions to capture the dynamic behavior of the system over time. Also, non-Newtonian effects such as viscoelastic, power-law, or couple-stress fluids can be incorporated to analyze more realistic complex fluid behaviors. Another possible direction is to extend the current two-dimensional model to three-dimensional geometries with irregular or porous walls can be considered to simulate real-world engineering systems.

Bibliography

[1] J. Fourier. *"The Analytical Theory of Heat"*. Cambridge University Press, 1822.

[2] H. S. Carslaw and J. C. Jaeger. *"Conduction of Heat in Solids"*. Oxford University Press, Oxford, 2nd edition, 1959.

[3] J. Crank. *"The Mathematics of Diffusion"*. Oxford University Press, Oxford, 2nd edition, 1975.

[4] M. N. Ozisik. *"Heat Transfer: A Basic Approach"*. McGraw-Hill, New York, 1985.

[5] F. P. Incropera, D. P. DeWitt, T. L. Bergman, and A. S. Lavine. *"Fundamentals of Heat and Mass Transfer"*. John Wiley & Sons, Hoboken, NJ, 7th edition, 2011.

[6] S. V. Patankar. *"Numerical Heat Transfer and Fluid Flow"*. Hemisphere Publishing Corporation, Washington, DC, 1980.

[7] R. Siegel and J. R. Howell. *"Thermal Radiation Heat Transfer"*. Taylor & Francis, New York, 4th edition, 2002.

[8] A. Bejan. *"Convection Heat Transfer"*. John Wiley & Sons, Hoboken, NJ, 4th edition, 2013.

[9] A.B. Zolotukhin and A.T. Gayubov. "analysis of nonlinear effects in fluid flows through porous media". *Journal of Petroleum Exploration and Production Technology*, 12:2237–2255, 2022. doi: 10.1007/s13202-021-01444-3.

[10] Kambiz Vafai. *"Handbook of Porous Media"*. CRC Press, 3rd edition, 2015. ISBN 9781466559985.

[11] Hui Zhao, Xiaoming Liu, and Jin Wang. "numerical analysis of heat transfer in a darcy–forchheimer porous medium". *International Journal of Heat and Mass Transfer*, 157:119963, 2020. doi: 10.1016/j.ijheatmasstransfer.2020.119963.

[12] B. R. Thomas. *"Introduction to Heat Transfer"*. Wiley, Hoboken, NJ, 7th edition, 2013.

[13] E. Vishnuvardhanarao and M. K. Das. "laminar mixed convection in a parallel two-sided lid-driven differentially heated square cavity filled with a fluid-saturated porous medium". *Numerical Heat Transfer, Part A: Applications*, 53(1):88–110, 2007.

[14] Fawang Liu, Vo Anh, Ian Turner, and Ninghu Su. "a two-dimensional finite volume method for transient simulation of time- and scale-dependent transport in heterogeneous aquifer systems". *Journal of Applied Mathematics and Computing*, 11:215–241, 2003.

[15] J. H. Ferziger and M. Perić. *"Computational Methods for Fluid Dynamics"*. Springer, Cham, Switzerland, 4th edition, 2020.

[16] O. C. Zienkiewicz, R. L. Taylor, and J. Z. Zhu. *"The Finite Element Method"*. Wiley, Hoboken, NJ, 7th edition, 2013.

[17] K .J. Bathe. *"Finite Element Procedures"*. Prentice Hall, Upper Saddle River, NJ, 2006.

[18] G. F. Carey and J. T. Oden. *"Finite Elements: A Survey of Applications in the Mechanics of Solids"*. Prentice-Hall, Englewood Cliffs, NJ, 1984.

[19] G .R. Liu. *"The Finite Element Method: A Practical Course"*. Springer, Berlin, Germany, 2000.

[20] Hrvoje Jasak and Željko Tuković. "automatic mesh motion for the unstructured finite volume method". *Transactions of FAMENA*, 30(2):1–20, 2006.

[21] D. Slone et al. "dynamic fluid–structure interaction using finite volume unstructured mesh procedures". *OCEAN Engineering*, 2004. Discusses FVM/FDM/FEM entailing remeshing for moving boundaries and free surfaces.

[22] D. A. Nield, A. Bejan, et al. *Convection in porous media*, volume 3. Springer, 2006.

[23] Moayed R. Hasan, Suhad A. Rasheed, and Ali N. Mahdi. "experimental study of forced convection heat transfer porous media inside a rectangular duct at entrance region". *Journal of University of Babylon for Engineering Sciences*, 27(1):211–231, 2019. doi: 10.29196/jubes.v27i1.1991.

[24] B. Vasu, B. Nithyadevi, A. Sathishkumar, and M. Kumar. "heat transfer enhancement using porous structures: A review". *Materials Today: Proceedings*, 45:2099–2106, 2021. doi: 10.1016/j.matpr.2020.11.886.

[25] M. S. Khan, M. A. Memon, I. Khan, and S. M. Eldin. "finite element based direct and iterative approach to investigate a magneto-micropolar flow through a rectangular channel". *Alexandria Engineering Journal*, 75:55–66, 2023.

[26] R. W. Fox, AT McDonald, and P. J. Pitchard. "introduction to fluid mechanics", 2004, 2006.

[27] R. K. Bansal. *"A textbook of fluid mechanics"*. Firewall Media, 2005.

[28] J. N. Reddy and D. K. Gartling. *"The finite element method in heat transfer and fluid dynamics"*. CRC press, 2010.

[29] J. Ahmed and M. S. Rahman. "handbook of food process design".

[30] Robert B. Bird, Ronald C. Armstrong, and Ole Hassager. *"Dynamics of Polymeric Liquids, Volume 1: Fluid Mechanics"*. John Wiley & Sons, New York, 2 edition, 1987.

[31] Robert W. Fox, Alan T. McDonald, and Philip J. Pritchard. *"Introduction to Fluid Mechanics"*. John Wiley & Sons, Hoboken, NJ, 8 edition, 2011.

[32] S. C. Brenner and R. L. Scott. *"The Mathematical Theory of Finite Element Methods"*, volume 15 of *Texts in Applied Mathematics*. Springer, New York, 3rd edition, 2008.

[33] A. Zahra. "application of the finite element method in thermal analysis of microchannels". Master's thesis, Capital University of Science Technology, 2024. Available at https://thesis.cust.edu.pk/zahra2024.

[34] L. C. Evans. *"Partial Differential Equations"*, volume 19 of *Graduate Studies in Mathematics*. American Mathematical Society, Providence, 2nd edition, 2010.

[35] A. Ern and J. L. Guermond. *"Theory and Practice of Finite Elements"*, volume 159 of *Applied Mathematical Sciences*. Springer, New York, 2004.

[36] Hongxing Rui and Hao Pan. "a block-centered finite difference method for the Darcy–Forchheimer model"s. *SIAM Journal on Numerical Analysis*, 50 (5):2612–2631, 2012. doi: 10.1137/110858239,2012.